

Fatty acids in oomycetes

Dissertation
zur Erlangung des Doktorgrades
der Naturwissenschaften

vorgelegt beim Fachbereich für Naturwissenschaften
der Johann Wolfgang Goethe - Universität
in Frankfurt am Main

von
Ann-Katrin Buch
aus Frankfurt am Main, Deutschland

Frankfurt 2021

vom Fachbereich Biowissenschaften der Johann Wolfgang Goethe - Universität
als Dissertation angenommen.

Dekan: Prof. Dr. Sven Klimpel

Gutachter : Prof. Dr. Marco Thines

Datum der Disputation : 27.09.21

Content

Abbreviations	III
Abstract	IV
Zusammenfassung	V
1. Introduction	1
1.1. Oomycetes.....	1
1.1.1. Biology and phylogeny of Oomycetes:	1
1.1.2. Pathogenicity of oomycetes	4
1.1.3. Prominent oomycetes.....	5
1.2. Fatty acids	7
1.2.1. Introduction to fatty acids	7
1.2.2. Functions of fatty acids.....	9
1.2.3. Fatty acid profiles	11
1.2.4. De novo synthesis of fatty acids	12
1.2.5. Enzymes involved in fatty acid synthesis	14
1.3. Scope of this work.....	15
2. Material and Methods	16
2.1. Strains.....	16
2.2. Media	16
2.3. Genomic DNA isolation.....	17
2.4. RNA isolation	18
2.5. DNA Amplification	18
2.6. Oligonucleotides used in this study.....	19
2.7. Phylogenetic analysis	25
2.8. FAME profiles	26
2.9. Genome assembly.....	28
2.10. Identification of enzymes involved in fatty acid synthesis.....	28
2.11. Analysis and characterisation of fatty acid elongases and desaturases.....	28
2.12. The pathway of the synthesis of very long chain polyunsaturated fatty acids	29
3. Results.....	29
3.1. Phylogenetic analysis	29
3.2. FAME analysis.....	32
3.3. Summary and comparison of oomycete fatty acid profiles.....	54
3.4. Characterisation of enzymes involved in long-chain fatty acid synthesis in <i>Pythium dissotocum</i> P100.30	60
3.5. Elongase of P100.30.....	62

3.6.	Desaturases of P 100.30	64
3.7.	Δ 4-desaturase	65
3.8.	Δ 5-desaturase	67
3.9.	Δ 6-desaturase	69
3.10.	Δ 12-desaturase	71
3.11.	Δ 15-desaturase	73
3.12.	Pathway of long chain fatty acid synthesis in the <i>Pythium dissotocum</i> strain P 100.30	75
4.	Discussion	80
4.1.	Fatty acids in oomycetes	80
4.2.	Endosymbiosis.....	84
4.3.	Pathway	85
4.4.	Sterols.....	87
4.5.	Reliability of FAME profiles and the possible fingerprinting of microorganisms 90	
5.	Conclusion	93
	References	94
6.	List of Figures	102
7.	Appendix.....	106
	Danksagung	Fehler! Textmarke nicht definiert.
	Curriculum vitae.....	Fehler! Textmarke nicht definiert.
	Record of conferences.....	Fehler! Textmarke nicht definiert.

Abbreviations

ALA, α -Linolenic acid

Bp, base pair

C-terminal, carboxyl-terminal

DGLA, Dihomo- γ -linolenic acid

DHA, Docosahexaenoic acid

DNA, Deoxyribonucleic acid

EPA, Eicosapentaenoic acid

ETA, Eicosatetraenoic acid

FAME, Fatty acid methyl ester

kb, kilobase

LA, Linoleic acid

LCPUFA, Long chain polyunsaturated fatty acids

ml, milliliter

mRNA, messenger RNA

rRNA, ribosomal RNA

MUFA, Monounsaturated fatty acids

NADPH, Nicotinamide adenine dinucleotide phosphate

ORF, open reading frame

PCR, polymerase chain reaction

PUFA, Polyunsaturated fatty acids

rRNA, Ribosomal ribonucleic acid

RNA, Ribonucleic acid

rpm, revolutions per minute

SFA, Saturated fatty acids

STA, Stearic acid

VLPUFA, Very long chain polyunsaturated fatty acids

μ g, microgram

Abstract

Oomycetes are recognized and well known for being destructive plant pathogens but they are less known for their ability to produce very long chain polyunsaturated fatty acids de novo.

Fatty acids are essential for human health but need to be acquired through the diet. To meet the increasing demand of ω -3 fatty acids new, sustainable sources need to be found. The aim of this study was to further extend the current knowledge of the fatty acid composition and their synthesis in Oomycetes

In this study 192 fatty acid methyl ester profiles were obtained from 23 different strains belonging to the *Peronosporomycetes*. The strains were grown at 20 °C and 27 °C to analyse the fatty acid content as well as the changes of the content in different temperatures. The analysis of the fatty acid profiles revealed that all of the oomycetes produce significant amounts of eicosapentaenoic acid. One *Pythium dissotocum* strain P100.30 was found to produce almost 40 % eicosapentaenoic acid of its total fatty acid content, this strain was chosen for further analysis. The genome and transcriptome sequencing revealed six enzymes involved in the synthesis of very long chain polyunsaturated fatty acids.

The enzymes were found in other oomycetes as well and revealed the existence of a similar enzymatic set in *Peronosporomycetes* as well as in *Saprolegniomycetes*. While the *Peronosporomycetes* are known to be sterol auxotrophs, the *Saprolegniomycetes* are sterol prototrophs. Sterols and fatty acids are important to maintain the structural integrity in the membranes of Oomycete membranes.

The fatty acid profiles showed branched fatty acids and while measurements and precautions were taken to avoid or remove potential bacterial contaminations, they did not disappear. One of the potential reasons could be an endosymbiotic relationship between oomycetes and bacteria.

Despite these results, which require further scrutiny in future studies, the fatty acid synthesis pathway of oomycetes could be elucidated in this study based on fatty acid profiling and genomic analyses.

Zusammenfassung

Oomyceten sind weithin bekannt als zerstörerische Pflanzenpathogene. Besondere Popularität innerhalb der *Peronosporomyceten* erlangte zum Beispiel *Phytophthora infestans*, der Verursacher der Kraut- & Knollenfäule, die zu der großen Hungersnot in Irland zwischen 1840 und 1845 führte. Bis zum heutigen Tage werden weltweit Ernteeinbußen von ungefähr 20 % auf Oomyceten zurückgeführt, und doch gibt es nur wenige, teils ineffektive Fungizide. Wofür Oomyceten weniger bekannt sind, ist ihre Fähigkeit langkettige mehrfach ungesättigte Fettsäuren de novo zu synthetisieren. Generell ist über die Stoffwechselwege bei Oomyceten relativ wenig bekannt. Galten sie früher alle als Sterol auxotroph wurde in den letzten Jahren in dem Genom von *Aphanomyces astaci* das Vorhandensein von Genen, die für Squalen-Epoxidasen codieren, nachgewiesen, welche auch in anderen *Saprolegniomyceten* gefunden wurde.

ω -3 Fettsäuren sind essenzielle Nährstoffe, die für die Funktion eines menschlichen Organismus unabdingbar sind. Eine gute Versorgung mit ω -3 Fettsäuren wird mit gesundheitlichen Vorteilen wie einer besseren Immunabwehr, verbesserten Fließeigenschaften des Blutes, einer Hemmung der Blutgerinnung sowie einer Blutdrucksenkung in Verbindung gebracht. Darüber hinaus wirken sie entzündungshemmend und beeinflussen den Triglycerid-Stoffwechsel positiv.

Da Menschen, wie alle höheren Lebensformen, langkettige ungesättigte Fettsäuren nicht selbst synthetisieren können, sind sie auf eine Zufuhr von diesen Nährstoffen durch ihre Ernährung angewiesen. Lebensmittel mit einem hohen Gehalt an Eicosapentaen- und Docosahexaensäure sind vor allem Seefisch und Meeresfrüchte. Aufgrund von Überfischung, einer zunehmenden Verschmutzung der Meere und somit einer Anreicherung von fettlöslichen Toxinen in solchen Lebensmitteln wird dringend eine neue Quelle von ω -3 Fettsäuren benötigt, um dem steigenden Bedarf gerecht zu werden.

Im Rahmen dieser Arbeit wurden 23 verschiedene Oomyceten, welche alle zu den *Peronosporomyceten* gehören, untersucht und Fettsäureprofile erstellt.

Dabei wurden die Stämme bei 20 °C und 27 °C für fünf Tage auf PDB-Agar mit 30 μ g/ml Rifampicin und 50 μ g/ml Nystatin kultiviert, um einen Vergleich der Fettsäureprofile bei unterschiedlichen Temperaturen erstellen zu können. Von jedem Stamm wurden mindestens drei Replikate der Fettsäureprofile erstellt.

Anschließend wurde ein *Pythium dissotocum* Stamm mit dem Namen P100.30, aufgrund seines Fettsäureprofils und seines Wachstumsverhaltens ausgewählt. Von diesem Stamm wurde das Genom und das Transkriptom sequenziert. Nach der Assemblierung des Genoms wurden die Enzyme, die in der Synthese der langkettigen mehrfach ungesättigten Fettsäuren beteiligt waren, identifiziert und charakterisiert. Mithilfe des Fettsäureprofils und der gefundenen Enzyme wurde der Syntheseweg der mehrfach ungesättigten Fettsäuren rekonstruiert.

Alle Fettsäureprofile der *Peronosporomyceten* zeigten, dass Oomyceten teils sehr große Mengen an Eicosapentaensäure (C20:5 ω 3) produzieren. Der Vergleich der Fettsäureprofile beim Wachstum bei 20 °C und 27 °C zeigte deutliche Unterschiede. Während bei 20 °C viele langkettige, mehrfach ungesättigte Fettsäuren produziert wurden, verschob sich das Fettsäuremuster zu kurzkettigeren, gesättigten oder nur einfach ungesättigten Fettsäuren bei 27 °C. Bei *Pythium dissotocum* Stamm P100.30 betrug der Anteil von Eicosapentaensäure im Fettsäureprofil fast 40 %, wenn er bei 20 °C kultiviert wurde.

Interessanterweise wurden in fast allen Fettsäureprofilen verzweigte Fettsäuren gefunden. Oomyceten sind jedoch nicht dafür bekannt verzweigte Fettsäuren zu produzieren, was eher als ein Merkmal von Bakterien angesehen wird. Um die Kulturen der Oomyceten von eventuellen bakteriellen Kontaminationen zu befreien, wurde zunächst die Antibiotikakonzentration erhöht. Dann wurden die Kulturen mit sogenannten Raper Ringen wachsen gelassen. Zuletzt wurden die Kulturen unter dem Mikroskop überimpft und nur einzelne Hyphen ohne erkennbare Kontaminationen aufgenommen. Die Fettsäureprofile wiesen jedoch trotz dieser Maßnahmen verzweigte Fettsäuren auf.

Im Genom von P100.30 wurden sechs Gene gefunden, die Enzyme kodieren, welche an der Synthese von langkettigen mehrfach ungesättigten Fettsäuren beteiligt sind. Dass diese Enzyme auch aktiv in *Pythium dissotocum* synthetisiert werden, konnte durch Mapping der genomischen Sequenzen auf das assemblierte Transkriptom bestätigt werden.

Unter den gefundenen Enzymen ist eine Elongase, welche C18 und C20 Substrate verlängert, jedoch mit einer starken Spezifität für C18 Substrate.

Weiterhin wurden fünf Desaturasen gefunden, welche durch Oxidation eine Doppelbindung in ein Molekül an einer bestimmten Stelle einbringen können. Unter den gefundenen Desaturasen befand sich eine Δ 4-Desaturase, bestehend aus 336

Aminosäuren, die $\Delta 4$ -Desaturase ist für die Desaturierung von Docosapentaensäure (C22:5 ω 3) verantwortlich. In der Sequenz wurden zwei Transmembran-Domänen gefunden, zwei Domänen, die im Cytosol lokalisiert sind und eine, welche im nicht-cytosolischen Raum lokalisiert ist. Das Resultat aus der enzymatischen Reaktion dieses Enzyms ist Docosahexaensäure (C22:6 ω 3). Die $\Delta 4$ -Desaturase ist zudem in der Reaktion auf einen Kälteschock involviert und kann Doppelbindungen in membrangebundene Fettsäuren einbringen.

Diese Desaturase scheint evolutionär nicht mit den anderen Desaturasen oder der Elongase verwandt. Sie weist große Ähnlichkeiten mit Desaturasen auf, die zur Familie der $\Delta 4$ -Sphingolipid-Desaturasen gehören. Der Vergleich mit Sequenzdaten von $\Delta 4$ -Desaturasen von anderen *Peronosporomyceten* und auch *Saprolegniomyceten* zeigte, dass diese Desaturasen hoch konserviert sind. Es gibt jedoch Unterschiede zwischen $\Delta 4$ -Desaturasen von *Saprolegniomyceten* und *Peronosporomyceten*, vor allem im Hinblick auf die Positionen der endoplasmatischen Retentionssignale und den Positionen ihrer Histidin-Boxen.

Die Sequenz der $\Delta 5$ -Desaturase, welche im Genom gefunden wurde, kodiert für ein 488 Aminosäure großes Protein. Diese Desaturase ist für die Desaturierung von entweder Dihomo- γ -Linolensäure oder Eicosatetraensäure verantwortlich.

Die ebenfalls gefundene Sequenz einer $\Delta 6$ -Desaturase kodiert für ein Protein, bestehend aus 457 Aminosäuren, und ist homolog zur $\Delta 5$ -Desaturase. Beide Desaturasen bestehen aus neun Domänen, die die Membran vier Mal durchqueren und somit ebenfalls zu den Membran-gebundenen Desaturasen zu zählen sind. Die $\Delta 5$ - und die $\Delta 6$ -Desaturase gehören beide zu den Front-End Desaturasen.

$\Delta 6$ -Desaturasen führen eine Doppelbindung in entweder Linolsäure (C18:2 ω 6) oder Linolensäure (18:2 ω 3) ein, was als einer der geschwindigkeitsbegrenzenden Schritte in der Synthese langkettiger Fettsäuren gehandelt wird.

Ein weiteres Enzym des Fettsäurestoffwechsels von *Pythium dissotocum*, das in den genetischen Daten gefunden werden konnte, ist eine $\Delta 12$ -Desaturase, die 398 Aminosäuren groß ist und für die Einführung einer ω -6 Desaturierung in Ölsäure (C18:1) verantwortlich. Es ist die erste Doppelbindung, die in der Synthese der mehrfach ungesättigten Fettsäuren von *Pythium dissotocum* eingefügt wird. Das Enzym ist ebenfalls membrangebunden und hat drei Transmembran-Domänen, zwei Domänen im Cytosol und drei Domänen im nicht-cytosolischen Bereich. $\Delta 12$ -

Desaturasasen sind in Pflanzen und Mikroorganismen weitverbreitet und gehören zu den Methyl-End-Desaturasasen.

Die Sequenz der $\Delta 15$ -Desaturase kodiert für 367 Aminosäuren und besteht aus elf Domänen, darunter fünf Transmembran-Domänen, drei Domänen im Cytosol und drei Domänen im nicht-cytosolischen Bereich. Die $\Delta 15$ -Desaturase wird auch als ω -3-desaturase bezeichnet, weil sie aus der ω -6 Fettsäure Linolsäure (C18:2 ω 6) durch die Desaturierung α -Linolensäure macht, und damit die erste ω -3 Fettsäure herstellt.

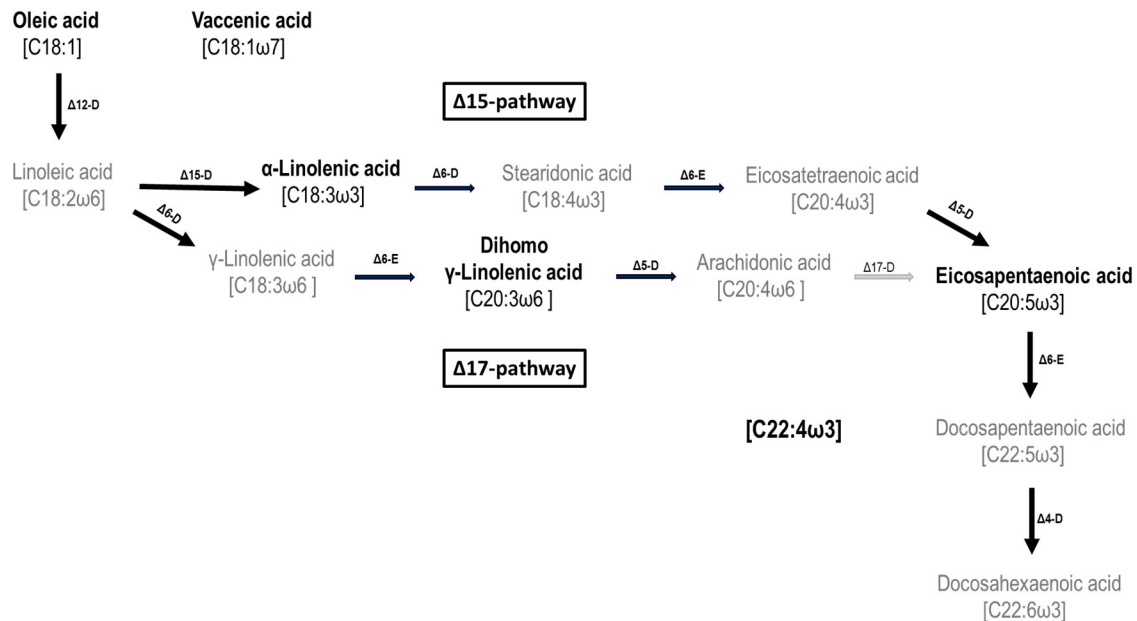


Abbildung 1: Syntheseweg von mehrfach ungesättigten Fettsäuren in dem *Pythium dissotocum* Stamm P100.30. Enzyme und Fettsäuren, die entweder im Genom oder in den Fettsäureprofilen gefunden wurden, sind schwarz, Fettsäuren und Enzyme die nicht gefunden wurden sind grau.

In Abbildung 1 ist der mögliche Syntheseweg der mehrfach ungesättigten Fettsäuren dargestellt. Die im Genom gefundenen Sequenzen, die für die verschiedenen Enzyme kodieren, sprechen für den $\Delta 15$ -Syntheseweg.

Die Fettsäuren, welche in den Fettsäureprofilen gefunden wurden, wiesen neben den verzweigten Fettsäuren noch zwei unbekannte Verbindungen auf, die als C22:4 ω 3 und als C18:2 ω 3 bezeichnet wurden.

Die Ergebnisse der FAME-Analyse zeigten Besonderheiten auf vor allem mit dem wiederholten Vorkommen der verzweigten Fettsäuren und den unbekanntem Verbindungen in den Fettsäureprofilen.

Das Vorkommen der verzweigten Fettsäuren, für welche besonders Bakterien bekannt sind, könnte für eine Art Endosymbiose sprechen, welche vor allem bei verschiedenen *Zygomyceten* nachgewiesen wurde. Bei einer solchen Vereinigung wird das in den Hyphen lebende Bakterium durch diese Hyphen geschützt und hilft dem Wirt bei der

Akquisition von Nährstoffen. Diese endosymbiontischen Bakterien könnten dann auch durch Zugabe von Antibiotika bei der Kultivierung nicht abgetötet werden.

Alle Oomyceten, die in dieser Arbeit untersucht wurden, gehören den *Peronosporomyceten* an, welche als Sterol-auxotroph gelten. Die Produktion von langkettigen, mehrfach ungesättigten Fettsäuren kann ihnen als Kompensation dienen, um bei geringer Verfügbarkeit von Sterol-Vorstufen die Membranintegrität zu gewährleisten.

Die Enzyme, welche für die Produktion von langkettigen, mehrfach ungesättigten Fettsäuren benötigt werden, wurden auch in den Genomen von verschiedenen *Saprolegniomyceten* gefunden. In durch andere Studien veröffentlichten Fettsäureprofilen wurden jedoch maximal Fettsäuren mit einer Kettenlänge von 20C Atomen gefunden. Ein Grund dafür könnte sein, dass sie keine langkettigen Fettsäuren für ihre Membranen brauchen, da sie Sterol prototroph sind.

Die Fettsäureprofile der untersuchten Oomyceten haben gezeigt, dass alle Oomyceten ω -3 Fettsäuren produzieren und der *Pythium dissotocum* Stamm P100.30 mit knapp 40 % Eicosapentaensäure (EPA) des Gesamt-Fettsäuregehalts sehr viel EPA produziert. Die in dem Genom gefundenen Enzyme stellen eine gute Quelle dar, um transgene Organismen für die Produktion von EPA zu generieren.

Der Syntheseweg der Fettsäuren, der durch die gefundenen Enzyme nachverfolgt werden konnte, bildet einen wichtigen Baustein, um den Stoffwechsel der ökonomisch und ökologisch wichtigen Gruppe der Oomyceten im Detail verstehen zu können.

1. Introduction

1.1. Oomycetes

1.1.1. Biology and phylogeny of Oomycetes:

The oomycetes belong to the kingdom of *Straminipila* and phylogenetically are related to brown algae and diatoms, even though many of them appear fungus-like (Lücking *et al.*, 2020).

Phylogenetically, fungi are closely related to animals while oomycetes diverged early within the Straminipila. In contrast to many photosynthetic *Straminipila*, oomycetes have developed a heterotrophic lifestyle. They are related to microorganisms containing phaeoplasts such as diatoms and brown algae, even though oomycetes are not known to carry plastids (Thines, 2018).

In the kingdom or the crown group of *Straminipila* the phylum of the *Oomycota* can be further divided into two fungal-like subclasses, the *Saprolegniomycetes* and the *Peronosporomycetes*. In the *Saprolegniomycetes* orders such as *Saprolegniales* and *Leptomitales* and within the main plant pathogenic Peronosporomycetes the order of the *Peronosporales sensu lato* are to be found (Fawke *et al.*, 2015; Archibald *et al.*, 2020).

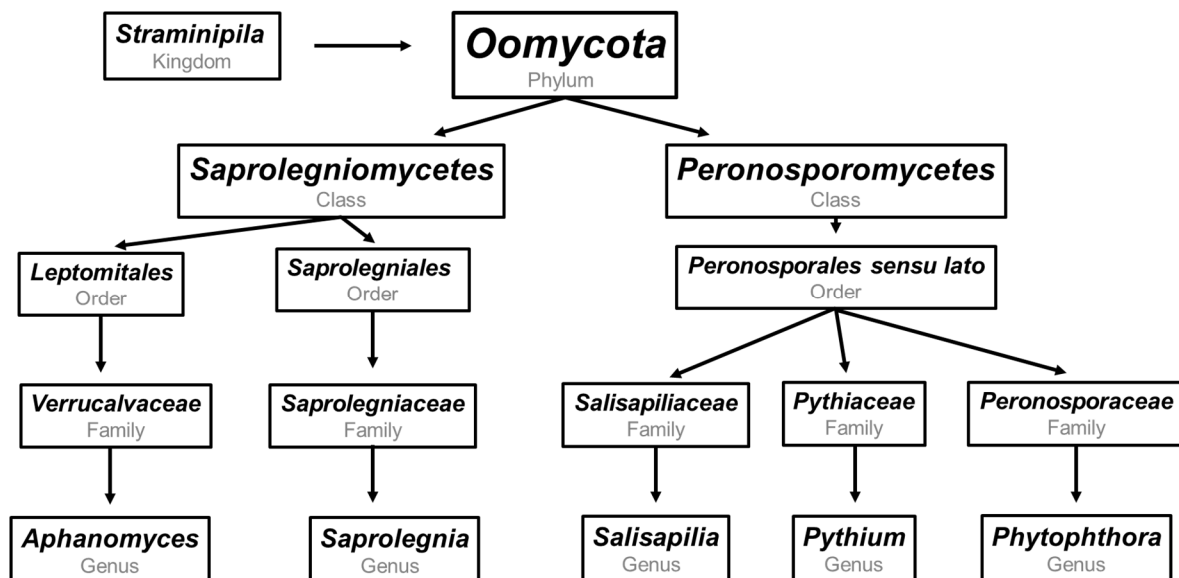


Figure 1: Overview of the phylogeny of the species used in this thesis.

The genera used in this study and their relationship are shown in Figure 1, the majority of the analysed species belonged to the genera of *Pythium* and *Phytophthora*.

Most oomycetes exhibit filamentous growth, just like many fungi, but some basal diatom-parasitizing *Saprolegniomycetes* and early-diverging lineages develop only holocarpic structures (Buaya *et al.*, 2020). Oomycetes are identifiable due to their structural features and evidence of oomycete-like structures have been found in fossils from the Devonian period and parasitism during the Carboniferous period, while the molecular clock dates the origin of oomycetes as early as the Silurian period (Fawke *et al.*, 2015). In the early stages of oomycete evolution they are believed to have started from marine environments as holocarpic parasites and later evolved to parasitize other eukaryotes (Judelson, 2017; (Thines, 2014)).

It remains unknown how many different oomycete species exist. More than 1200 species are described so far, the dark figure of unknown or undescribed species could be many times higher, especially since many early diverging holocarpic oomycetes are not discovered yet (Thines, 2018).

The structure that contributed to the name of the oomycetes are the Oogonia, part of the reproductive structures, combining the Greek word for egg and fungus (Judelson & Ah-Fong, 2019; Patel *et al.*, 2018; Ho, 2018; Thines, 2018).

The “fungal-like-organisms” are often referred to as water moulds, despite of their ubiquitous occurrence. They can be found in all kinds of habitats, continents and climate zones, for example in fresh water habitats, seawater and many more ecological niches while sometimes even showing an amphibious lifestyle (Patel *et al.*, 2018; Thines, 2018).

While there are lots of differences, similarities to fungi can be observed in their morphology and similar infection strategies (Fawke *et al.*, 2015). An often highlighted difference to real fungi is that oomycetic hyphae are rarely septated and coenocytic while fungal hyphae are septated most of the time and only some fungi develop coenocytic hyphae (Thines, 2018). Oomycetes are diploids during their vegetative life stage while fungi are, during most of their lifecycle, haploids, have cell wall micro fibrils primarily made out of glucans and cellulose instead of chitin, and undergo oogamous reproduction (Fawke *et al.*, 2015; Thines, 2018). Oomycetes reproduce asexually by wind or water dispersal of spores. The formation of Sporangia on a Sporangiphore results in the release of motile biflagellate zoospores. Sporangia and Sporangiphores differ among the oomycetes with their shape, mode of germination and their location in respect to their host tissue (Judelson, 2009).

The oospores, the result of the sexual reproduction, have thick walls and are haploid resting structures to overcome inhospitable conditions and enhance genetic fitness as this is the site where Meiosis and Karyogamy happens. Unique to Oomycota are their distinct female and male Gametangia, the Oogonium and Antheridium (Judelson, 2009).

An important feature of the oomycetes, distinguishing them from true fungi, can be found in their metabolism. Genome mining revealed that oomycetes have the genetic toolkit to produce enzymes to grow on a variety of carbon and nitrogen sources and to protect them from toxic compounds. The secondary metabolism, normally describing the production of metabolites that are not crucial for survival, is limited in the oomycetes compared to fungi. Most of the oomycetes are unable to produce pigments or to digest toxic xenobiotics (Judelson, 2017). In fungi proteinaceous mating hormones are employed for communication of sexual compatibility while oomycetes use secondary metabolites (Judelson, 2009).

Differences to fungi can also be found in the biochemical pathway of lysine synthesis, their ability to synthesize very long chain fatty acids de novo and in the sterol pathway (Archibald *et al.*, 2020). Sterols are essential components of membranes, important to control permeability and fluidity. Most oomycetes belonging to the *Peronosporomycetes* are sterol-auxotroph, such as *Pythium* and *Phytophthora*, as they acquire sterols through their pathogenic lifestyle (Dahlin *et al.*, 2017; Gaulin *et al.*, 2010). Recent studies in *Aphanomyces euteiches*, belonging to the *Saprolegniomycetes*, showed that they can synthesize fucosterol, just like brown algae, making them sterol prototroph and simultaneously strengthening the phylogenetic relationship between *Oomycota* and brown algae (Gaulin *et al.*, 2010). A loss of the SqE-genes, responsible for oxidosqualene synthesis, is responsible for the auxotrophy of some oomycetes while genes predicted to play part in the sterol synthesis de novo have been found in genomes of members of the *Saprolegniales* (Dahlin *et al.*, 2017).

1.1.2. Pathogenicity of oomycetes

Plant pathogenic oomycetes can exhibit hemibiotrophic, biotrophic or necrotrophic lifestyles, some even a combination of such. Obligate biotrophs, such as *Plasmopara halstedii* on *Helianthus annuus*, are completely dependent on the tissue of the host.

Many members of the phylum of *Oomycota* feed saprotrophically on plant or animal debris or as parasites on such. Their role as members of the decomposition cycle highlights their importance in different ecosystems as they are often among the first decomposers, clearing the way for secondary colonisers (Thines, 2018).

Oomycetes have evolved different infection strategies to parasitize their host and acquire the host's nutrients for their growth. The three main infection strategies include a necrotrophic lifestyle, a hemibiotrophic and a biotrophic lifestyle. Necrotrophic pathogens kill their host to feed on the tissue, this lifestyle is often associated with a broad host range and *Pythium ultimum* is a well-known necrotrophic oomycete that is able to thrive in soil or plant debris. Toxins or cell wall degrading enzymes are secreted to kill the host followed by the nutrient uptake by the pathogen. In contrast to that, *Phytophthora infestans* requires its host to be alive and at the end of the disease cycle changes to a necrotrophic lifestyle. This change of habit makes *Phytophthora infestans* a hemibiotrophic pathogen while at the same time the hemibiotrophic lifestyle leads to a less broad host range as the necrotrophic one. Biotrophic pathogens require their host to be alive and the pathogen will not damage the host in a detrimental way. This lifestyle is accompanied by a very narrow host range and an obligate biotrophy can be observed in *Helianthus annuus* and its oomycete pathogen *Plasmopara halstedii*. *Plasmopara halstedii*, as an obligate biotroph, can only grow on living tissue, axenical cultures are not established yet. To take up nutrients from their living host obligate biotroph pathogens have established a non-destructive relationship with their respective host, resulting in less severe symptoms (Ah-Fong *et al.*, 2019; Fiore-Donno and Bonkowski, 2021).

Genetic research on oomycetes has developed during the years. Genome sequencing and assemblies of different oomycetes have given insights into genome organisation, metabolic pathways and phylogenetic work (Schornack *et al.*, 2009). Work with *Phytophthora* species, who are feared pathogens, led to a better understanding of how oomycetes can parasitize their host plant without evoking plant defense mechanisms. During the past years CRISPR-Cas has facilitated and revolutionized genetic work with

Oomycetes and especially in *Phytophthora infestans* (Schornack *et al.*, 2009; Javed *et al.*, 2021).

1.1.3. Prominent oomycetes

The family of *Peronosporaceae* hosts some parasites who gained notoriety in the past. *Phytophthora* species are, in general, quite host specific such as *Phytophthora infestans*, a well-known and studied pathogen on *Solanum*. *Phytophthora infestans* is the causal agent for the late blight that caused the great potato famine in the 19th century, leading to the death of around a million people and the emigration of around two million people in Ireland. The great potato famine in Ireland in the 19th century and the loss of the majority of the potato yields many years in a row was facilitated by monoculture of a non-resistant potato variety. Until today *Phytophthora infestans* is regarded as a threat to global food security and it causes enormous economic losses every year (Binyam Tsedaley, 2014; Yoshida *et al.*, 2013). *Phytophthora ramorum* is the causal agent of the sudden oak death and around 100 species of hardwood are susceptible to the pathogen. Its host range is one of the largest within the *Phytophthora* spp. (Jennifer M. Davidson *et al.*, 2005).

In the genus *Pythium* many opportunistic plant pathogens, saprotrophic and necrotrophic strains can be found, causing root rot, a common and frequently occurring disease on crop plants while not being as host specific as *Phytophthora* strains (Hein *et al.*, 2009). While *Phytophthora* strains are mainly plant pathogenic, *Pythium* strains are pathogens on plants, algae and animals. This diverse host range is displayed in the genus of *Pythium* being a highly divergent heterophyletic group (Uzuhashi *et al.*, 2010).

What the *Pythiaceae* are less known for is their ability to act as biocontrol agents. In this concept the rapidly growing *Pythium oligandrum* strain shall compete in the rhizosphere by a direct approach with the potential pathogen over space and nutrients and by mycoparasitising the pathogen and excreting antimycotic compounds. Indirectly it can stimulate the plant defence mechanisms and promote plant growth all while not being harmful to the host. This provides an advantage especially in closed hydroponic systems where vegetables, crops and fruits are grown as the amount of fungicides used can be reduced (Vallance *et al.*, 2009). *Pythium* species reproduce via zoospores

that need surface water to move in. In hydroponic systems the requirements to grow are optimal for *Pythiaceae*, even though they are often referred to as soil-borne fungi due to the fact that their oospores can survive in soil for a long time, making it hard to reuse agricultural fields after an infection (Ho, 2018);(Vallance *et al.*, 2009; Thines, 2014).

Important animal-infecting diseases such as Saprolegniosis and Pythiosis are caused by different *Saprolegnia* strains and *Pythium insidiosum*. *Pythium insidiosum* infects mammals and causes very rare but often deadly infections predominantly in animals such as horses, rabbits and cats but humans as well. Since oomycetes in general are quite insensitive to existing fungicides and only few drugs directly targeted towards oomycetes exist, the therapies to overcome a Pythiosis are very aggressive and harmful, including amputations of diseased areas, for example a leg or an eye, and chemotherapy (Gaastra *et al.*, 2010).

Aphanomyces astaci, also belonging to the *Saprolegniales*, was introduced in the late 18th century to Europe by northern American cray fish who are resistant to the pathogen and act as vectors. Unfortunately European and Australian cray fish species are not resistant and *Aphanomyces astaci*, causing the crayfish plague, is a big threat to the existence of the European crayfish populations. Until today it is in the top 100 of the world's worst invasive alien species, eradicating native crayfish populations all over the world. *Aphanomyces astaci* is a fatal pathogen for European crayfish populations and is responsible for the decline of native crayfish populations all over Europe (Tuffs and Oidtmann, 2011).

Oomycetes are known to cause significant economic losses by infecting crop plants each year while treatments are rare. Greenhouses and hydroculture systems are frequently affected by severe infections of oomycetes (Timothy C. Paulitz & Richard R. Bélanger, 2001).

What oomycetes are less known for are the secondary metabolites they produce and their ability to produce fatty acids de novo (Sun *et al.*, 2013).

Even though the interest in combating those pathogens is huge and no agricultural important plant has developed an effective resistance yet (Fawke *et al.*, 2015), lots of knowledge is yet to be gained.

Oomycetes are a constant threat for agriculture (*Derevnina et al.*, 2016), therefore they are under research by many different research groups. Advances in genomics led to an understanding of how oomycetes parasitize their host and overcome plant defense

mechanisms. In order to keep their host alive while feeding on it and overcome barriers by the host defense mechanisms oomycetes secrete different effectors to their host (Fawke *et al.*, 2015; Jiang and Tyler, 2012; Judelson and Ah-Fong, 2019; Schornack *et al.*, 2009).

1.2. Fatty acids

1.2.1. Introduction to fatty acids

Biological macromolecules are grouped into four major classes (proteins, nucleic acids, carbohydrates and lipids). Fatty acids are part of the fourth group of biological components, the lipids. Lipids are a heterogenic group of molecules that are lipophilic and hydrophobic (Müller-Esterl and Brandt, 2009).

Fatty acids are carboxylic acids with an aliphatic chain and that can be saturated or unsaturated, depending on the occurrence of double bonds in the carboxylic chain. Most naturally occurring unbranched fatty acids have an even number of carbon atoms. Saturated fatty acids have no double bonds between their carbon atoms and unsaturated fatty acids can have one or more C=C double bonds. These double bonds are typically not conjugated and separated through a methylene group and are cis-configured. The amount of double bonds and the lengths of the carboxylic chain are substantial for the properties of the molecule. In general, if the chain is short and many double bonds are present, the fat is going to be liquid at room temperature, typically referred to as an oil. After the double bonds get hydrated and are saturated, they will be hard at room temperature, such as coconut oil for example (Müller-Esterl and Brandt, 2009).

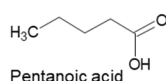
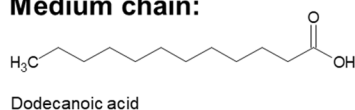
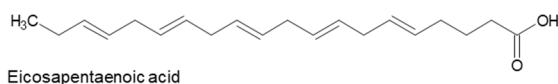
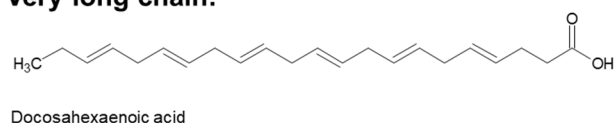
Short chain:**Medium chain:****Long chain:****Very long chain:**

Figure 2: Example of short, medium, long and very long chain fatty acids

Short-chain fatty acids typically have fewer than six carbon atoms, are not saturated and are crucial for gastrointestinal health. Pentanoic acid, visualized in Figure 2, also known as valeric acid, can be found in the plant *Valeriana officinales*. Medium-chain fatty acids have an aliphatic tail of six to twelve carbon atoms and are the easiest fatty acids to metabolize as the absorption, use and storage do not require additional energy. A well-known medium-chain fatty acid is dodecanoic acid or lauric acid, comprising half of the fatty acid content of coconut milk. Long-chain fatty acids have carbon chains from 13 to 21 carbon atoms and especially the polyunsaturated fatty acid eicosapentaenoic acid is an important precursor of eicosanoids in humans. Very long-chain fatty acids have 22 carbon atoms or more in their aliphatic tail and the most popular fatty acid in this group is docosahexaenoic acid. It is polyunsaturated and has an aliphatic tail with 22 carbon atoms. Saturated fatty acids have no double bonds in their carbon chain because they are saturated with hydrogen atoms. Hence, they are less likely prone to oxidise. Unsaturated fatty acids have one or more double bonds in their aliphatic tail as they have lost hydrogen atoms in a hydration process (Ahmad, 2017).

Typically the carbon chain consists of 14-24 carbon atoms while C16, palmitic acid, and C18, stearic acid, are the most prevalent ones in humans. Palmitic acid synthesis takes place in the cytosol while longer chain fatty acids will be synthesized and modified at the cytosolic membrane of the endoplasmic reticulum. Different ways of fatty acid classification exist and in the usage of different authors even mixed. In this

this is the most common classification will be used. Fatty acids are commonly classified based on the length of their carbon chain and the number of double bonds (Müller-Esterl and Brandt, 2009).

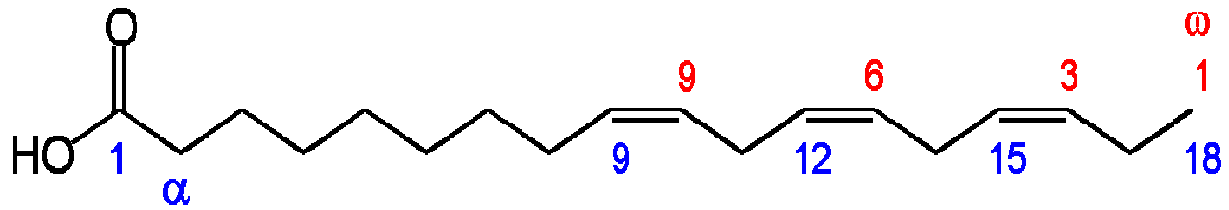


Figure 3: α -Linolenic acid C18:3 ω 3

In contrast to nucleotides, sugars or amino acids, lipids can form high molecular joints without developing covalent bonds (Müller-Esterl & Brandt, 2009).

The first carbon atom at the carboxyl-group end is numbered one and the carbon atoms are counted until the ω -end. The nomenclature of ω -3 fatty acids displays the location of the first introduced double bond, counted from the ω -end of the carboxylic chain. To clarify the location of double bonds the carbon atoms are counted starting from the methyl-group, the ω -end, to the first double bond. In the case of alpha-linolenic acid (Fig.3) there are 18 C-atoms and the first double bond starts at the third C-atom, counted from the ω -end (Rustan and Drevon, 2001).

Eicosapentaenoic acid and docosahexaenoic acid are both very long chain polyunsaturated fatty acids and essential for human diet and must be obtained directly or indirectly through other polyunsaturated fatty acids (Food and Agriculture Organization of the United Nations, 2010).

1.2.2. Functions of fatty acids

Fatty acids in general play important roles as they are involved in structural integrity, are important modules for energy production and conservation, are precursors in the synthesis of secondary metabolites, gene regulation and messenger molecules in the cellular communication (Devanadera *et al.*, 2019; Dolch *et al.*, 2017; Meyer *et al.*, 2004).

Especially important are ω -3 fatty acids as precursors of the eicosanoid family of signalling molecules such as prostaglandins, leukotrienes and thromboxanes (Wang *et al.*, 2013). As structural components of membrane phospholipids they are irreplaceable and, adding to that, they exhibit regulatory effects and physiological

activities. VLCPUFAs are an important factor for the integrity of membranes and cell walls. A special role comes to fatty acid in child nutrition as they are important for a normal development of the infant brain (Wang *et al.*, 2013). Recent studies even suggested anticancer properties of special fatty acids from marine oomycetes caused by the apoptotic and cytotoxic effects (Devanadera *et al.*, 2019).

Fatty acids are not soluble in water, which makes them an excellent energy saving resort as they don't influence the osmotic balance, and are amphiphilic. These storage lipids consist of three fatty acid molecules esterified with glycerine. Those triacylglycerins can form lipid droplets, up to 1 μM in size (Müller-Esterl & Brandt, 2009).

One of the main sources in human diet is cold water fish, even though new products coming from microorganisms such as krill are now on the market (Food and Agriculture Organization of the United Nations, 2010). Vegetarian products with linolenic acid (C18) are not sufficient as humans, as well as most animals and plants, have lost the ability to efficiently synthesize VLCPUFAs, except from breastfeeding woman (Food and Agriculture Organization of the United Nations, 2010). The overfishing of the seas, accumulated heavy metals and fat soluble pollutants in the fish caused by environmental pollution elevate the need for a new source of ω -3-fatty acids (Oliver *et al.*, 2020).

Oomycetes have the ability to produce very long chain polyunsaturated fatty acids (VLCPUFA) *de novo* instead of accumulating them via their diet, as almost all plants and animals need to do as they have lost the ability to produce VLCPUFAs during evolution (Pang *et al.*, 2015).

Fatty acids are essential nutrients in the human diet and the raised interest in such fatty acids is clearly tied to the increase of nutrition related chronic diseases (Food and Agriculture Organization of the United Nations, 2010). While extensive research has been done in this field studies show that low carb- and high-fat-and low fat- and high carb-diets are not correlated to beneficial health effects but correlations have been found between the high intake of around 250 mg/day of specific dietary fats, such as the polyunsaturated fatty acids EPA and DHA, and a low intake of easily digested carbohydrates and beneficial health effects such as a lowered risk of heart diseases, blood pressure, heart rate, triglycerides, likely inflammation, endothelial function, cardiac diastolic function, reduced risk of fatal CHD and sudden cardiac death (Food and Agriculture Organization of the United Nations, 2010; Oliver *et al.*, 2020).

Unfortunately it is not only necessary to consume enough ω -3 fatty acids, the ratio between ω -6 fatty acids and ω -3 fatty acids should be balanced and is a crucial factor for health. The full potential of health benefits resulting from an intake of ω -3 fatty acids can only be fully obtained if the ratio of ω -3: ω -6 is as low as possible. Consumption of ω -3 fatty acids was able to increase the formation of endogenous anti-inflammatory and pro-resolving lipid mediators while inhibiting the formation of pro-inflammatory eicosanoids derived from ω -6 fatty acids. Even though fats are energy-dense nutrients, they play a much bigger role than being just energy sources as they are more likely key nutrients, especially fatty acids, affecting early growth and development and at the same time nutrition-related chronic diseases later in life (Food and Agriculture Organization of the United Nations, 2010).

Defined mixtures of saturated fatty acids with monounsaturated and polyunsaturated fatty acids isolated from marine oomycetes even seem to have anticancerogenic properties following studies done by Devanadera *et al.* (2019).

1.2.3. Fatty acid profiles

Fatty acid methyl ester are transesterified fatty acids. In the presence of a catalyst, for example a strong acid or a strong base, a glyceride reacts with alcohol resulting in a mixture of fatty acid esters and alcohol. This reaction is reversible. When methanol is used as an alcohol the resulting product is called a fatty acid methyl ester (Eder, 1995). Fatty acid methyl esters are commonly found in biodiesel as they are, through the esterification, protected from oxidation and are not as corrosive as free fatty acids even when they are stored for a long time (Dahiya, 2020).

As fatty acid profiles from bacteria are very distinct and allow species determination based on fatty acid profiles, they might provide a utility to characterize and differentiate oomycetic species (Larkin and Groves, 2003; Augustyn *et al.*, 1991). Claims are that when factors such as incubation temperature, growth medium and storage on agar medium are kept consistent the fatty acid profiles are distinct, consistent and reproducible and allow differentiating individual isolates by their FAME profiles (Larkin *et al.*, 2003). The need to identify *Phytophthora* and other pathogens is necessitated by the potential threat those pathogens pose to agriculture worldwide in order to implement appropriate control mechanisms (Larkin *et al.*, 2003). Even though

characterization methods, for example genetic fingerprinting, are routinely used already, many of them are not able to clearly distinguish isolates because of minor genetic differences, which unfortunately do not display differences in potential epidemiological differences (Larkin *et al.*, 2003).

1.2.4. De novo synthesis of fatty acids

As mentioned, the loss of ability to produce VLCPUFAs is associated with the so called “more advanced taxa” and, since humans don’t have a $\Delta 12$ - or $\Delta 15$ -desaturase, they cannot synthesize ω -3 or ω -6 fatty acids de novo (Kihara, 2012).

Fatty acids derive from multiple condensation steps of C₂-units in the cytosol. Each C₂ elongation step is made out of a consecutive action of four steps, a condensation, reduction, dehydration and reduction, involving four different enzymes organized in a multifunctional complex, the fatty acid synthase. In this multi-enzyme complex the substrate is handed from one domain to the other, synthesizing palmitic acid from the precursors acetyl-CoA and malonyl-CoA with the help of NADPH. The synthesis of long chain fatty acids is located in the endoplasmic reticulum by membrane bound desaturases and elongases (Domergue *et al.*, 2003). Desaturases are comparable to oxygenases except for the fact that they do not transfer molecular oxygen directly to its substrate but use activated molecular oxygen to abstract a hydrogen atom from the carboxyl chain and create a double bond between two carbon atoms while releasing a molecule of water with the abstracted hydrogen atoms (Meesapyodsuk and Qiu, 2012).

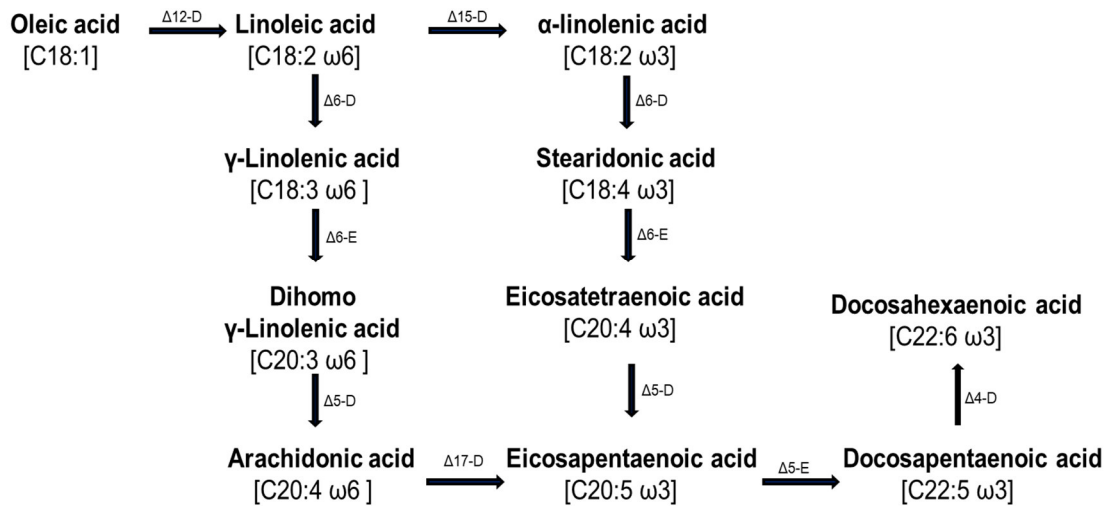


Figure 4: the aerobic-synthesis pathway of ω -3 Fatty acids

The oomycetic VLCPUFAs are de novo synthesized via an aerobic elongase/desaturase pathway (Figure 4). Starting from stearic acid the synthesis is mediated by the consecutive action of elongases and desaturases (Müller-Esterl & Brandt, 2009). The homeostasis of unsaturated fatty acids is achieved by a feedback regulation of fatty acid desaturase gene transcription through a signalling pathway (Wang *et al.*, 2013).

A study of Tu *et al.* (2010) showed, that the expression of key enzymes involved in VLCPUFA-synthesis is upregulated when the dietary level of PUFAs is low and downregulated when the PUFA-level is high. Those key enzymes involve a $\Delta 5$ - and $\Delta 6$ -desaturase and an elongase. The changes in gene expression did not however result in a changed amount of VLCPUFAs as the concentration of EPA and DHA seems to be controlled by available free substrates for the elongases and desaturases. The ω -3 VLCPUFA abundance seems to be regulated by the competitive interaction of distinct substrates involved in the synthesis than by alterations in the expression of key enzymes of the pathway (Tu *et al.*, 2010).

Substrate preference is dependent on the organism the desaturase derives from as they differ distinctively, for example the ω -3-desaturase from *Saprolegnia diclina* exclusively desaturates substrates with a 20 carbon atom chain and a ω -6 desaturation as its substrate (Wang *et al.*, 2013).

1.2.5. Enzymes involved in fatty acid synthesis

Membrane-bound fatty acid desaturases can be divided into three distinct clusters. These membrane-bound desaturases introduce double bonds into fatty acids that are either esterified as acyl-CoA or bound to the glycerol moiety of glycerolipids (Wang *et al.*, 2013).

In the first cluster the $\Delta 9$ -desaturases group together, the $\Delta 9$ -desaturase is the only desaturase that can be found in all living organisms. Since this desaturase can be found in plants, animals fungi and microorganisms it seems to be essential for life and the $\Delta 9$ -desaturase is thought to be the origin for the evolution of the different desaturases as the differences of these enzymes are based on the position of the double bond created. Phylogenetic research revealed that $\Delta 9$ -desaturases are the ancestors of all membrane-bound desaturases and the evolving $\Delta 12$ -desaturases are ancestral to ω -3-desaturases. Phylogenetic analysis supports the ω -3-desaturases originating from $\Delta 12$ -desaturases in a prokaryotic lineage. The second cluster contains methyl-end ω -3-desaturases originating in a prokaryotic lineage from a $\Delta 12$ -desaturase gene. The $\Delta 15$ -desaturase, the ω -3-desaturase and the $\Delta 12$ -desaturase are missing in higher plants and animals. The origination of the $\Delta 15$ -desaturase from a $\Delta 12$ -desaturase seems likely possible since the substrate of the $\Delta 15$ -desaturase is linoleic-acid, the product of the $\Delta 12$ -desaturase. In the 3rd cluster front-end-desaturases form a group including the $\Delta 5$ -, $\Delta 6$ - and $\Delta 8$ -desaturases. While $\Delta 5$ -, $\Delta 6$ - and $\Delta 8$ -desaturases share a same origin, $\Delta 5$ and $\Delta 6$ are paralogs. The independent acquirement of a cytochrome b5 domain by desaturases might have provided a selective advantage by an increased efficiency, ω -3 fatty acid desaturases lack this cytochrome b5-like domain though. Interestingly, comparing phylogenetic trees originated from desaturase genes reveals that the alignments of the desaturase genes are consistent with conventional species trees (López Alonso *et al.*, 2003).

The availability of precursors, for example alpha-linolenic acid (ALA), regulates the synthesis of very long chain polyunsaturated fatty acids instead of alterations on the transcription level. The higher the dietary amount of ALA is, the higher the EPA and DHA content will be. ALA and DHA rely on the same desaturase and compete while ALA has an advantage due to a slight substrate specificity of the desaturase for ALA (Tu *et al.*, 2010).

Elongation of polyunsaturated fatty acids has been linked to ELO-type genes which have been first characterized from yeast. ELO1 is involved in the elongation of medium chain fatty acids that are monounsaturated or unsaturated while ELO2 and ELO3 elongate long chain fatty acids. Nevertheless, the elongation of polyunsaturated fatty acids is poorly described compared to the elongation of medium chain or saturated fatty acids (Domergue *et al.*, 2003).

1.3. Scope of this work

Oomycetes are well known as destructive pathogens but considering their ability to produce long and very long chain polyunsaturated fatty acids they represent a potential source for eicosapentaenoic acid (EPA) and docosahexaenoic acid (DHA). EPA and DHA seem to have a beneficial effect on the human vascular system, have anti-inflammatory properties and are important for the infant brain development and have gained popularity as dietary supplements. Due to the overfishing and pollution of the seas, a new, clean source is needed.

Elucidating the pathway of the production of VLCPUFAs is an important step in order to understand and, in future work, utilize the findings.

The scope of this work is to combine results from traditional methods, like FAME-profiles, with the genetic background information supplied by genomic and transcriptomic data.

Elucidating the pathway and identifying the enzymes involved will lead to a better understanding and appreciation of oomycetes, which are mostly viewed as dangerous pathogens but can probably also be utilised for human wellbeing.

2. Material and Methods

2.1. Strains

The oomycetes used in this study were obtained either from the culture collection of Prof. Dr. Marco Thines or the CBS-KNAW culture collection (Westerdijk, Netherlands), and are detailed in table 1.

Table 1: List of the isolates used in this study

Name	Genus	Source
P100.31	<i>Pythium dissotocum</i>	Isolated by Lisa Nigrelli
P100.30		
P77.13		
P101.2		
P101.3		
P100.4		
P100.39		
V21.2	<i>Pythium flavoense</i>	Isolated by Lisa Nigrelli
P76.3	<i>Pythium oopapilum</i>	Isolated by Lisa Nigrelli
V2.4	<i>Pythium kashmirensense</i>	Isolated by Lisa Nigrelli
lev 1805	<i>Pythium ultimum</i>	Prof. Dr. Marco Thines culture collection
T30-4	<i>Phytophthora infestans</i>	Prof. Dr. Marco Thines culture collection
LT 7204	<i>Salisapilia tartarea</i>	Isolated by Lisa Nigrelli
P 2Z.2	<i>Phytophthora lacustris</i>	Isolated by Lisa Nigrelli
P 2Z.3		
P 2Z.5		
P100.18		
EMTS 1.2.1		
S7.1	<i>Phytophthora ramorum</i> CBS 111762	Westerdijk Fungal Biodiversity Centre (previously the Fungal Biodiversity Centre, CBS-KNAW)
Ph.ramorum		
EMTD 7	<i>Halophytophthora</i> sp.	Isolated by Lisa Nigrelli
EMTD 12		
EMTS 23		

2.2. Media

All oomycetes, investigated in this study, were grown on PDB-V8-medium containing 13.25 g Potato-Dextrose-Broth (Carl Roth, Karlsruhe, Germany), 10 ml of clarified V8-

juice (V8-Gemüsesaft, Alnatura, Birkenbach, Germany) and 7.5 g Agar-Agar (Carl Roth, Karlsruhe, Germany) per litre. In advance, the V8-juice was clarified by mixing with $10 \text{ g l}^{-1} \text{ CaCO}_3$, incubated for 30 minutes under permanent stirring, and centrifuged at high speed for 20 min at room temperature. The supernatant was transferred into a new tube. This process was repeated three times until the juice was translucent, and was subsequently stored at $-20 \text{ }^\circ\text{C}$.

After autoclaving at $121 \text{ }^\circ\text{C}$ for 21 minutes and a cool-down period to approximately $60 \text{ }^\circ\text{C}$ two antibiotics were added. While Rifampicin (Carl Roth, Karlsruhe, Germany), which was used at a final concentration of $30 \text{ } \mu\text{g ml}^{-1}$, is directed against bacteria, Nystatin (Carl Roth, Karlsruhe, Germany) is a fungicide, used to inhibit growth of Fungi, and was used at a final concentration of $50 \text{ } \mu\text{g ml}^{-1}$.

Pure cultures of the isolates were cultivated in 6 cm petri dishes (Avantor, Radnor, Pennsylvania, United States) at room temperature for 3-5 days and stored in the fridge until they were needed. Fresh mycelium was generated by cutting out cubes of around 0.5 cm side length from the active edge of the mycelium and transferring it to a fresh PDB-V8-plate by using a sterile inoculation loop in a microbiological safety cabinet (MSC). The plates were sealed with Parafilm (Avantor, Radnor, Pennsylvania, United States) and grown in the dark at room temperature.

2.3. Genomic DNA isolation

Genomic DNA isolation was performed according to a protocol of McKinney *et al.* (1995) with slight modifications as detailed below.

Mycelium from approx. 0.5 cm^2 was harvested and grinded with liquid nitrogen in a pre-chilled mortar for around 15 minutes. Care was taken that the sample did not thaw. Subsequently, the sample was transferred to a new 2 ml-tube and 200 μl of extraction buffer (50 mM TRIS pH=8, 200 mM NaCl₂, 0.2 mM EDTA, 0.5 % SDS) supplemented with 5 μl RNase A ($20 \text{ } \mu\text{g ml}^{-1}$) was added. The sample was thoroughly vortexed and incubated at $37 \text{ }^\circ\text{C}$ for 30 minutes in a Peqlab Thriller (Avantor Radnor, Pennsylvania, United States), while inverting the tubes every five minutes manually. Subsequently, 25 μl of Proteinase K (20 mg ml^{-1}) was added and the mixture was incubated for additional 15 min at $37 \text{ }^\circ\text{C}$ in the Peqlab Thriller as detailed above. 200 μl of phenol chloroform/isoamylalcohol (Roti Phenol/chloroform/isoamylalcohol 25:24:1, Carl Roth,

Karlsruhe, Germany) was added and the tube was inverted for ten times or until the sample was completely mixed. The aqueous and hydrophobic phases were separated by centrifugation for two minutes at maximum speed in an Eppendorf 5430R centrifuge (Eppendorf, Hamburg, Germany). The aqueous layer was transferred into a new 2 ml-tube after which 200 μ l of chloroform/isoamylalcohol (Roti C/I 24:1, Carl Roth, Karlsruhe, Germany) was added. Centrifugation was repeated as described above. Again, the aqueous layer was transferred to a new 2 ml-tube and 5 μ l RNase A (20 μ g ml⁻¹) was added to remove any residual RNA. The mixture was incubated for 30 minutes at 37 °C in the Peqlab Thriller. 18 μ l of 3 M sodium acetate and 400 μ l (two volumes) of absolute ethanol was added to precipitate the nucleic acids. The precipitated DNA was pelleted by centrifugation at 6000 g for ten minutes at 4 °C in the prechilled centrifuge. To remove the salts from the precipitated DNA, the pellet was washed twice by adding 500 μ l of 70 % ethanol and centrifugation at 6000 g for five minutes. Any residual ethanol was removed by pipetting off and the pellet was air dried. The pellet was resuspended in sterile dH₂O and stored at -20°C until further usage. The integrity of the DNA was checked by gel electrophoresis in a 0.5 % agarose gel stained with ethidium bromide. The DNA amount was quantified by using a Qubit 1 fluorometer with a dsDNA HS assay kit (Invitrogen, Carlsbad, California, United States).

2.4. RNA isolation

Total RNA for transcriptome sequencing was isolated from fresh mycelium using the Nucleospin® RNA plant kit from Macherey & Nagel following the manufacturer's instructions.

Total RNA amount was determined by using a Qubit fluorometer 1 with a Qubit RNA HS assay kit (Invitrogen, Carlsbad, California, United States).

2.5. DNA Amplification

The DNA was amplified using the polymerase chain reaction (PCR). The polymerase chain reaction involves three steps, first the denaturation of the DNA separating the double helix of the DNA. The annealing is the second step where the oligonucleotide primers anneal to the single strand DNA followed by the third step, the elongation, in

which the Taq-polymerase synthesizes the complementary DNA strand starting from the annealed oligonucleotide primers.

The amplification reactions were carried out using a volume of 25 μ l and genomic DNA between 1-10 ng. For an amplification reaction 1x Mango Taq PCR buffer, 0.2 mM dNTPs, 2 mM MgCl₂, 0.8 mg ml⁻¹ BSA, 0.4 mM forward and reverse primers and 0.5 Units Mango Taq Polymerase (Bioline GmbH, Luckenwalde, Germany) were combined with the DNA. The mixture was placed in a Master cycler pro (Eppendorf, Hamburg, Germany) equipped with a vapo.protect lid using an initial denaturation at 94 °C for 4 min followed by 28 cycles of denaturation at 94 °C for 40 s, a primer-specific annealing temperature for 20 s, and an elongation step at 72 °C for 30-60 s and a final elongation at 72 °C for 10 minutes.

For the identification of species the internal transcribed spacer oligonucleotides were used, the reverse primer LR0 is a reverse complement to LR-0R described by (Moncalvo *et al.*, 1995) and the oomycete specific forward primer DC6 was described by (Cooke *et al.*, 2000) used with an annealing temperature of 55 °C.

To verify the sequence of the enzymes involved in the fatty acid synthesis Ranger Taq Polymerase (Bioline GmbH, Luckenwalde, Germany) was used due to its proofreading activity and the ability to produce long DNA fragments. Specific oligonucleotide primer were designed using Primer3 (Untergasser *et al.*, 2012) and are shown in Table 2 with their respective annealing temperatures.

A 12.5 μ l PCR reaction was set up with 1x Ranger Taq buffer, 0.375 μ M forward and reverse primer and 0.13 U of the Ranger Taq polymerase. The conditions for the two-step PCR are as follows: an initial denaturation step at 95 °C for 3 min, 28 cycles of a denaturation at 98 °C for 20 s, annealing and elongation combined at 60 °C for 8 min, and a final elongation for 10 min.

2.6. Oligonucleotides used in this study

All oligonucleotide primer used in this study (Table 1 and 2) were purchased from Sigma-Aldrich (St. Louis, Missouri, United States).

The nucleotides in table 2 were used to verify the sequences of the enzymes used in the synthesis of poly-unsaturated fatty acids derived from the genome assembly. The oligonucleotides were designed with Primer3. (Untergasser *et al.*, 2012)

The oligonucleotides from Table 3 were used for the identification of isolates.

Table 2: Oligonucleotides designed for sequence verification

Name	Genlocus	Orientation	Sequence [5' -> 3']	
ab1	Δ 6-elongase	forward	ACATGAGAATCTTGGCCTTCTTAC	
ab2		reverse	TACATCAGGTCTACTACGTTGTGT	
ab3		forward	CATTCTCGAGTTTGGCATCTTCTC	
ab4		reverse	GTGGAAGAAGTACCTGACCATCAT	
ab5		forward	TGTAGAATCAAGAAGCTCATCGTC	
ab6		reverse	GTCTCATTTTGTCTACGGATCGA	
ab7	Δ 12-desaturase	forward	GCCTTTCTCACTTGTCTCTTTACA	
ab8		reverse	GTTCTACCACCTCTTCAAGAACG	
ab9	Δ 5-desaturase	forward	ACGAACCCATCCACAAGACT	
ab10		reverse	TCTGCATACCACGGTCTCAG	
ab11		forward	CCTGTGGATTTCAACCGCAA	
ab12		reverse	TCTCAAACCTCTTCGCTCGT	
ab13		Δ 6-desaturase	forward	CCATGGACGAAGACTTGCTG
ab14			reverse	AAGGAGTTCGACATCCCGTT
ab15	forward		AATGACGGAAGGAGGAGGC	
ab16	reverse		GGAGCACCCCTGAAAAGTTGG	
ab17	forward		CAGCGAGCTCTTGACGTTAC	
ab18	reverse		AAGATCAAGTCCATGGGCCT	
ab19	Δ 15-desaturase	forward	TCGGGTCCGGTGTAGATTGAG	
ab20		reverse	CATCGTCATGTGTTTCGCTGT	
ab21	Δ 4-desaturase	forward	ATTGTGGGGCTACTGGAGTT	
ab22		reverse	GCACGATCATGGGGTTCTC	
ab23		forward	CACATCCAACGCGACTACAG	
ab24		reverse	GACAAGATCCACTCGCGTTC	
ab25	Δ 6 elongase	forward	GCACTCGACGCAACCA	
ab26		reverse	TCCAGTTCACGACGCCT	
ab27		forward	GACGCAACCATGACTC	
ab28		reverse	CGTCGTGCCATTATGA	
ab29	Δ 5-desaturase	forward	CAGTTCACCTTCACGC	
ab30		reverse	CAAGTACACCGTGCTG	
ab31	Δ 15-desaturase	forward	GCTAGTTCTTGCACGG	
Name	Genlocus	Orientation	Sequence [5' -> 3']	
ab32	Δ 6 elongase	reverse	TGGGCGTGTACTACTG	
ab33		forward	CTCATTCTCGAGTTTGC	
ab34		reverse	TCTGCTCGTACATGTG	
ab35		forward	CGAGGATCTTGGACAG	
ab36		reverse	CGCCTGAGTCTGTATC	
ab37		Δ 12-desaturase	forward	CGTCGACTACCTCTTC
ab38	reverse		CTACCTCGTGCTCATC	
ab39	forward		CCAACTCTACTGGTTCG	
ab40	reverse		CAAGTACAACGGCAAG	

ab41	$\Delta 5$ -desaturase	forward	ATGTTGTGCTCACCTC
ab42		reverse	CCAGGACATCTTCGAG
ab43		forward	CGACGTA CTTCAGTA
ab44		reverse	CAATTCCAGTGGACGA
ab44b		reverse	TCCATTTCCACACTCG
ab45		forward	CTCACGACCAAGTTCT
ab46		reverse	GGTACTTGGCCTTCAA
ab47		forward	AGTTGTGCGAGTAGTC
ab48		reverse	ttgatG TTCAGGCGAA
ab49	$\Delta 6$ -desaturase	forward	CATCCACCCATCCATC
ab50		reverse	CCTGCTGATCCACTAC
ab51		forward	GTAGTGGATCAGCAGG
ab52		reverse	GTTGGTACTCTGCACA
ab53	$\Delta 15$ -desaturase	forward	GAGTTCCATCATCGCT
ab54		reverse	GATCTTCTACCCGCAG
ab55		forward	AGAAACGTACCAGCTC
ab56		reverse	CTGTGATCTGGAGAGC
ab57	$\Delta 4$ -desaturase	forward	ATTTCAAGTCCACGGG
ab58		reverse	GAAGACCTGGAAGACC
ab59		forward	TTCAAGCGATACCACA
ab60		reverse	ACGCTCCACA ACTTG
ab61	$\Delta 12$ -desaturase	forward	TCTTGTAGAACACGACCTTG
ab62		reverse	TTCTTGGTCACAGGGAAAC
ab63		forward	CAGCATGAGGAAGATCTTGT
ab64		reverse	GACAAA ACTTACACCCTTGC
ab65		forward	CTTGAAGAGGTGGTAGAACG
ab66		reverse	CAGACCCACGGCAATTC
ab67		forward	CAGCACGGTCATTACGGC
ab68		reverse	CTTAAAGCTGACACGGGCAG
ab69		forward	GGCCGTGTTCAAGTTCTACC
ab70		reverse	TTGCGACCACCAACTCTACT
ab71		forward	TTGGTTTGGATTGGACTGCG
ab72		reverse	GACCCTCCACAAGTCTTCA
ab73	$\Delta 5$ -desaturase	forward	TTCGTGCGGTGGTAGT
ab74		reverse	GCATCAGCGCATGGAA
ab75		forward	CATTTGAGCGCGTGGA
ab76		reverse	TTGTTCCCGGGTGTGT
Name	Genlocus	Orientation	Sequence [5' -> 3']
ab77		forward	CTCGTGTTGTGGTGACC
ab78		reverse	AGTTCTGGGGCGTGTT
ab79		forward	ACGACTTGACCTGCGA
ab80		reverse	TTACACCAACGTCGCG
ab81		forward	ATGGTCGCGAGGTTG
ab82		reverse	TGCGGTTGAAATCCACA
ab83		forward	TGTTGTGCTTGGCCAC
ab84		reverse	CGTGTGTGCTGCTTGT
ab85	$\Delta 6$ -desaturase	forward	GTGAGATGGCTTCAGTT

ab86		reverse	GATGAGGTGAAGAGAAGT
ab87		forward	CAAATAACCACTCTCGC
ab88		reverse	ATATTGCCTCAAAGCG
ab89		forward	GACATCCGGACGATTG
ab90		reverse	CATGGACTTGATCTTGAC
ab91		forward	CTGGACCAGTTCTACATC
ab92		reverse	CCGATGCTGAACACCA
ab93		forward	TACTTTGCCGGTATGAG
ab94		reverse	AGTCGAGTGCCTTTATT
ab95		forward	GTCTGTATCCCATCAGTC
ab96		reverse	GCTTTCTTCTTCAACACC
ab97		forward	CCAACGCTCTGAGATC
ab98		reverse	GAGAAGATCCATCCCATC
ab99	Δ 15-desaturase	forward	CGAAGATTTGATTCCCG
ab100		reverse	TGGCGAATAGGAGCGT
ab101		forward	GATGGAGAGCTGTACAC
ab102		reverse	CCGATACTGGCTAGATC
ab103		forward	ATCCGCAGCTAGTCGA
ab104		reverse	ATAGGTTAGAATAGGGCG
ab105		forward	TACCTATCCAGTCCATTG
ab106		reverse	TGATCCAGTCATATACGG
ab107		forward	CAGGACGAGATCTTCTAC
ab108		reverse	GGTGTAGATTGAGTGTTG
ab109		forward	TCTTAGTATGAGCCCTTC
ab110		reverse	GACACTAACACGAACAC
ab111	Δ 4-desaturase	forward	CTGATGTAGAGCCAAATG
ab112		reverse	GGTACAACAACCTTACCTG
ab113		forward	ATCGTTGGTGATTTTGG
ab114		reverse	GCTTAGAGGAAAGAGAGG
ab115		forward	CTTCCTTCCCTTCCACTC
ab116		reverse	TTGAGGATCCCGTAGTA
ab117		forward	CTCTTCTACCTGCTCTTC
ab118		reverse	ACAAGACGCAGATCTC
ab119		forward	AATGTCTCTCTGTCTCAG
ab120		reverse	GAGAACGGCATTATTGAC
ab121		forward	TTTCGTGAACTTGAAGC
ab122		reverse	AGTATCATTCCGTTCCC
Name	Genlocus	Orientation	Sequence [5' -> 3']
ab123		forward	GTGGTGTA AACAGACAG
ab124		reverse	CACGACAAGTACTGGG
ab125		forward	CTCGTCAACCCAAAGA
ab126		reverse	CTGTCAATAATGCCGTTT
ab127		forward	GCAACGACATCATCATC
ab128		reverse	GAGATCTGCGTCTTGT
ab129	Δ 15-desaturase	forward	GTTAGAAGACGAAGGAAG
ab130		reverse	GTAGTATGTTGTCTGACG
ab131		forward	TGATCCAGTCATATACGG

ab132		reverse	GAATCCTTCCACGGTC
ab133		forward	GTTGAGCAGGTGGTAG
ab134		reverse	CTCCACAGTCATTTTCG
ab135		forward	CAACGTTGGAGGATTTAG
ab136		reverse	TTTCTGTGATCTGGAGAG
ab137	$\Delta 6$ elongase	forward	AATAGCCCACAAGCCC
ab138		reverse	TGAGCATTGGGAAGACC
ab139		forward	TACCTTGTCCAGTTCTAC
ab140		reverse	AAGCAGGTTGACACAAT
ab141		forward	TTGATGCGAGCTCTTG
ab142		reverse	AGACCTTGTACTGGCC
ab143		forward	TCCCAACGTAATACTGAG
ab144		reverse	CGTTCAGGATGATGGT
ab145		forward	TGCTGTACCTGTTCTTT
ab146		reverse	GTGGCTTCAATATCGTAC
ab147		forward	CATTATCCACTGTGTAGC
ab148		reverse	AAGGGGTCTCTCTCTC
ab149		forward	CTTGAGAAGCTCCACA
ab150		reverse	GTCCAGGAAGAGCATG
ab151	$\Delta 12$ -desaturase	forward	GATACAGAGACCGAGTC
ab152		reverse	ATGACGAATGGATGGG
ab153		forward	GATAGGTTGGAGATGGAA
ab154		reverse	ACAGTACAGTAGGCTAAC
ab155		forward	ATGTGGGACTCGTCTT
ab156		reverse	GAAGAACCAGTAGATCGG
ab157		forward	CTTCGAACGCTCCATC
ab158		reverse	GAGAAGATGTGGTGGG
ab159		forward	TCAAGTTCTACCTCGTG
ab160		reverse	TCTTCCAGTACAAGACG
ab161		forward	CTCACCTTCTTCCCTTTA
ab162		reverse	CAGTTTCAGCGTGTATC
ab163		forward	GTTGAGTTGACGTTGAC
ab164		reverse	GCTCTCATGGTCGTAG
ab165	$\Delta 5$ -desaturase	forward	GTAGTCGTTTCGATCTTCT
ab166		reverse	CTACAAATCCAAGCTCTC
ab167		forward	CGGAGACCAACATCAA
ab168		reverse	CATGTTTCATGCCTTGG
Name	Genlocus	Orientation	Sequence [5' -> 3']
ab169		forward	GAGGAGCCAGGCAAAT
ab170		reverse	CTCTCTATGGCGTGCT
ab171		forward	GATGTAGATGCGGTAGAA
ab172		reverse	CTCGTGTTTCATGGTCG
ab173		forward	GGTTTCCAGGGATGAG
ab174		reverse	TAAGAGCCAAACCAGATC
ab175		forward	TGTTTAGTGGCCAATGA
ab176		reverse	GGTGAACCTCTCGTAC
ab177	$\Delta 6$ -desaturase	forward	GTGAGATGGCTTCAGTT

ab178		reverse	CAACGTTTCGATTGGATAG
ab179		forward	ACTTCTCTTCACCTCATC
ab180		reverse	CATGAGAACGAGGAGATA
ab181		forward	CAGTTCCACAGTATACAC
ab182		reverse	ATGACGTTGTTCCAGTA
ab183		forward	CGATCATGGGTCTGTT
ab184		reverse	GTTCCCTGTTATCAATCG
ab185		forward	TCCAAGGAGTTCATCAC
ab186		reverse	TGTTCCAGATCTTCGTC
ab187		forward	TCACTCGCAACATAAAC
ab188		reverse	CTTGCTAGACGATGCT
ab189	$\Delta 6$ elongase	forward	TTAAGAATCTGTCCAGGG
ab190		reverse	ATGATCCAGTTCCTCAC
ab191		forward	TACATGACTGGGATCTTC
ab192		reverse	GTTTCTCTACAACCCTCT
ab193		forward	GCTGCTTCCACTTCTT
ab194		reverse	TAGAGACCGAGAACATTC
ab195		forward	TACCTTCTCAGTGCCG
ab196		reverse	GGGCGTAACAGTGACT
ab197	$\Delta 12$ -desaturase	forward	TCATCACTGCATCCTG
ab198		reverse	GAAAATGCTAGAGTGACC
ab199		forward	TTGGTTTGGATTGGACT
ab200		reverse	CACAAGTCTTCATCACTC
ab201		forward	ACCACATCTTCTCCAAG
ab202		reverse	ATTGATAAGACCCAGAG
ab203	$\Delta 5$ -desaturase	forward	AGAGAAAACCACCAGAG
ab204		reverse	GACAAAGTACTCGTTCAC
ab205		forward	TTACACCAACGTTCGCG
ab206		reverse	CAAAGAACGTTCGTGATC
ab207		forward	AGTGTGAGTATCCGAAC
ab208		reverse	AGGGAAGAACTGGAAG
ab209	$\Delta 6$ -desaturase	forward	ACTTCTCTTCACCTCATC
ab210		reverse	AAGATTCCAACGGTCC
ab211		forward	TATCTCCTCGTTCATG
ab212		reverse	CATCTCCTTGCTCCAC
ab213		forward	GTTTCTGATCAAGCACC
ab214		reverse	TTCCACTACTACTGTACG
Name	Genlocus	Orientation	Sequence [5' -> 3']
ab215		forward	TCCCGATCAAGGCATT
ab216		reverse	GAGTTCGTTGCTGCTG
ab217	$\Delta 15$ -desaturase	forward	CTACGACCAAGACAGATA
ab218		reverse	ACGTTGGTTGTTGTTG
ab219		forward	CTTGATCTCCGTGAGC
ab220		reverse	GTTTGGACGAAGATTGAT
ab221	$\Delta 4$ -desaturase	forward	CGTAGAGTGTGGTCA
ab222		reverse	TACTTGGCCATGATGAG
ab223		forward	TCTAAGCCACTTCGTATT

ab224	reverse	GTTCCGGAGTCTAGTCAG
ab225	forward	CTCTTCTACCTGCTCTTC
ab226	reverse	GAATGGGAGAGATGGAG

Table 3: Oligonucleotides used to identify isolates

Genlocus	Primer name	Source		Primer sequence
28 S rRNA	LR0	reverse complement of LR-OR von Moncalvo et al 1995	fw	GCTTGAGTTCAGCGGGT
	DC6-F	modified primer DC6 designed by (Cooke et al. 2000)	rev	GAGGGACTTTTGGGTAATCA

2.7. Phylogenetic analysis

For the reconstruction of phylogenetic relationships multiple different markers are available. Loci from the nuclear as well as from the mitochondrial genome can be used to resolve the genetic relationship of organisms.

For this study, the internal transcribed spacer region was chosen, amplifying parts of the 18S rRNA, the 5.8 S rRNA and the highly variable internal transcribed spacer regions (ITS1, ITS2) between these two genes. The internal transcribed spacer was chosen because it is a commonly accepted molecular barcode in the oomycete and mycological community, it is able to identify organisms to species level, and exhibits a large number of reference sequences in public databases.

Sequencing was conducted by the laboratory centre of the Senckenberg Biodiversity and Climate Research Centre (Frankfurt am Main, Germany) after diluting the PCR reaction to the DNA concentration requested by the facility.

Using the software Geneious (Geneious version 9.1.8, www.geneious.com) forward and reverse sequences were assembled and poor-quality ends trimmed. From GenBank (<https://www.ncbi.nlm.nih.gov/Genbank/>) similar, representative reference sequences were downloaded by using the nucleotide database search blastn (Altschul *et al.*, 1990). Subsequently, all of the sequences were aligned with MAFFT version 7 (Kato *et al.*, 2002), a multiple alignment program for amino acid or nucleotide sequences. The alignment was done with the default values with slight modifications,

the direction of the sequence was adjusted according to the first sequence and using the G-INS-i-alignment method. The resulting alignment was used to calculate a phylogenetic tree with the program MEGA 6 (Tamura *et al.*, 2011) using the Minimum Evolution algorithm with the Tamura-Nei model, and 500 bootstrap replicates. The Minimum evolution algorithm calculates a tree based on the assumption that the shortest sum of the tree branches is the correct one.

2.8. FAME profiles

The whole-cell fatty-acid-methyl-ester analysis (FAME) was done by using gas chromatography combined with a mass spectrometer of N-methyl-N-(trimethylsilyl) trifluoroacetamide (MSTFA) derivatized fatty acid methyl esters.

The fatty acid methyl ester were prepared as describe below:

Mycelium of each respective strain was grown at either 20 °C or 27 °C in 9 cm petri dishes on PDB-V8-medium supplemented with Rifampicin and Nystatin as described above. The oldest and youngest part of the mycelium was discarded as depicted in Figure 5.

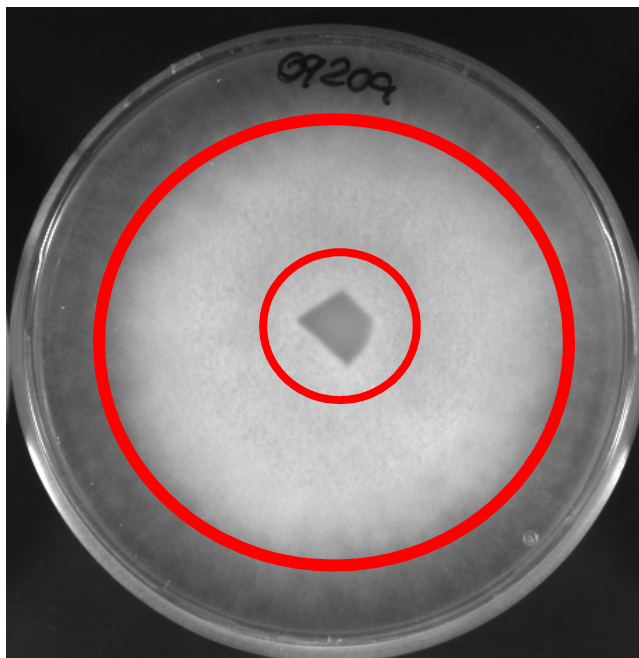


Figure 5: Visualization of the mycelium used for the FAME analysis. All mycelium within the inner circle and outside of the outer circle were discarded.

The mycelium between the two red circles was used for fatty acid methyl ester analysis. For most of the oomycetes the mycelium grew very densely and could be pulled off the

agar easily. With a sterile inoculation loop remaining agar pieces were scraped off to remove as much Agar-agar from the mycelium as possible. The mycelium was stored at -20 °C after collection until the esterification process.

The collected samples for the fatty acid methyl ester analysis were first transferred in a 1.8 ml glass vial and dried until no more liquid residues were visible, and the sample appeared to be dry.

To the dried sample 500 µl of the FAME-solution (methanol / toluene / sulfuric acid 50:50:2 V/V) was added and the vial was closed with a Teflon seal. The sealed vial was shortly vortexed until the solution takes on the colour of the sample and was subsequently incubated at 55 °C overnight.

After the incubation, the samples were cooled down to room temperature and 400 µl of the Destroyer reagent (0.5 M NH₄HCO₃, 2 M KCl) was added. Because a precipitate might form, or gases (Carbon dioxide) might emerge the vial was kept open and only after a possible emergence of gas the vial was closed and vortexed again. Subsequently, the solution was centrifuged at 20 °C for 5 minutes at 4000 – 5000 rpm. 75 µl of the supernatant, the organic phase, which contained the fatty acids, was transferred in a GC-vial and 25 µl of the MSTFA solution (N-Methyl-N-(trimethylsilyl) trifluoroacetamid) was added. The mixture was incubated at 37 °C for 30 minutes and afterwards injected into an Agilent 7890A Gas Chromatograph implemented in an Agilent 5975C Series GC/MSD (Agilent, Santa Clara, USA), which allowed the quantification of the substance by the integrated mass selective detector.

The program “Automated Mass Deconvolution and Identification Software” AMDIS (version 2.64) was used to identify the different fatty acids, which had been detected by the GC/MS, by comparing the retention time of the fatty acids of interest to the retention times of known fatty acids, which were obtained from a reference library.

After the analysis of the fatty acids of the different oomycetes, one strain was chosen for further investigation by taking the amount of long chain fatty acids and the growth rate into account equally. From all investigated organisms *Pythium dissotocum* strain P100.30 produced both, a high amount of Eicosapentaenoic acid and it grew very fast, and was therefore chosen for the following tests.

For the complete genome and transcriptome sequencing the strain P100.30 was grown at 20 °C for 5 days on PDB-V8-medium in the dark until the first hyphae reach the edge of the plate. The oldest and youngest mycelium was discarded as described earlier. The DNA and RNA were extracted as described earlier.

The isolated RNA and genomic DNA was sent to a LGC genomics (Hoddesdon, Herts, United Kingdom) and sequenced on Illumina sequencing platform using paired end sequencing of shotgun libraries with a read length of 100 and insert sizes of 300 bp and 800 bp and two long jump distance libraries of 3000 and 8000 bases. The RNA was sequenced using the Illumina RNASeq platform.

2.9. Genome assembly

Genome assembly of the *Pythium dissotocum* strain P100.30 was done by Deepak Kumar Gupta. Transcriptomic data was assembled by Dr. Rahul Sharma.

2.10. Identification of enzymes involved in fatty acid synthesis

In order to identify the enzymes involved in the fatty acid synthesis the gene ontology table was used to find domains typically present in protein sequences involved in elongation or desaturation of fatty acids. If such domains were found the putative proteins sequences were checked for Interproscan IDs in the gene ontology table. The gene coordinates derived from the gene ontology table were checked with the program Bioedit and sequences of the putative proteins were extracted. The putative protein sequence was analysed with InterproScan to check for protein domains typically found in elongases and desaturases. Additionally, the sequence was blasted to the NCBI-website to check for similar protein sequences. For the sequences found Oligonucleotides were designed based on the genome sequence of said protein to verify the sequence, shown in Table 2.

The results of the verification, the sequenced PCR-results, were compared to the CDS and compared to the transcriptomic data.

2.11. Analysis and characterisation of fatty acid elongases and desaturases

After the verification of the sequences and transcripts of the enzymes involved in fatty acids the remaining six enzymes were blasted to the NCBI-website to check for similar

enzymes in other organisms. The verified sequences of the five desaturases and the elongase were then, to search for and to classify protein families, analysed with Interproscan (Jones *et al.*, 2014).

Protein sequence alignments were made with Geneious R9.1.8 (www.geneious.com) with the MAFFT alignment using the blosum 62 scoring matrix with a gap open penalty of 1.53 and the offset value of 0.123 (Kato *et al.*, 2002). The conserved motifs in the protein sequences were searched in Geneious R9.1.8 with the embedded search tool based on the EMBOSS 6.5.7 tool fuzzpro (Rice *et al.*, 2000).

2.12. The pathway of the synthesis of very long chain polyunsaturated fatty acids

The pathway of the synthesis of polyunsaturated fatty acids was retraced by combining the fatty acids found in the FAME profiles with the enzymes detected in the genomic and transcriptomic data.

3. Results

3.1. Phylogenetic analysis

In the start of the study a phylogenetic reconstruction of the species to be analysed was conducted in order to classify them. After the isolation of the DNA a PCR with ITS primers was done and reference sequences from GenBank (Clark *et al.*, 2016) were used to facilitate the identification. Those sequences were added to the alignment with which the phylogenetic tree was calculated from.

In the tree shown in Figure 7 it is evident that the strains annotated as *Pythium* strains belonged to a highly divergent group. Four new genera have previously been described and separated from this group, named *Ovatisporangium*, *Elongisporangium*, *Pilasporangium* and *Globisporangium* (Uzuhashi *et al.*, 2010). The *Pythium ultimum* isolate, now *Globisporangium ultimum*, belonged to one of the separated groups. The previous separation was supported by the phylogenetic analysis done in this study with strong support.

Pythium dissotocum and *Pythium oopapillum* strains were closely related as the genetic difference is small. This close phylogenetic relationship was displayed in their similar growth patterns as well. Even though P100.30 and its close relatives matched to *Pythium coloratum*, *Pythium lutarium* as well as *Pythium dissotocum*, morphological as well as further phylogenetic investigations clearly identified P100.30 as a *Pythium dissotocum* strain.

Close relatives of the *Pythium dissotocum* strains were the *Pythium sp.* strains while *Pythium kashmirensis* strains were on the opposite branch, both of these *Pythium* species grew noticeably slower than the *Pythium dissotocum* and *oopapillum* strains. The *Saprolegnia bulbosa* sequence, clustering within the *Pythium* species complex, was retrieved as a reference sequence from Genbank. A BLAST search back to the dataset of GenBank was done and showed highly similar sequences matching to the *Saprolegnia* sequence labelled as *Pythium sp.* and *Pythium insidiosum*. The result of the search and the clustering of a *Saprolegniomycete* within the *Peronosporomycete* species complex were clear indications for this sequence being incorrectly identified and labelled.

Most of the *Phytophthora* isolates used in this study belonged to *Phytophthora lacustris* and were, grouped together, the sister clade to *Phytophthora ramorum*.

Phytophthora infestans were clearly separated from the *Phytophthora lacustris* strains. *Phytophthora infestans* was closer related to *Phytophthora parasitica* while the *Halophytophthora* strains were clearly separated from all the other *Phytophthora* strains.

The *Salisapilia tartarea* strains were clearly distinguished from the rest of the *Peronosporomycetes* regarding their phylogenetic relationship and their different growth rates and patterns. When grown axenically the *Salisapilia tartarea* strain LT7204 grew into a flower-like pattern shown in Figure 6.

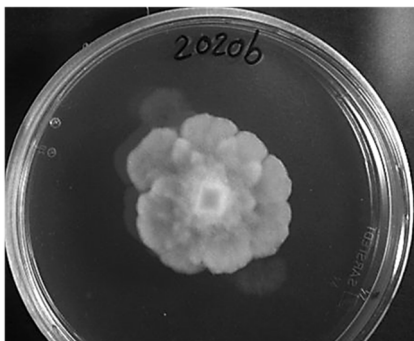


Figure 6: Axenical growth pattern of the *Salisapilia tartarea* strain LT7204 on PDB-agar at 20 °C after 5 days.

Almost all of the isolates described so far belonged to the *Peronosporomycetes*, the outgroup rooting the tree was *Aphanomyces* species harbouring *Aphanomyces astaci* and *Aphanomyces euteiches* as well as *Saprolegnia parasitica*. These isolates belonged to the *Saprolegniomycetes*, a sister order of

the *Peronosporomycetes* in the phylum of the *Oomycota*.

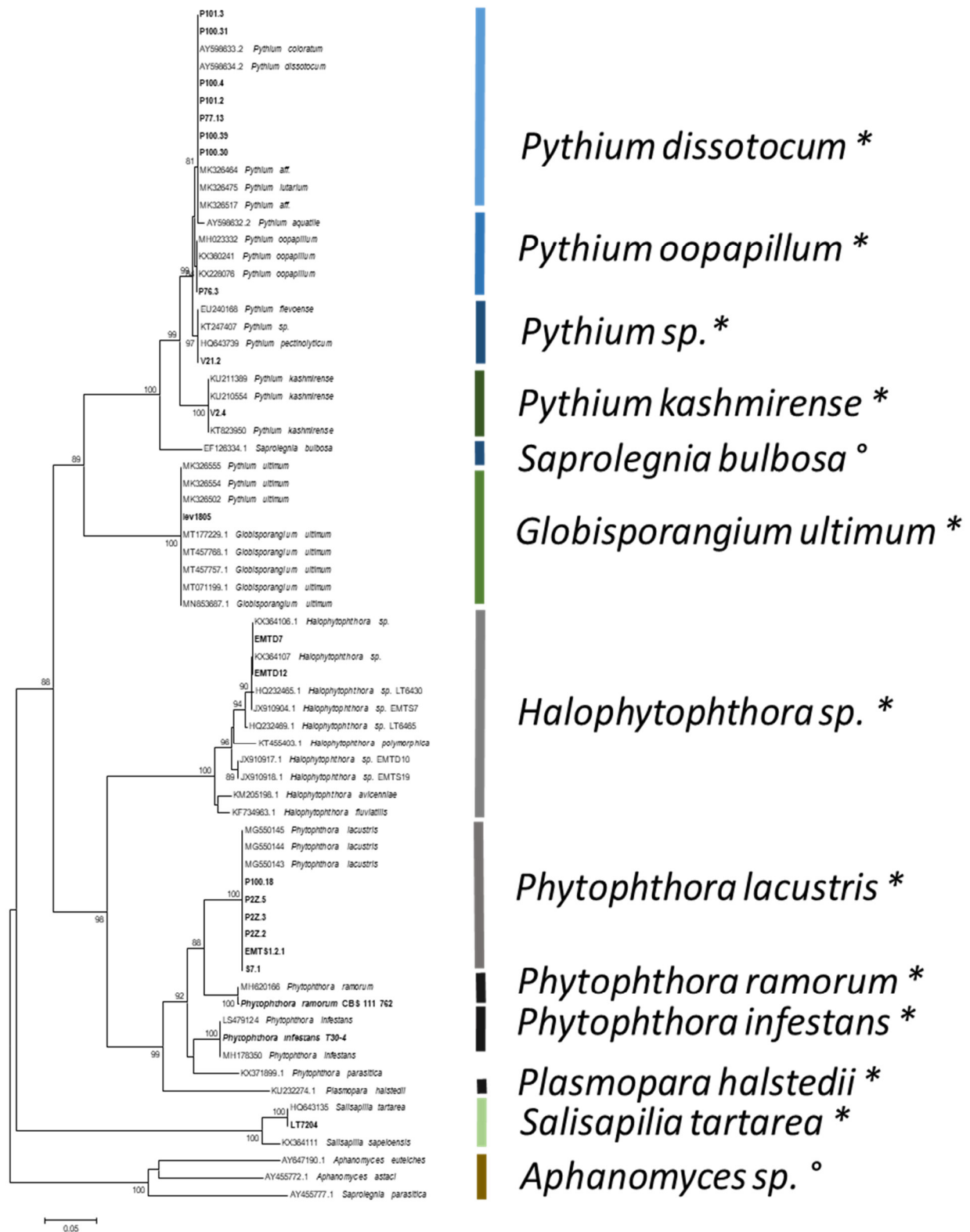


Figure 7: Phylogenetic tree inferred from Minimum Evolution analysis based on ITS sequences with 500 bootstraps. The numbers above the branches indicate the respective support, bootstrap values below 75 % are not shown. The spacer bar indicates the number of base substitutions per position. Isolates used in this study are marked with bold letters. Asterisks mark isolates belonging to the *Peronosporomycetes*, the degree sign marks the isolate belonging to the *Saprolegniomycetes*.

3.2. FAME analysis

All of isolates were grown on agar plates containing antibiotics and fungicides to obtain enough material for the fatty acid methyl ester analysis. Growth in liquid culture was poor for most of the isolates and the old mycelium could not be easily excluded from the analysis as they grow out from the agar plug used for inoculation into a mycelium ball.

The cultures grown on 9 cm diameter petri dishes agar plates were harvested after five days. An agar plug with an edge length of 0.5 cm was used as to inoculate the plates while the oldest and the newest mycelium was excluded using a form.

The cultures were harvested by carefully peeling off the mycelium from the agar which was easily doable for most isolates since the mycelium grew densely. After harvesting the mycelium was stored at -20 °C until the esterification. The storage time was needed because some strains grew sparsely or very slow and many culture plates were needed to get a sufficient amount for the esterification.

Multiple measurements were taken per isolate but often contaminations appeared in the FAME profiles. This was observed only in the FAME profiles, not on the agar plates. Bacterial contaminations were evident in the FAME profiles since oomycetes are not known to produce branched fatty acids as this is a trademark of bacteria. Growth of the isolates was repeated when the first branched fatty acids appeared on the fatty acid methyl ester profiles. As was mentioned in the Methods parts of this thesis, the measurements taken to prevent bacterial contaminations included an increased antibiotic-concentration from 30 µg/ml to 50 µg/ml Rifampicin, the usage of Raper rings (Raper, 1937) (a small plastic ring surrounding the inoculation agar plug to prevent bacteria from colonizing the agar plate while the oomycetes grow underneath the ring) and multiple transfers of hyphae under the microscope. After these actions the esterification and measurement of fatty acids was repeated.

In total 192 FAME-profiles of 23 isolates belonging to 6 different genera were obtained. 55 profiles from isolates grown at 27 °C and 137 from profiles grown at 20 °C.

The isolates P100.31, P100.39, P100.4, P101.2, P101.3, *Phytophthora ramorum* CBS 111 762, *Phytophthora infestans* T30-4, V2.4 and V21.2 did not grow at all or very poorly at 27 °C so only FAME-profile from growth at 20 °C could be obtained for these isolates.

In some measurements only one or two fatty acids were detected. Those measurements were excluded.

The fatty acid profiles of the different isolates display that the oomycetes produced a variety of different fatty acids. The fatty acids with an 'i' in front of the number of carbon atoms, for example Ci16:9, are branched fatty acids. Oomycetes are not known to produce branched fatty acids, this is a trademark of bacteria.

Above each name of the isolates the number of fatty acid profiles obtained for the given strain are given and out of those profiles the mean is displayed in the Table while the standard deviation indicates the average amount of variability between the given values. In the appendix the Table with all the values the Figures are based on can be found.

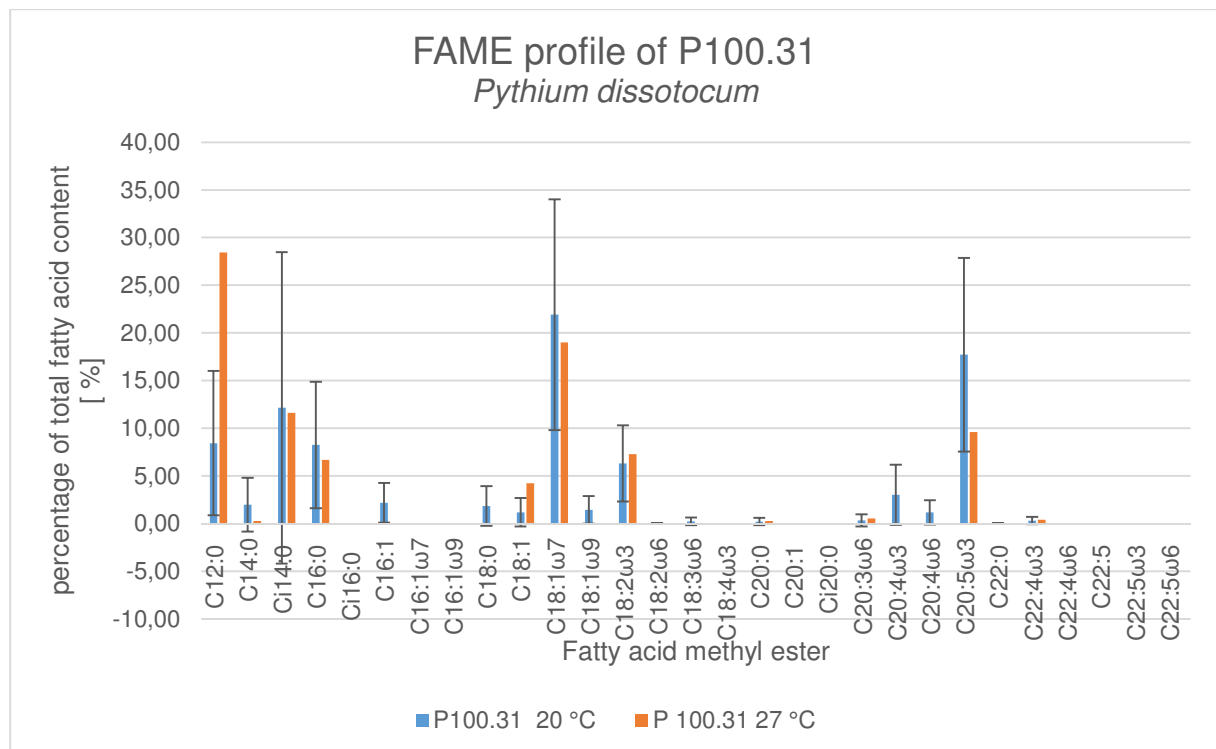


Figure 8: Fatty acid profile of the *Pythium dissotocum* strain P100.31 grown at 20 °C and 27 °C. Values shown are averages of all fatty acids methyl ester profiles obtained.

Figure 8 shows the FAME-profiles from the *Pythium dissotocum* strain P100.31, in total twelve FAME-profiles could be obtained. Eleven of the fatty acid profiles were from samples grown at 20 °C and one was grown at 27 °C. In general, growth at 27 °C was not good and two profiles were discarded because only one fatty acid was measured which was i16:0 with 100 %.

The fatty acids with the highest produced amounts at 20 °C were Ci14:0 with 12.15 % (branched tridecanoic acid), C18:1ω7 (vaccenic acid) with 21.1 % and C20:5ω3

(eicosapentaenoic acid) with 17.71 %. Since only one fatty acid profile of isolates grown at 27 °C could be used there is no standard deviation.

The fatty acid with the highest detected amount was lauric acid, C12:0, with 28.43 %, followed by vaccenic acid with 19 % and Tridecanoic acid, Ci14:0, with 11.62 %. The detected amount of eicosapentaenoic acid was comparably low with 9.59 %.

The values measured deviated greatly from the mean values, especially in the detected Ci14:0 with 16.34 %, in 18:1 ω 7 with 12.1 % and C20:5 ω 3 (eicosapentaenoic acid) with 10.16 %.

The difference in the fatty acid profiles produced at the different temperatures was mainly a shift towards fatty acids with shorter chains as the detected amount of lauric acid was increased by almost 20 % while the amount of eicosapentaenoic acid declined by 8 %.

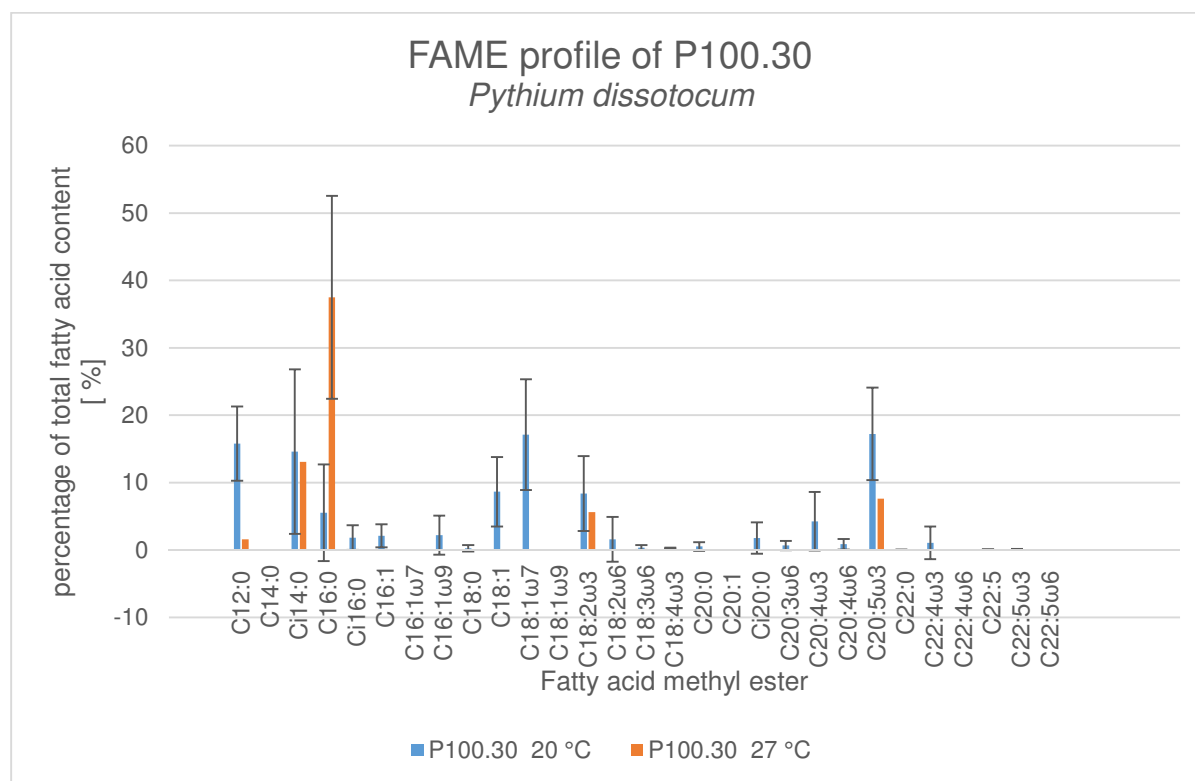


Figure 9: Fatty acid profile of the *Pythium dissotocum* strain P100.30 grown at 20 °C and 27 °C. Values shown are averages of all fatty acids methyl ester profiles obtained.

Of the isolate P100.30, a *Pythium dissotocum* strain as well, twelve fatty acid profiles of isolates grown at 20 °C and six of isolates grown at 27 °C were obtained and the results are shown in Figure 9.

At 20 °C grown isolates had the highest amounts of fatty acid in C12:0, lauric acid, with 15.77 %, Ci14:0, tridecanoic acid, C18:1 ω 7, vaccenic acid, and C20:5 ω 3 with 17.22 %.

The standard deviation showed that the data set was highly variable with values ranging from 12.21 % in Ci14:0 to 6.88 % in C20:5 ω 3.

In the samples grown at 27 °C the fatty acid profile was significantly less variable as lesser different fatty acids were detected, nevertheless the most abundant fatty acids stayed the same in both temperatures. 16.68 % lauric acid was found, 14.18 % tridecanoid acid, 21.26 % vaccenic acid and 17.18 % eicosapentaenoic acid.

The standard deviation showed that the data set is highly variable.

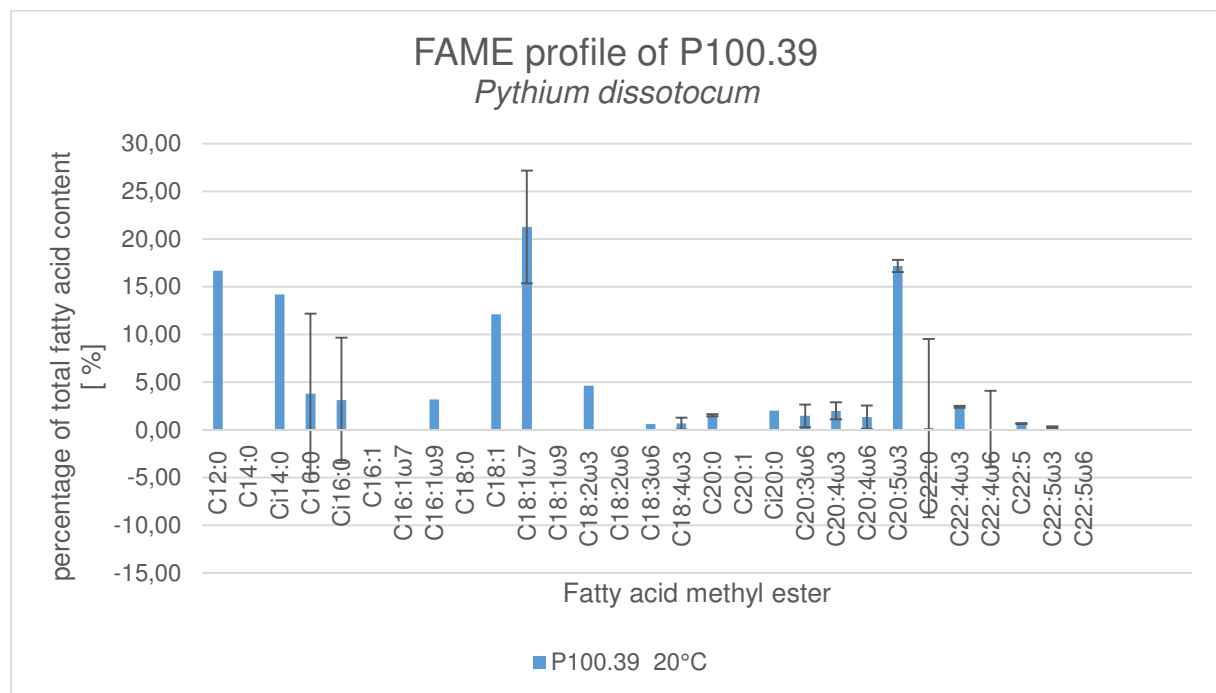


Figure 10: Fatty acid profile of the *Pythium dissotocum* strain P100.39 grown at 20 °C. Values shown are averages of all fatty acids methyl ester profiles obtained.

Of the isolate P100.39, as well a *Pythium dissotocum* strain, three profiles could be obtained. The isolates were grown at 20 °C, at 27 °C the organisms did not grow. The results of the FAME-measurements are shown in Figure 10.

Vaccenic acid was the most prominent fatty acid with 21.26 %, followed by eicosapentaenoic acid with 17.18 % and lauric acid with 16.68 %. Tridecanoic acid was found to be 14.18 % of the total fatty acid profile. Vaccenic acid could only be detected in one sample, resulting in no standard deviation. The standard deviation in the other samples showed a high diversity of the measurements.

Of the *Pythium dissotocum* strain P100.4 three FAME-profile could be used grown at 20 °C. Growth at 27 °C was very poor and not enough material could be collected for the measurements. The results are shown in Figure 11.

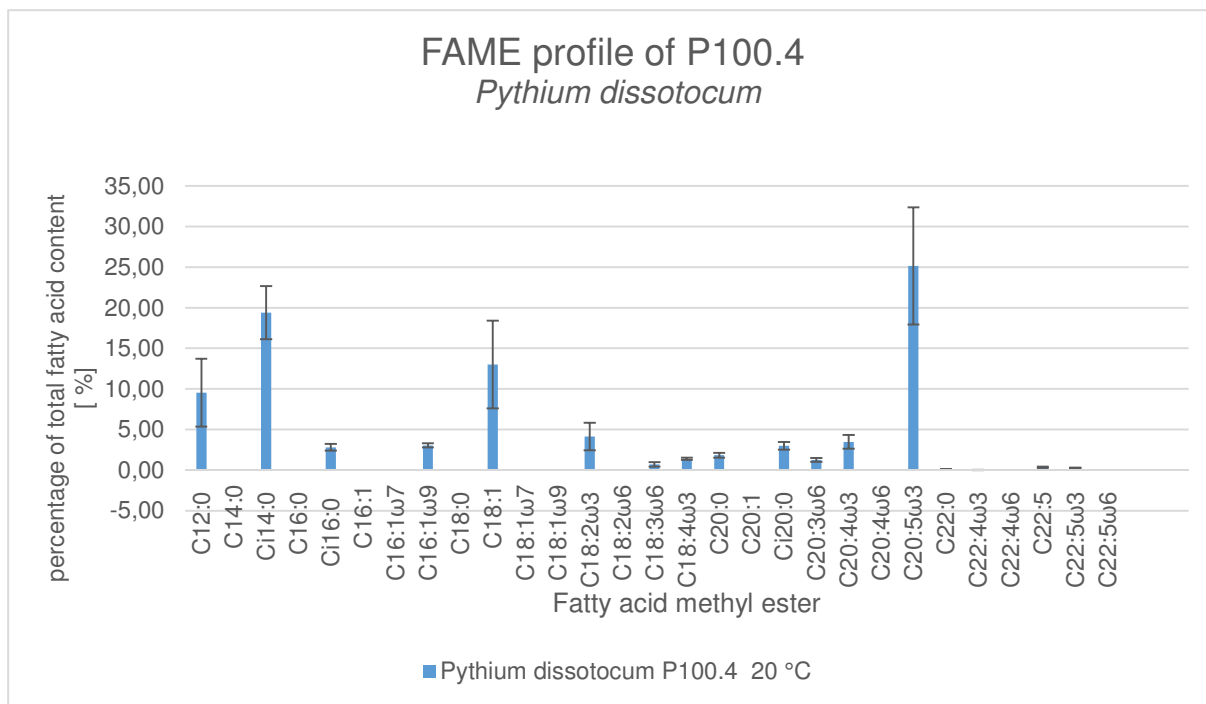


Figure 11: Fatty acid profile of the *Pythium dissotocum* strain P100.4 grown at 20 °C. Values shown are averages of all fatty acids methyl ester profiles obtained.

Tridecanoid acid, Ci14:0, was present with 19.4 %, stearic acid, C18:1, with 13.01 % and eicosapentaenoic acid with 25.17 %. The standard deviation showed that the data set is highly variable.

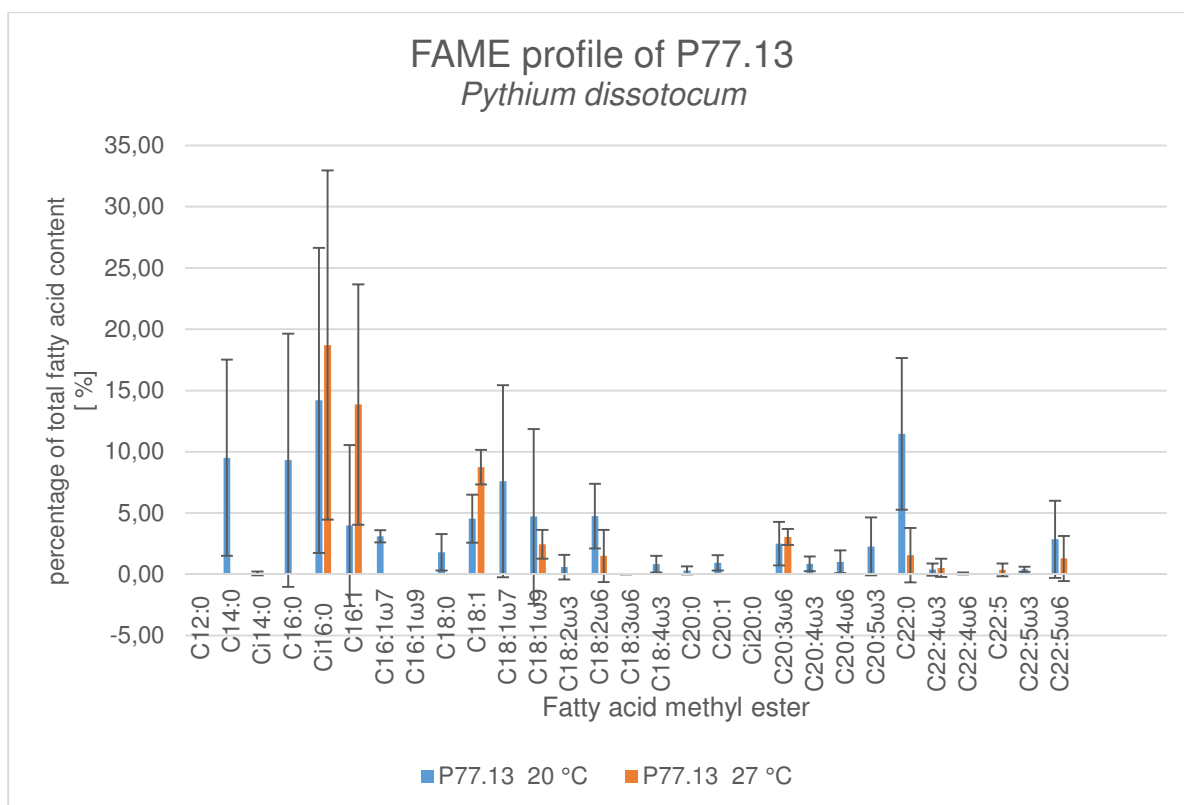


Figure 12: Fatty acid profile of the *Pythium dissotocum* strain P77.13 grown at 20 °C and 27 °C. Values shown are averages of all fatty acids methyl ester profiles obtained.

The fatty acid profile of the *Pythium dissotocum* strain P77.13 consisted of eight samples grown at 20 °C and three samples grown at 27 °C and the fatty acids found are shown in Figure 12.

The biggest part of the FAME profile of samples grown at 20 °C consists of lauric acid with 9.51 % and a standard deviation of 8.0 %, palmitic acid, C16:0, with 14.2 % and a standard deviation of 12.45 % and eicosapentaenoic acid with 11.47 % and a standard deviation of 6.19 %.

Most prominent fatty acids in the FAME profile of P77.13 isolates grown at 27 °C were palmitic acid, C16:0, with 18.70 %, where the standard deviation of 14.24 % shows the diversity of the data, Ci16:0, the isobranched version of palmitic acid, was present with 13.85 % and a standard deviation of 9.8 % and stearic acid with 8.75 % and a low standard deviation of 1.41 %.

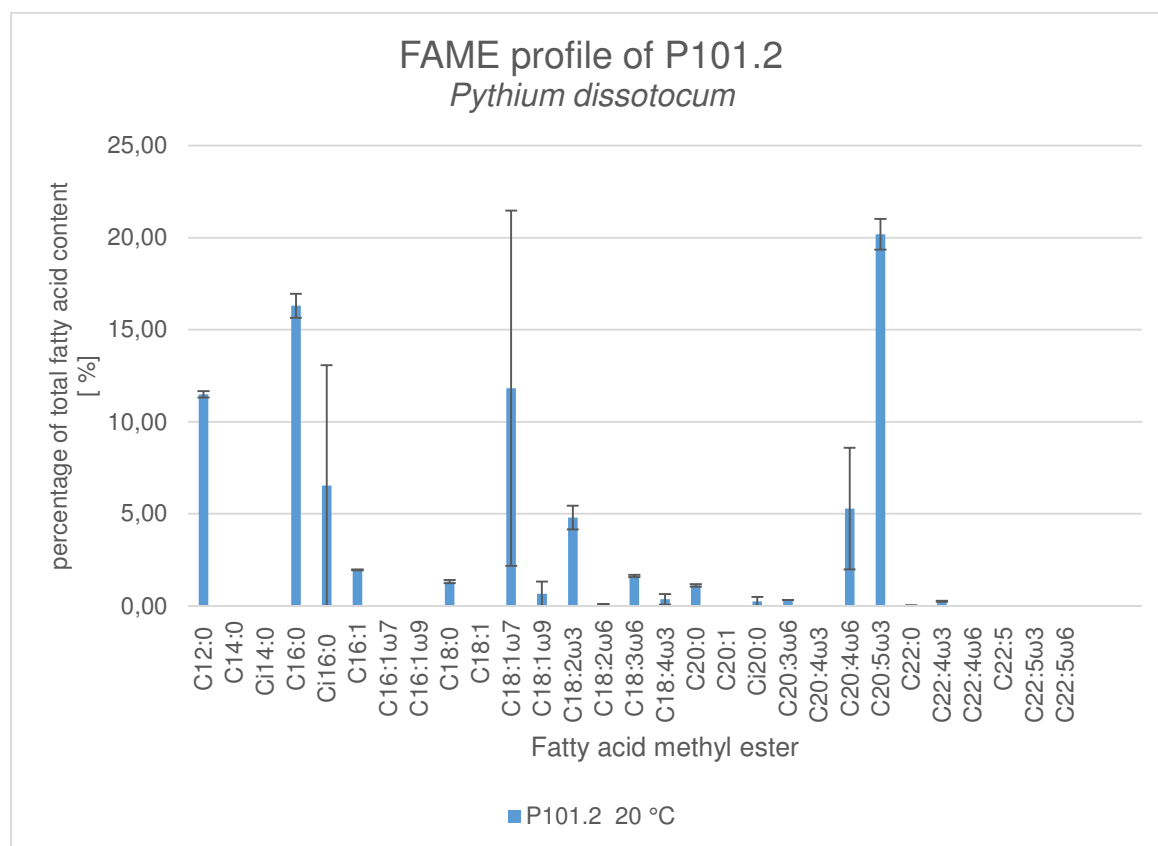


Figure 13: Fatty acid profile of the *Pythium dissotocum* strain P101.2 grown at 20 °C. Values shown are averages of all fatty acids methyl ester profiles obtained.

The *Pythium dissotocum* strain P101.2 was only cultivable at 20 °C, there was almost no growth in temperatures over 25 °C. Four measurements were done with the samples grown at 20 °C, no measurement from samples grown at 27 °C and the results are shown in Figure 13.

Eicosapentaenoic acid was present with 20.19 % and a very low standard deviation of only 0.84 %. Palmitic acid, C16:0, was found with 16.3 % and a very low standard deviation of only 0.66 %. 11.82 % of the total fatty acid content was vaccenic acid with a very high standard deviation of 9.65 %.

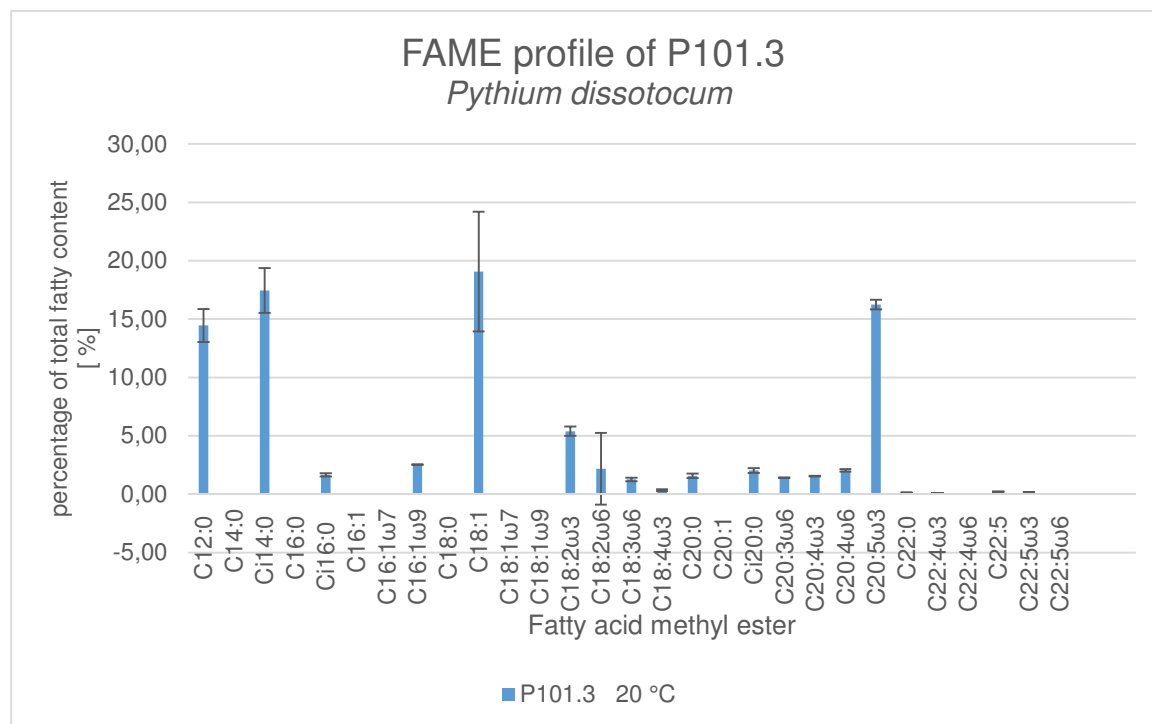


Figure 14: Fatty acid profile of the *Pythium dissotocum* strain P101.3 grown at 20 °C. Values shown are averages of all fatty acids methyl ester profiles obtained.

The isolates of the *Pythium dissotocum* strain P101.3 showed, like P101.2, poor growing abilities at 27 °C, only measurements of isolates grown at 20 °C were used for the fatty acid methyl ester profiles and the results are shown in Figure 14.

The branched fatty acid tridecanoic acid, Ci14:0, was present with 17.45 % in the total fatty acid content as well as C18:1 with 19.08 % and eicosapentaenoic acid with 16.25 %. Standard deviation was low in Ci14:0 with 1.93 % and eicosapentaenoic acid with 0.42 % while it was 5.13 % in C18:1.

In all of the FAME profiles of the *Pythium dissotocum* strains eicosapentaenoic acid was found and even though the amount varied, in most of the strains, especially when grown in 20 °C, eicosapentaenoic acid was among the top three fatty acids.

Only of three of the six *Pythium dissotocum* strains fatty acid profiles grown at 27 °C could be obtained. Growth at 27 °C of the other isolates was either both, slow and poor, or not existent, even in the three strains the fatty acid profiles could be obtained from the growth at 27 °C was not optimal. Comparison of the fatty acids from isolates

grown at 27 °C and isolates grown at 20 °C revealed a clear shift from fatty acids with longer carbon chains to fatty acids with shorter chains.

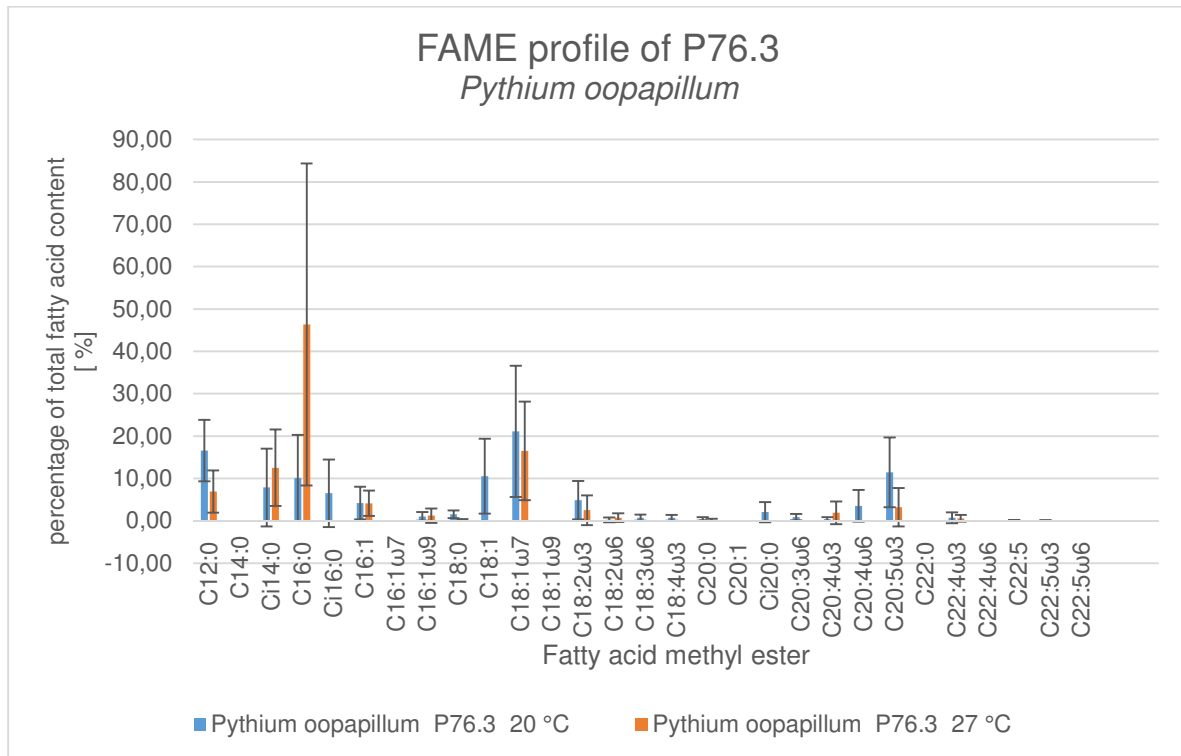


Figure 15: Fatty acid profile of the *Pythium oopapillum* strain P76.3 grown at 20 °C and 27 °C. Values shown are averages of all fatty acids methyl ester profiles obtained.

From the *Pythium oopapillum* strain P76.3 eight fatty acid profiles of samples grown at 20 °C and three of samples grown at 27 °C could be obtained and the results are shown in Figure 15.

In the fatty acid profiles grown at 20 °C vaccenic acid, C18:1ω7 was present with 21.10 %, lauric acid, C12:0, with 16.57 % and eicosapentaenoic acid with 11.42 %.

In the samples grown at 27 °C palmitic acid (C16:0) was the most prominent fatty acid with 46.35 % followed by vaccenic acid (C18:1ω7) with 16.49 % and the branched fatty acid Tridecanoic acid (Ci14:0) with 12.52 %.

The fatty acid content shifted with an increasing temperature to a composition of predominantly shorter chain fatty acids. In both cases the standard deviation was high, indicating that the data set is very variable.

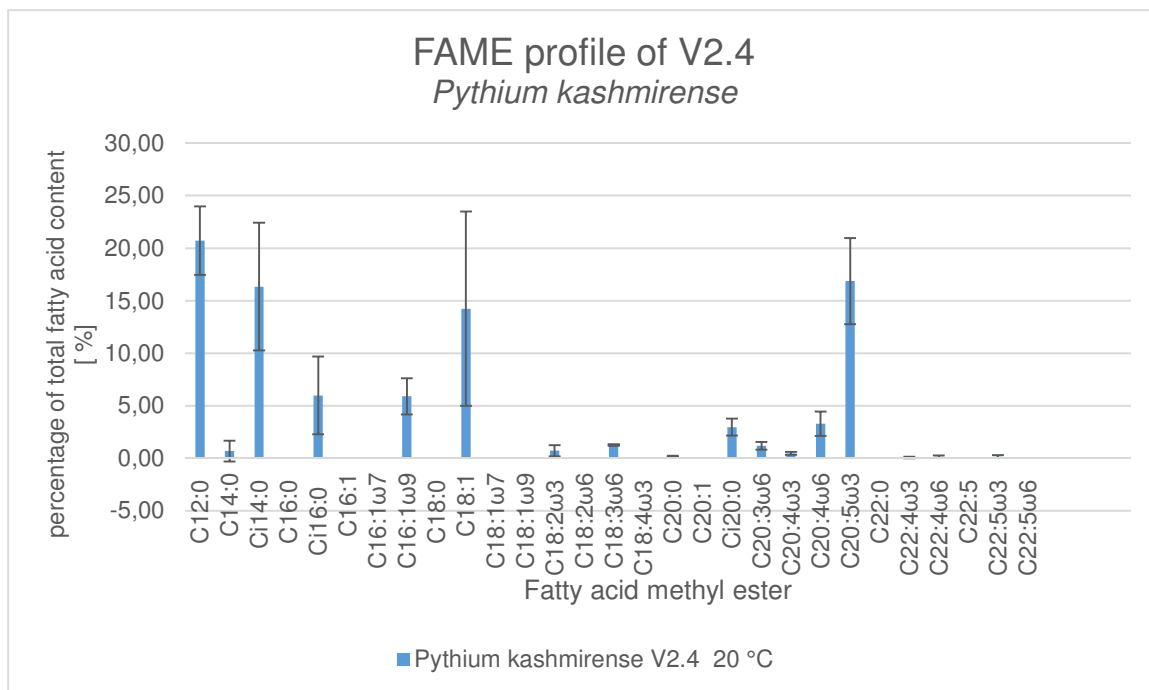


Figure 16: Fatty acid profile of the *Pythium kashmirens* strain V2.4 grown at 20 °C. Values shown are averages of all fatty acids methyl ester profiles obtained.

The *Pythium kashmirens* strain V2.4 did not grow well at 27 °C and no fatty acid profile from isolates grown at this temperature could be obtained. Three fatty acid profiles could be obtained from the isolates grown at 20 °C. This is shown in Figure 16. The highest amount detected of a fatty acid was Lauric acid (C12:0) with 20.72 %, Eicosapentaenoic acid was detected with 16.87 % and the branched fatty acid Tridecanoic acid (C14:0) with 16.35 %. The standard deviation for each of those values ranged from 3.27 % to 6.08 % and was considerably low compared to the other fatty acid profiles of other strains.

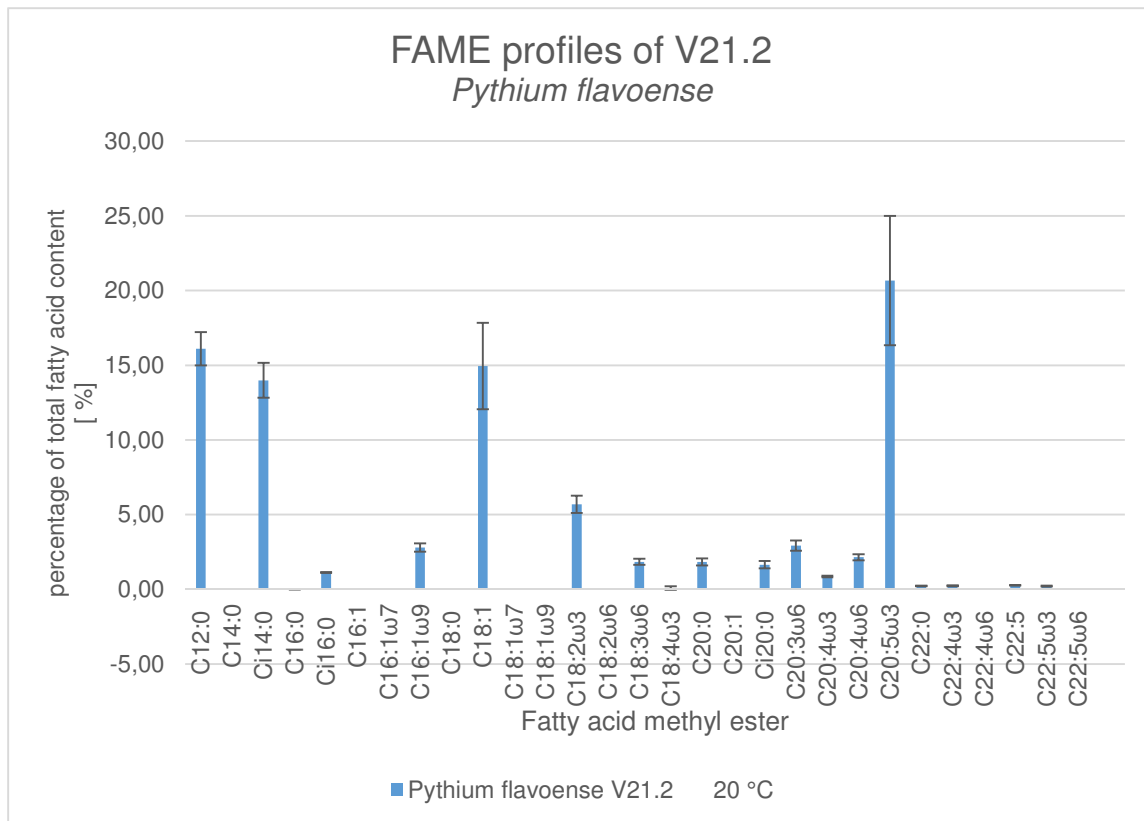


Figure 17: Fatty acid profile of the *Pythium flavoense* strain V21.2 grown at 20 °C. Values shown are averages of all fatty acids methyl ester profiles obtained.

The *Pythium flavoense* strain V21.2 did not grow at 27 °C, only samples from 20 °C were taken and the fatty acid profiles were the result which is shown in Figure 17.

The fatty acid with the highest detected amount was eicosapentaenoic acid (C20:5ω3) with 20.66 %, then lauric acid (C12:0) with 16.11 % and stearic acid (C18:1) with 14.95 %.

The standard deviation for eicosapentaenoic acid was 4.33 %, for lauric acid 1.12 % and for stearic acid 2.90 %.

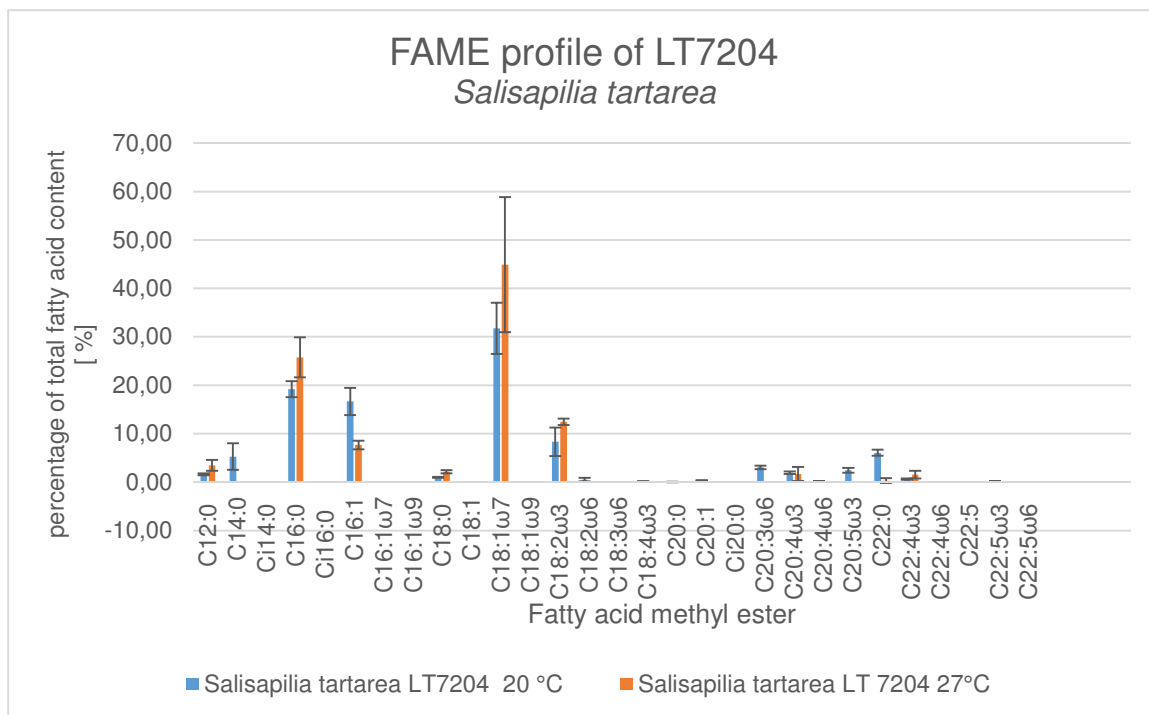


Figure 18: Fatty acid profile of the *Salisapilia tartarea* strain LT7204 grown at 20 °C and 27 °C. Values shown are averages of all fatty acids methyl ester profiles obtained.

The *Salisapilia tartarea* LT7204 strain grew extremely slow at 27 °C but three fatty acid profiles could be obtained and from isolates grown at 20 °C six fatty acid profiles were obtained, shown in Figure 18.

The fatty acid with the highest amounts from the isolates grown at 20 °C was vaccenic acid (C18:1ω7) with 31.73 %. Palmitoleic acid (C16:1) was found with 16.66 % and palmitic acid (C16:0) with 19.20 %. The standard deviation was comparably low with 5.29 % for vaccenic acid, 2.82 % for palmitoleic acid and 1.64 % for palmitic acid.

The fatty acid profiles from the isolates grown at 27 °C had a high amount of vaccenic acid (C18:1ω7) with 44.90 % and a standard deviation of 13.97 %, showing that the values were very different from each other. Palmitic acid (C16:0) was found to provide 25.75 % of the total fatty acid content while those values only differed from the mean by the standard deviation of 4.11 %. The compound labelled as C18:2ω3 12.46 % was found to have a standard deviation of 0.66 %.

No eicosapentaenoic acid was found in the fatty acid profile of the strains grown at 27 °C while the profiles obtained from the 20 °C cultures showed a small amount with 2.43 %. With an increasing temperature the amount of vaccenic acid increased by almost 50 %.

All of the six *Phytophthora lacustris* strains were able to grow at 20 °C and at 27 °C. Of the *Phytophthora lacustris* strain P2Z.2 seven fatty acid profiles from cultures grown at 20 °C could be obtained and six fatty acid profiles from cultures grown at 27 °C. The result is shown in Figure 19.

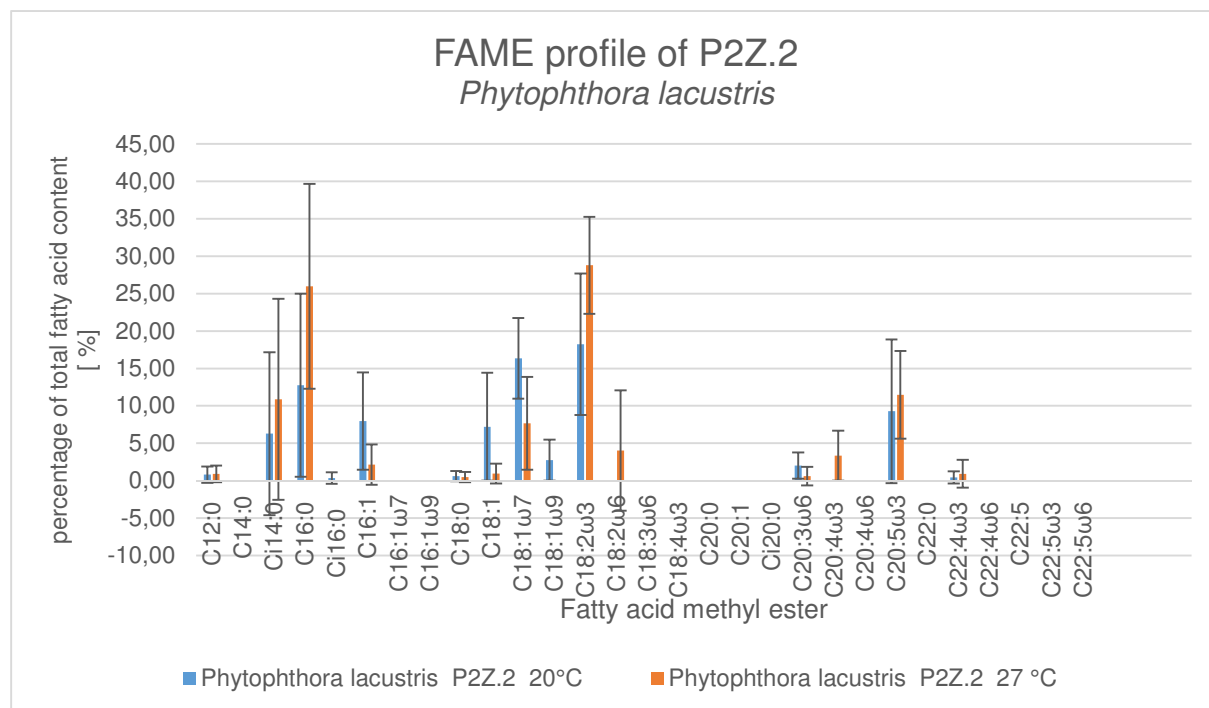


Figure 19: Fatty acid profile of the *Phytophthora lacustris* strain P2Z.2 grown at 20 °C and 27 °C. Values shown are averages of all fatty acids methyl ester profiles obtained.

At 20 °C the fatty acid profile consisted of 18.32 % of the compound labelled as C18:2ω3, 16.36 % of vaccenic acid (C18:1 ω7) and 12.75 % palmitic acid (C16:0).

The standard deviation was especially in palmitic acid high with 12.23 %, 9.45 % in C18:2ω3 and 5.4 % in vaccenic acid.

Eicosapentaenoic acid was detected to be 9.27 % of the total fatty acids detected.

At 27 °C palmitic acid (C16:0) was detected with 25.99 %, C18:2ω3 with 18.23 % and eicosapentaenoic acid with 11.48 %.

Comparing the fatty acid profiles revealed that the amount of palmitic acid almost doubled with the rise in temperature as well as the amount of eicosapentaenoic acid rose to from 9.27 % to 11.48 %.

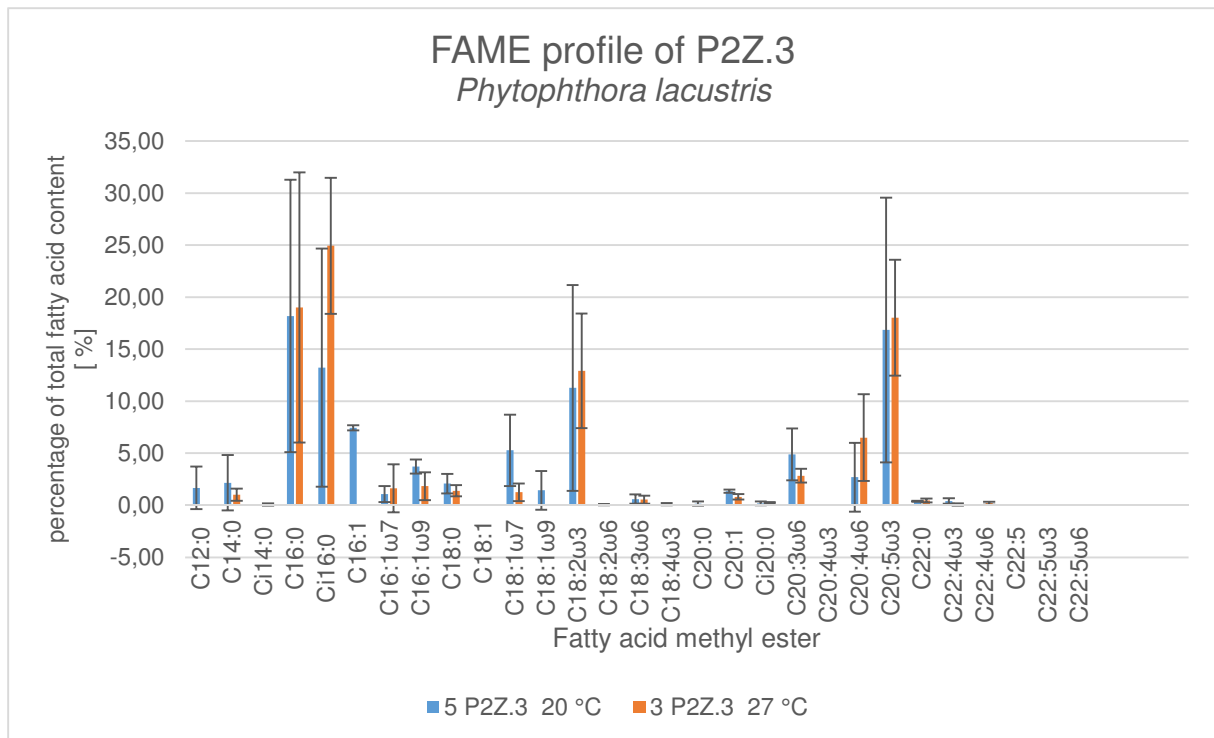


Figure 20: Fatty acid profile of the *Phytophthora lacustris* strain P2Z.3 grown at 20 °C and 27 °C. Values shown are averages of all fatty acids methyl ester profiles obtained.

In Figure 20 the measurements of the FAME profiles from the *Phytophthora lacustris* strain P2Z.3 are shown. From P2Z.3 five fatty acid profiles could be obtained from cultures grown at 20 °C and three fatty acid profiles from cultures grown at 27 °C.

The highest amount of fatty acids in the profile from cultures grown at 20 °C was 18.19 % of palmitic acid (C16:0), 16.84 % of eicosapentaenoic acid and 13.23 % of the isobranched palmitic acid (Ci16:0). Standard deviation showed in all of these fatty acids that the data set is extremely variable.

Fatty acid profiles from cultures grown at 27 °C had 24.94 % of the isobranched palmitic acid (Ci16:0), 19.01 % of palmitic acid and 18.03 % of eicosapentaenoic acid. The fatty acid profiles changed with an increase in temperature with an increase in the amount of eicosapentaenoic acid as well as an increase in short chain fatty acids like palmitic acid.

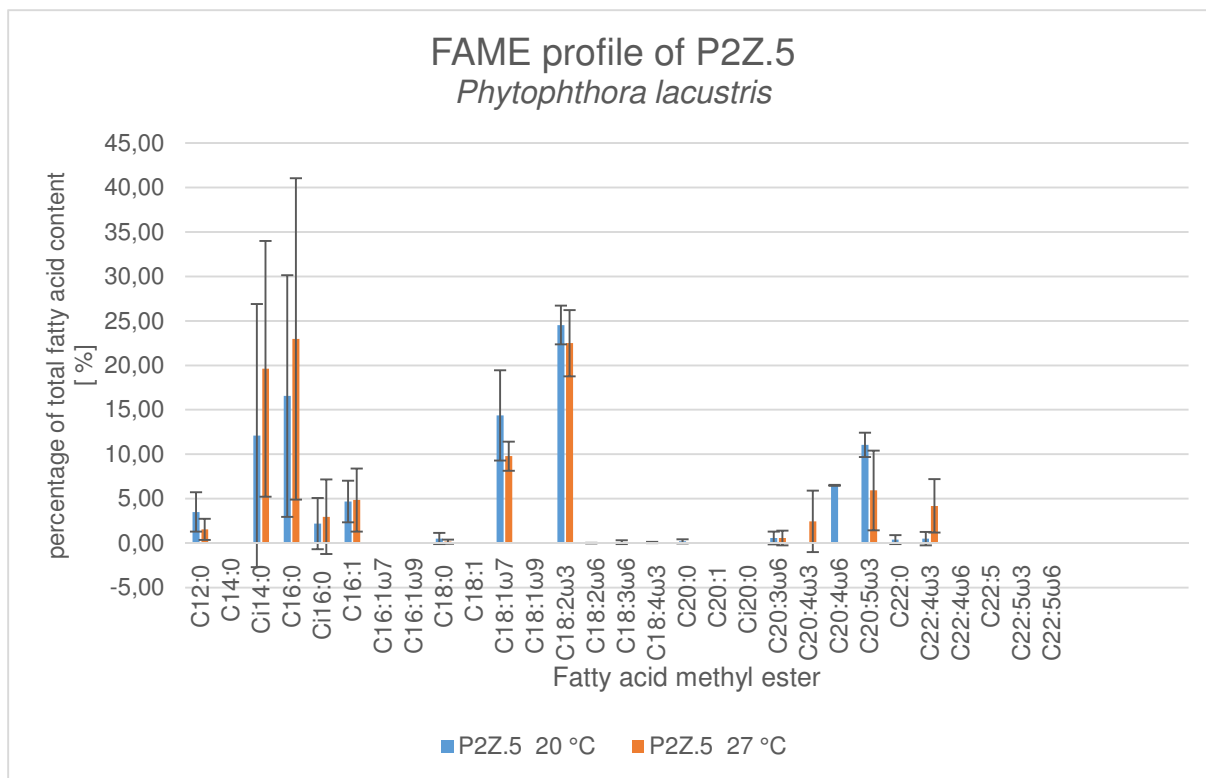


Figure 21: Fatty acid profile of *Phytophthora lacustris* strain P2Z.5 at 20 °C and 27 °C. Values shown are averages of all fatty acids methyl ester profiles obtained.

The isolates of the *Phytophthora lacustris* strain P2Z.5 were cultivable at both temperatures and five fatty acid profiles of isolates grown at 20 °C were obtained and three fatty acid profiles of cultures grown at 27 °C, the results are shown in Figure 21. When grown at 20 °C the compound C18:2ω3 contributed 24.54 % to the total fatty acid content, palmitic acid 16.56 % and vaccenic acid 14.36 %. Eicosapentaenoic acid was present with 11.05 %.

The fatty acid profile of isolates grown at 27 °C was comprised of 22.49 % C18:2ω3, 22.99 % of palmitic acid and 19.62 % branched tridecanoic acid. The amount of eicosapentaenoic acid was only 5.93 %.

With an increase of temperature the amount of vaccenic acid decreased by almost 1/3 while the amount of short chain fatty acids increased.

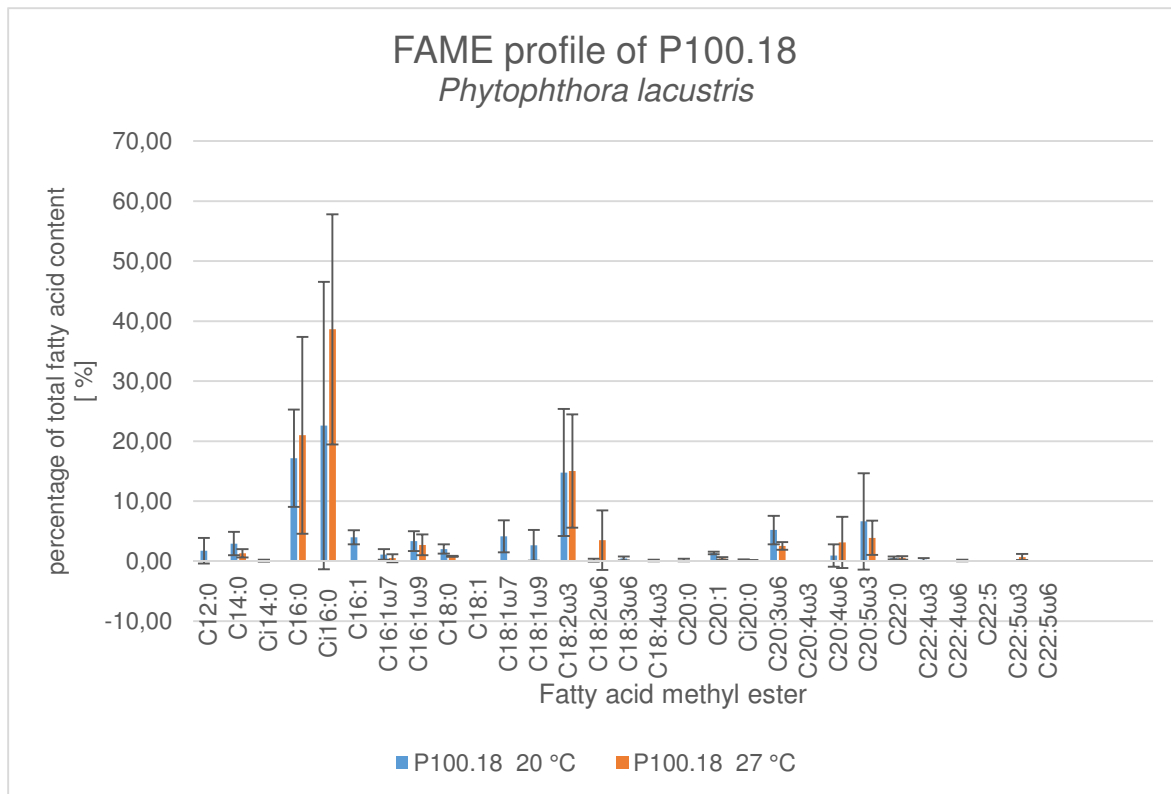


Figure 22: Fatty acid profile of *Phytophthora lacustris* strain P100.18 at 20 °C and 27 °C. Values shown are averages of all fatty acids methyl ester profiles obtained.

Of the *Phytophthora lacustris* strain P100.18 five fatty acid profiles of cultures grown at 20 °C and three fatty acid profiles from cultures grown at 27 °C could be obtained (Figure 22).

When grown at 20 °C branched palmitic acid was present with 22.58 %, unbranched palmitic acid with 17.16 % and C18:2ω3 with 14.78 %.

When grown at 27 °C branched palmitic acid was present with 38.63 %, unbranched palmitic acid with 20.98 % and C18:2ω3 with 15.01 %.

While the amount of C18:2ω3 stayed constant with the rising temperature the amount of the branched palmitic acid almost doubled and the amount of palmitic acid rose from 17.16 % to 20.98 %.

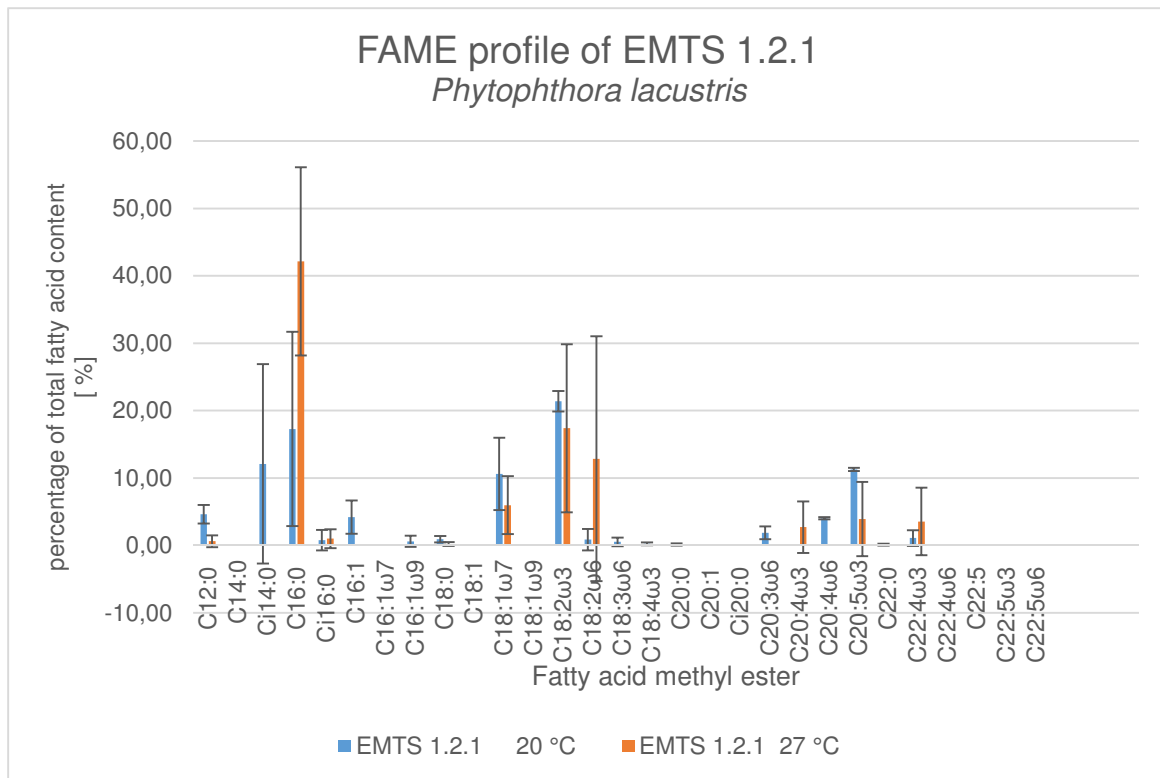


Figure 23: Fatty acid profile of *Phytophthora lacustris* strain EMTS1.2.1 at 20 °C and 27 °C. Values shown are averages of all fatty acids methyl ester profiles obtained.

The *Phytophthora* strain EMTS 1.2.1 grew good in both temperatures, 20 °C and 27 °C, and five fatty acid profiles could be obtained from samples grown at 20 °C and three fatty acid profiles from samples grown at 27 °C. The results are shown in Figure 23.

When grown at 20 °C the fatty acid profile consisted of 21.39 % C18:2ω3, 17.28 % palmitic acid and 12.09 % branched tridecanoic acid. Eicosapentaenoic acid was found to be 11.26 % of the total fatty acid content.

Cultures grown at 27 °C had their fatty acid profiles consist of 42.16 % palmitic acid, 17.38 % C18:2ω3, 12.85 % linoleic acid (C18:2ω6) and 3.91 % eicosapentaenoic acid. With the rising cultivation temperature the amount of palmitic acid was more than doubled while the amounts of other fatty acids and the longer chain fatty acids like eicosapentaenoic acid decreased.

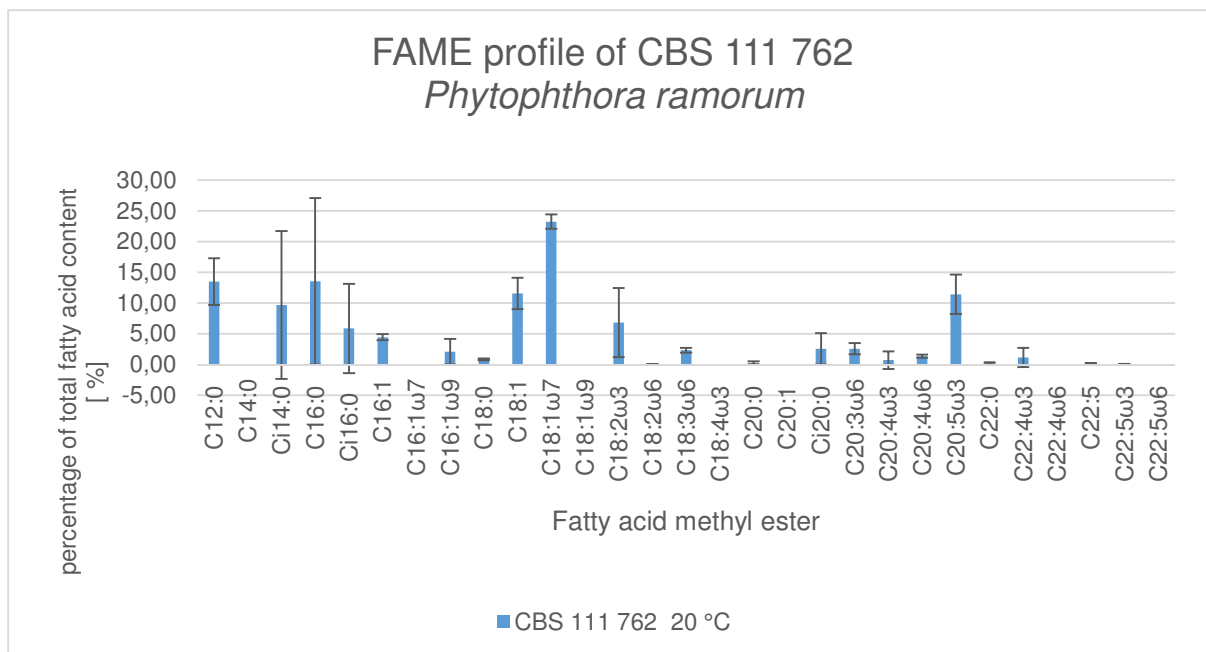


Figure 24: Fatty acid profile of the *Phytophthora ramorum* strain 111 762 at 20 °C. Values shown are averages of all fatty acids methyl ester profiles obtained.

The *Phytophthora ramorum* strain CBS 111 762 did not grow at 27 °C but from cultures grown at 20 °C five fatty acid profiles could be obtained, the results are shown in Figure 24.

The most prominent fatty acids in the profile of isolates grown at 20 °C were 23.26 % vaccenic acid, 13.55 % palmitic acid, 13.48 % lauric acid and 11.43 % eicosapentaenoic acid. The standard deviation was high, especially in the fatty acids with a carbon chain lengths of 16 and lower.

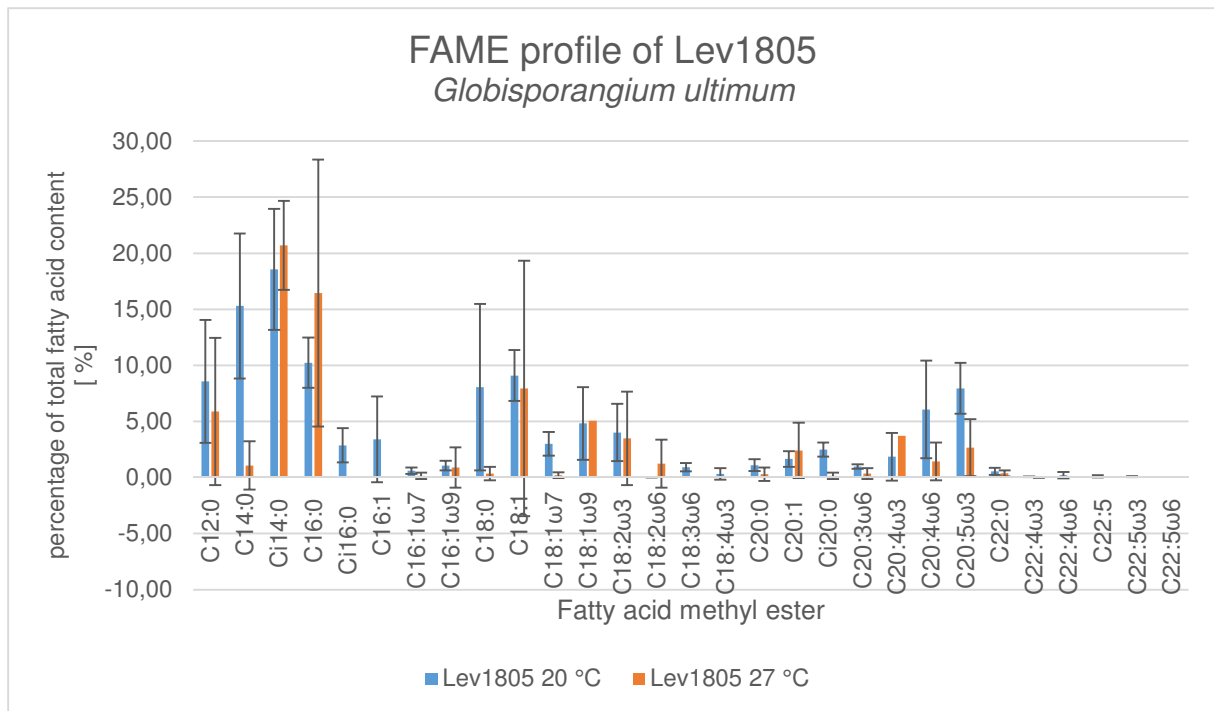


Figure 25: Fatty acid profile of the *Globisporangium ultimum* strain lev1805 grown at 20 °C and 27 °C. Values shown are averages of all fatty acids methyl ester profiles obtained.

The *Globisporangium ultimum* strain grew slow but steady and eleven fatty acid profiles from samples grown at 20 °C and six samples grown at 27 °C were obtained and are displayed in Figure 25.

Out of the 11 fatty acid profiles from cultures grown at 20 °C unbranched tridecanoid acid was present with 15.30 %, branched tridecanoic acid with 18.57 % and palmitic acid with 10.23 %.

The total fatty acid content of the six fatty acid profiles obtained from cultures grown at 27 °C consisted of 20.70 % branched tridecanoic acid, 16.45 % palmitic acid and only 1.08 % of unbranched tridecanoic acid.

Eicosapentaenoic acid was found in the fatty acid profile from 20 °C to be 7.95 % of the total fatty acid content and in the profiles from 27 °C to be 2.66 %.

With the temperature rising the amount of branched tridecanoic acid rose to 20.70 % as well as the amount of palmitic acid.

In *Globisporangium ultimum* almost 60 % of the fatty acids detected were fatty acids with a 16-carbon atom chain or shorter whereas in other *Pythium* species the majority of fatty acids had 18 carbon atoms or more.

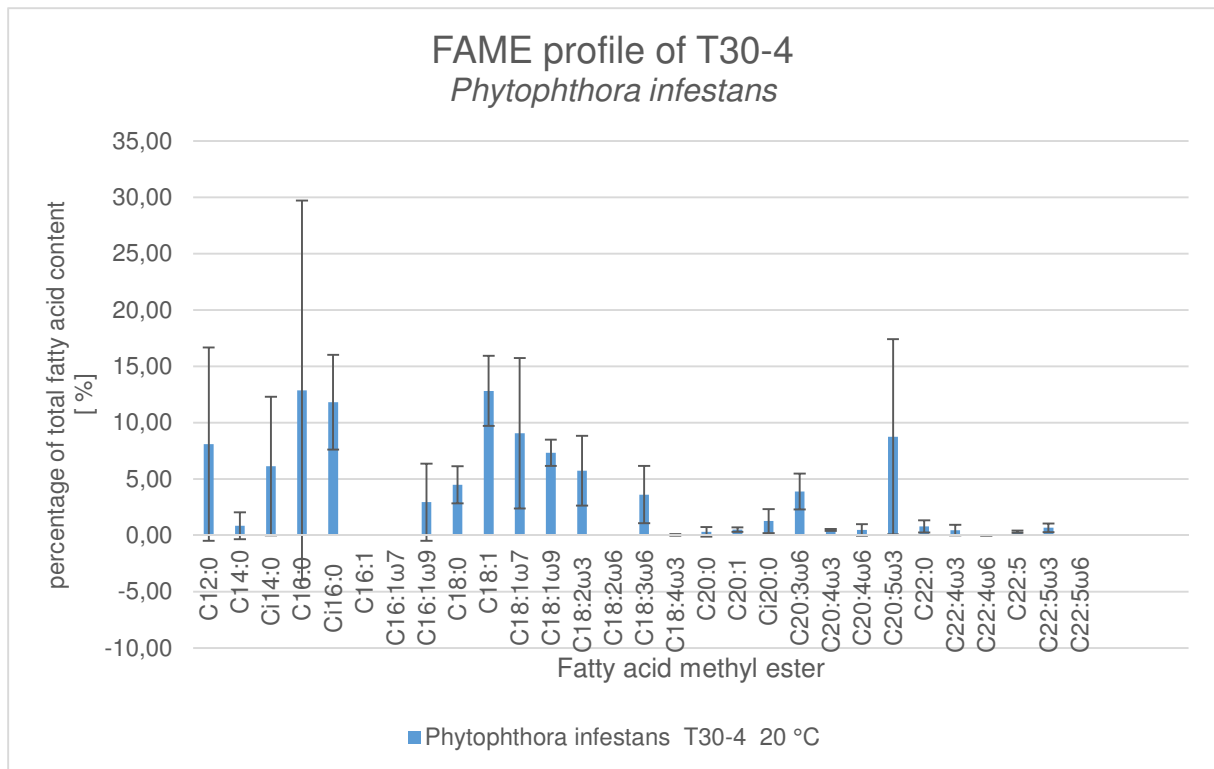


Figure 26: Fatty acid profile of the *Phytophthora infestans* strain T30-4 grown at 20 °C. Values shown are averages of all fatty acids methyl ester profiles obtained.

Phytophthora infestans grew comparably slow at 20 °C and six fatty acid profiles could be obtained but no fatty acid profiles from cultures grown at 27 °C, the results are shown in Figure 26.

In the fatty acid profiles palmitic acid was found to be 12.89 % of the total fatty acid content, C18:1 with 12.83 % and eicosapentaenoic acid with 8.76 %.

The standard deviation was very high with 8.66 % for eicosapentaenoic acid and 16.84 % for palmitic acid, indicating a highly divers dataset.

All of the *Halophytophthora* strains used in this study grew significantly slower than the *Pythium* or even the *Phytophthora* strains.

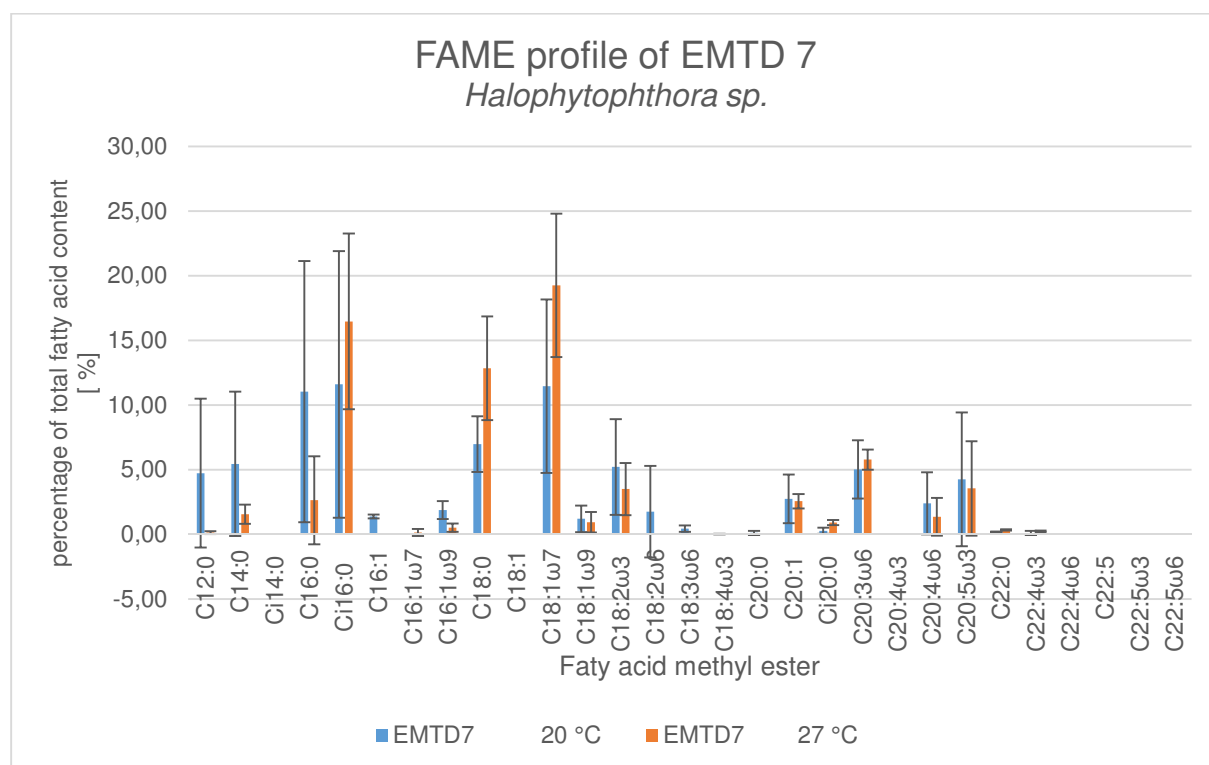


Figure 27: Fatty acid profile of the *Halophytophthora* sp. strain EMTD 7 grown at 20 °C and 27 °C. Values shown are averages of all fatty acids methyl ester profiles obtained.

From the strain EMTD 7 and its growth at 20 °C five fatty acid profiles could be obtained and from its growth at 27 °C four fatty acid profiles were obtained, the results are shown in Figure 27.

In the fatty acid profiles grown at 20 °C unbranched palmitic acid was found to comprise 11.04 %, branched palmitic acid 11.61 %, vaccenic acid (C18:1ω7) 11.46 % and eicosapentaenoic acid (C20:5ω3) 4.27 %.

The fatty acid profiles were highly diverse as the standard deviation shows.

In the fatty acid profiles from the samples grown at 27 °C the most prevalent fatty acid was vaccenic acid (C18:1ω7) with 19.27 % followed by branched palmitic acid (Ci16:0) with 16.48 % and stearic acid (C18:0) with 12.84 % eicosapentaenoic acid (C20:5ω3) was 3.57 % of the total fatty acid content.

The amount of branched fatty acids detected rose with the increasing temperature as well as the amount of vaccenic acid while the amount of longer chained fatty acids decreased as it can be seen in the detected amount of eicosapentaenoic acid.

From the *Halophytophthora* strain EMTS 23 four fatty acid profiles from samples grown at 20 °C were obtained and three fatty acid profiles from samples grown at 27 °C. The results are shown in Figure 28.

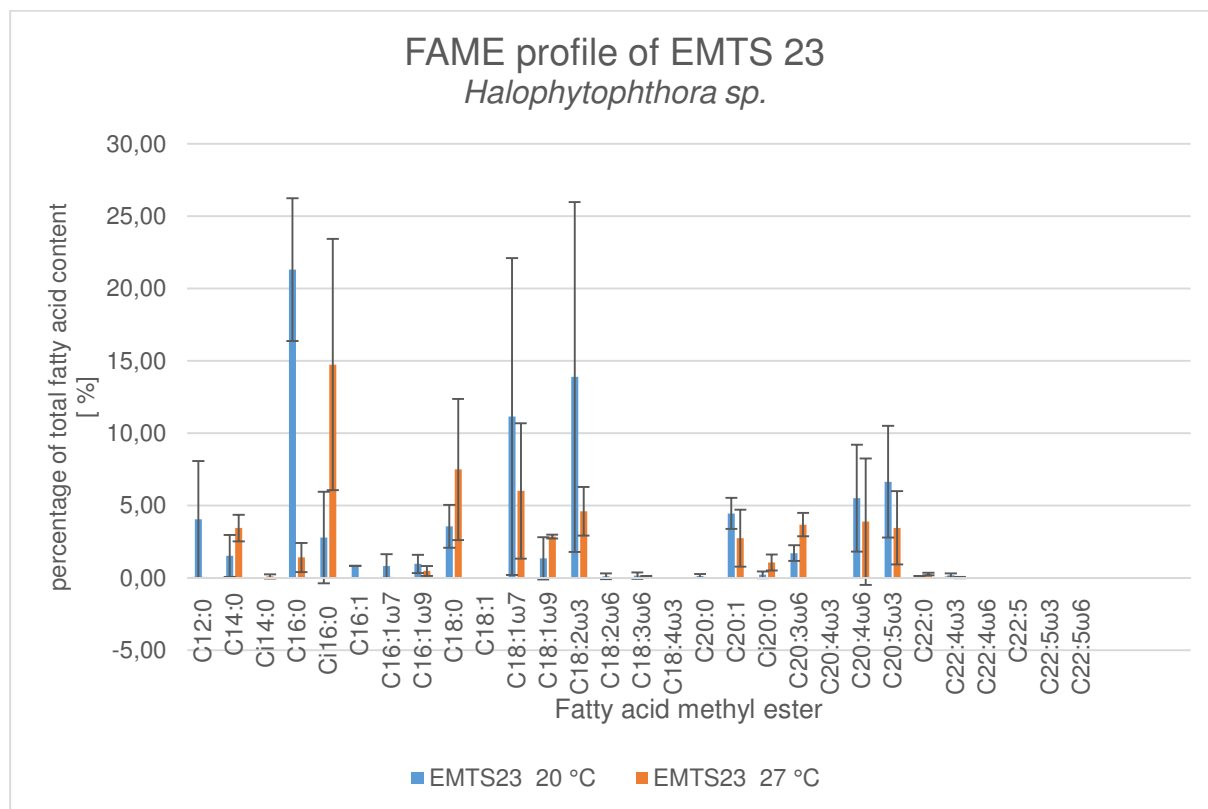


Figure 28: Fatty acid profile of the *Halophytophthora* sp. strain EMTS 23 grown at 20 °C and 27 °C. Values shown are averages of all fatty acids methyl ester profiles obtained.

The fatty acid content from samples grown at 20 °C consisted mainly of palmitic acid with 21.31 %, C18:2ω3 with 13.88 % and vaccenic acid (C18:1ω7) with 11.15 %.

When grown at 27 °C most prevalent fatty acids were branched palmitic acid (Ci16:0) with 14.74 %, stearic acid (C18:0) with 7.49 % and vaccenic acid (C18:1ω7) with 6.01 %. The increasing temperature shifted the fatty acid profile from unbranched fatty acids like palmitic acid to the branched form of the fatty acid.

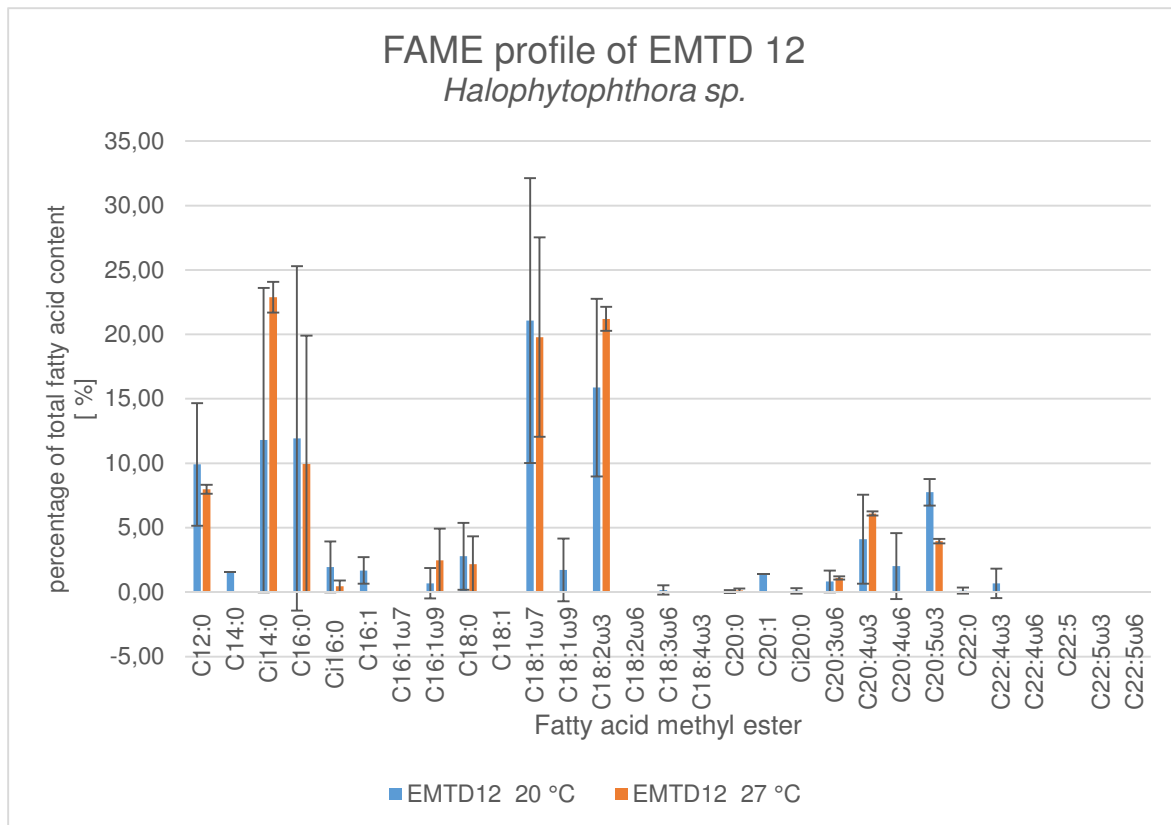


Figure 29: Fatty acid profile of the *Halophytophthora* sp. strain EMTD 12 grown at 20 °C and 27 °C. Values shown are averages of all fatty acids methyl ester profiles obtained.

The *Halophytophthora* strain EMTD 12 grew slow but five fatty acid profiles were obtained from growth at 20 °C and three fatty acid profiles from growth at 27 °C. The results are shown in Figure 29.

At 20 °C vaccenic acid was the most prevalent fatty acid with 21.07 % followed by C18:2ω3 with 15.87 % and the branched tridecanoic acid (Ci14:0) with 11.79 % and Palmitic acid (C16:0) with 11.93 % with almost similar amounts.

The standard deviation was very high for these fatty acids, for branched tridecanoic acid 11.81 % and palmitic acid with 13.38 %.

The fatty acid profile of the isolates grown at 27 °C consisted of 22.89 % branched tridecanoic acid (Ci14:0), 19.79 % vaccenic acid (C18:1ω7) and 21.21 % C18:2ω3.

The amount of detected eicosapentaenoic acid (C20:5ω3) was 7.75 % at 20 °C and 3.95 % at 27 °C.

The different temperatures of the growth of EMTD 12 resulted in an increase of the branched fatty acid tridecanoic acid and in a decrease of long chain fatty acids, like for example eicosapentaenoic acid.

3.3. Summary and comparison of oomycete fatty acid profiles

In Figure 30 solely the ω -3 fatty acids percentages of the total fatty acids detected in the isolates are shown as these polyunsaturated fatty acids are of special interest.

The fatty acid profiles used for this graphic are fatty acid profiles without branched fatty acids. For some isolates no profiles without branched fatty acids could be obtained so they were excluded in this analysis.

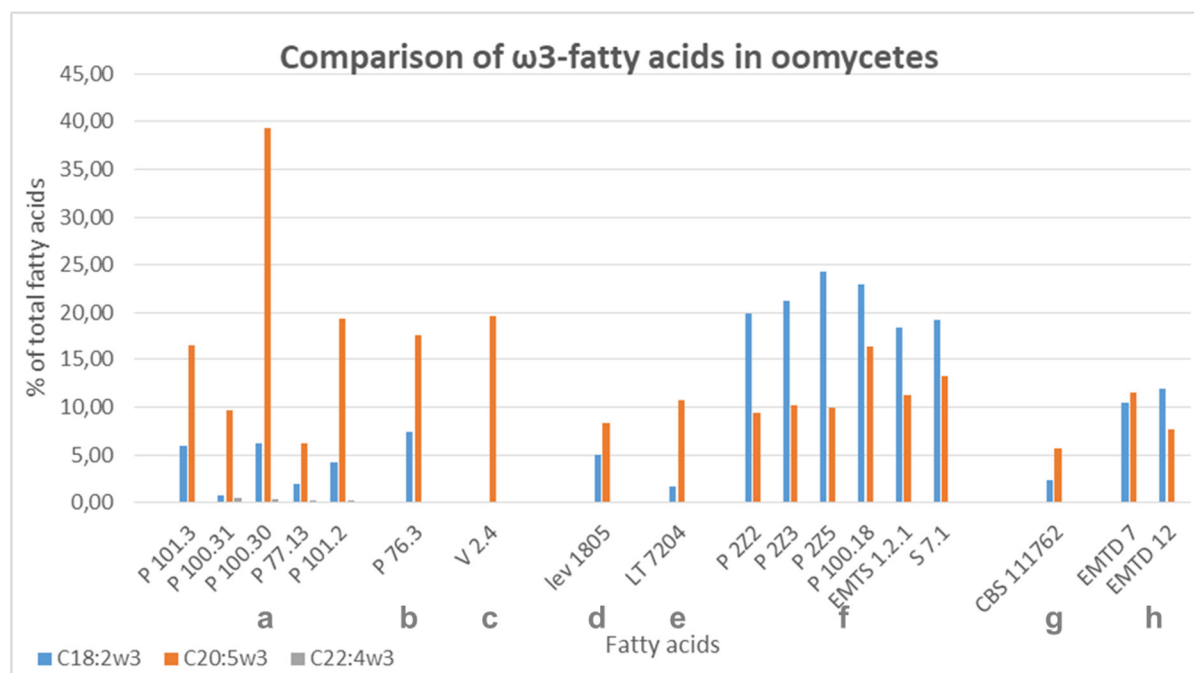


Figure 30: Comparison of ω 3 fatty acids of different oomycetes. Isolates with the letter a are *Pythium dissotocum*, b is *Pythium oopapillum*, c is *Pythium kashmirensis*, d is *Pythium ultimum*, e is *Salisapilia tartarea*, f is *Phytophthora lacustris*, g is *Phytophthora ramorum* and h is *Halophytophthora* sp..

Pythium dissotocum, *Pythium oopapillum* and *Pythium kashmirensis* strains produced significantly more eicosapentaenoic acid than the other isolates, between 15 % and 20 % of the total fatty acids were eicosapentaenoic acid (EPA). The detected amount of α -linolenic acid is lower than the EPA amount and ranges below 10 %, between 0.8 % and 6.2 % in all of the *Pythium dissotocum*, *Pythium oopapillum* and *Pythium kashmirensis* strains.

Globisporangium ultimum, lev1805, produced only 5.06 % of α -linolenic acid, 8.32 % eicosapentaenoic acid and 0.02 % of C22:4 ω 3.

Salisapilia tartarea produced as well comparably less ω -3 fatty acids in total with 1.64 % α -linolenic acid, 10.68 % eicosapentaenoic acid and 0.08 % C22:4 ω 3.

In the *Pythium kashmirensis* isolate V2.4 α -linolenic acid could not be detected but the amount of eicosapentaenoic acid detected was 19.58 % and of C22:4 ω 3 it was 0.07 %.

What the isolates have in common so far is that more eicosapentaenoic acid than α -linolenic acid was detected.

In *Phytophthora ramorum* the amount of ω -3 fatty acids in the total fatty acid composition was low with 2.32 % α -linolenic acid, 5.61 % eicosapentaenoic acid and 0.06 % of C22:4 ω 3, still more eicosapentaenoic acid was found than α -linolenic acid.

In the *Halophytophthora sp.* strains the amounts of ω -3 fatty acids detected was balanced.

In the *Halophytophthora* strain EMTD 7 10.52 % α -linolenic acid, 11.58 % eicosapentaenoic acid and 0.09 % C22:4 ω 3 were detected and in the EMTD 12 strain 11.98 % α -linolenic acid, 7.67 % eicosapentaenoic acid and 0.09 % C22:4 ω 3. In both strains the total amount of ω -3 fatty acids was comparably low.

Phytophthora lacustris strains produced high amounts of α -linolenic acid, between 20 and 25 % of the total fatty acid content. Eicosapentaenoic acid amounts ranged between 9.4 % and 16.4 % but all of the isolates produced more α -linolenic acid than eicosapentaenoic acid.

In all of the isolates traces of a compound labelled as C22:4 ω 3 was detected, even though in some cases it is not obvious in the Figure. The detected amount ranged from 0.08 % to 0.5 % in the fatty acid profile of *Pythium dissotocum*. In the strains P100.30 and P100.31 the highest amount with 0.38 % in P100.30 and 0.52 % in P100.31 was detected. In *Pythium oopapillum*, *Pythium kashmirensis*, *Pythium ultimum* and *Salisapilia tartarea* the detected amount was low, ranging from 0.02 % to 0.08 %. The maximum amount detected in *Phytophthora lacustris* was 0.11 % in the isolate S7.1, the other isolates produced less C22:4 ω 3. In *Phytophthora ramorum* and the *Halophytophthora sp.* isolates the detected amounts were equally low.

In Table 4 all long chain fatty acids produced by the analysed species are shown.

Table 4: Long chain fatty acids produced from the oomycetes. Starting from oleic acid to the compound labelled as C22:4 ω 3

Fatty acids	<i>Pythium dissotocum</i>					<i>Phytophthora ramorum</i>
	P 101.3	P 100.31	P 100.30	P 77.13	P 101.2	CBS 111762
C18:1	17,22	3,46	11,87	21,36		7,96
C18:1 ω 7		18,98	21,537	2,45	11,82	23,26
C18:2 ω 6		0,08		0,02	0,08	2,32
C18:2 ω 3	5,93	0,81	6,21	2,00	4,16	0,05
C18:3 ω 6	1,43	0,83		1,99	1,68	2,42
C18:4 ω 3	0,30				0,07	
C20:3 ω 6	1,41	2,13	0,16	0,97	0,35	3,63
C20:4 ω 3	1,59					0,13
C20:4 ω 6	2,17	3,12		5,20	1,98	1,33
C20:5 ω 3	16,64	9,72	39,28	6,20	19,34	5,61
C22:1/22:3 ω 3	0,08	0,11	1,06	0,04	0,04	0,13
C22:4 ω 3	0,08	0,52	0,38	0,24	0,27	0,06

Fatty acids	<i>Phytophthora lacustris</i>					
	P 222	P 223	P 225	P 100.18	EMTS 1.2.1	S 7.1
C18:1	6,35	2,22	8,21	7,07	4,69	19,41
C18:1 ω 7	19,21	19,14	18,45	3,12	14,54	1,99
C18:2 ω 3	19,93	21,21	24,25	23,00	18,43	19,26
C18:2 ω 6	0,03	0,16	0,09	0,11	4,01	0,10
C18:3 ω 6	0,90	1,08	0,55	0,33	1,26	0,92
C18:4 ω 3		0,23	0,16	0,22	0,45	
C20:3 ω 6	2,09	1,91	1,44	2,43	2,06	3,50
C20:4 ω 3						
C20:4 ω 6	3,56	0,98	6,44	4,70	3,84	4,23
C20:5 ω 3	9,45	10,22	9,93	16,45	11,29	13,21
C22:1/22:3 ω 3	0,25	0,15	0,10	0,19	0,02	0,22
C22:4 ω 3	0,09	0,04	0,03	0,03	0,04	0,11

Fatty acids	<i>Pythium oopapillum</i>	<i>Pythium kashmirensis</i>	<i>Globisporangium ultimum</i>	<i>Salisapillia tartarea</i>	<i>Halophytophthora sp.</i>	
	P 76.3	V 2.4	lev 1805	LT 7204	EMTD 7	EMTD 12
C18:1	15,81	26,75	16,63	20,30	8,71	32,84
C18:1 ω 7	5,12		5,12	41,25	9,09	13,91
C18:2 ω 3	0,02		0,01	0,04	10,52	11,98
C18:2 ω 6	7,43		5,06	1,64		
C18:3 ω 6	1,78	1,30	0,94	0,09	0,58	
C18:4 ω 3	1,47				0,06	
C20:3 ω 6	1,87	0,97	0,89	2,06	2,58	
C20:4 ω 3	1,28	0,42		0,21		
C20:4 ω 6	3,76	3,16	3,59	1,87	1,67	0,40
C20:5 ω 3	17,63	19,58	8,32	10,68	11,58	7,67
C22:1/22:3 ω 3	0,06	0,06		0,16	0,01	0,31
C22:4 ω 3	0,04	0,07	0,02	0,08	0,09	0,09

The fatty acid profiles differed not only in the amounts of each fatty acid but as well in the number of fatty acids detected. In all of the analysed oomycetes the highest amounts of fatty acids were C18 fatty acids, like oleic acid and vaccenic acid, as well as C20:5 ω 3.

The ω -3 fatty acids are highly sought after because they are important nutrients in human diet.

In Table 5 the percentages of ω -3 and ω -6 fatty acids are summed up and shown. Noteworthy is the fatty acid profile of P100.30, it consisted of almost 50 % ω -3 fatty acids and only 0.16 % of the total fatty acids were ω -6 fatty acids. In general, the amount of ω -6 fatty acids in all oomycetes analysed was comparably low, all of them produced more ω -3 fatty acids.

P100.18, a *Phytophthora lacustris* strain, had 39.89 % ω -3 fatty acids compared to 7.58 % ω -6 fatty acids. The *Phytophthora lacustris* strains all produced a high amount of ω -3 fatty acids, the amount ranging from 29.7 % to 39 %. In the *Pythium dissotocum* strains the amount of ω -3 fatty acids showed a broader range between 8 % and 49 % ω -3 fatty acids. The ω -6 fatty acid amount in *Phytophthora lacustris* was comparably low between 4 % and 11 %.

The amount of ω -3 and ω -6 was almost balanced in *Phytophthora ramorum*, 8.2 % ω -3 and 7.4 % ω -6 of total fatty acids.

In some oomycetes high levels of vaccenic acid (C18:1 ω 7) were found. In LT7204, a *Salisapillia tartarea* strain, 41.25 % of total fatty acid content was vaccenic acid.

The three *Phytophthora lacustris* strains P2Z.2, P2Z.3, P2Z.5 and the *Pythium dissotocum* strain P100.30 produced almost 20 % vaccenic acid.

Table 5: Percentages of total ω -3/ ω -6 fatty acid content of different isolates

Fatty acid	<i>Pythium dissotocum</i>					<i>Pythium oopapilum</i>
	P 101.3	P 100.31	P 100.30	P 77.13	P 101.2	P 76.3
ω -3	24,61	11,16	46,93	8,48	23,89	27,92
ω -6	5,01	6,16	0,16	8,17	4,08	7,43

Fatty acid	<i>Phytophthora lacustris</i>						<i>Phytophthora ramorum</i>
	P 2Z2	P 2Z3	P 2Z5	P 100.18	EMTS 1.2.1	S 7.1	CBS 111762
ω -3	29,73	31,85	34,47	39,89	30,22	32,80	8,25
ω -6	6,58	4,13	8,53	7,58	11,17	8,75	7,43

Fatty acid	<i>Salisapilia tartarea</i>	<i>Pythium ultimum</i>	<i>Pythium kashmirese</i>	<i>Halophytophthora sp.</i>	
	LT 7204	lev 1805	V 2.4	EMTD 7	EMTD 12
ω -3	12,76	13,40	20,13	22,27	20,05
ω -6	4,07	5,43	5,42	4,83	0,40

After analysing the fatty acid profiles from the oomycetes the *Pythium dissotocum* strain P100.30 was chosen for further analysis.

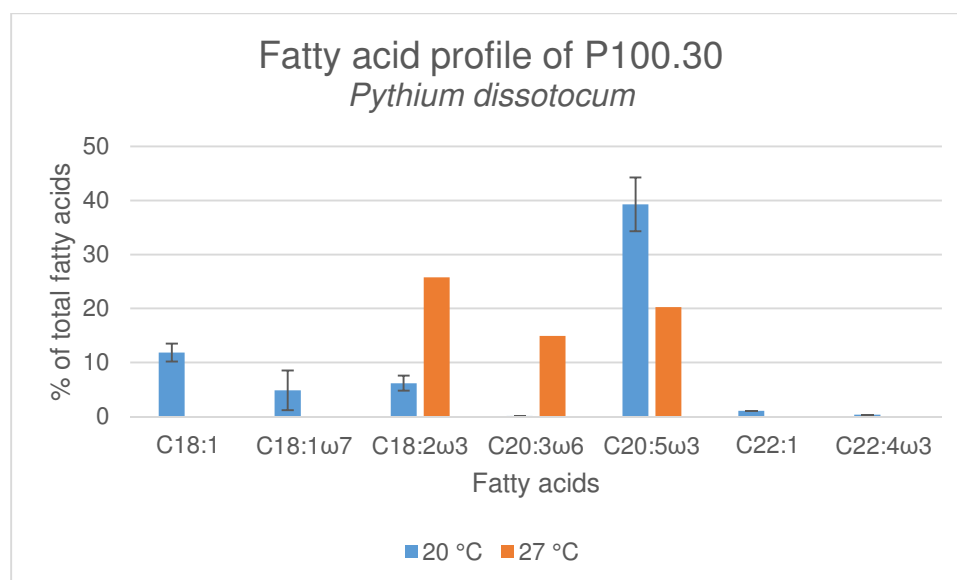


Figure 31: Fatty acid profile of *Pythium dissotocum* strain P100.30 without FAME measurements that showed branched fatty acids

The fatty acid profiles shown in Figure 31 display the FAME profiles obtained without branched fatty acids. P100.30 produced significant amounts of eicosapentaenoic acid. In comparison to the FAME profiles with branched fatty acids the amount of fatty acids detected was significantly lower as only 7 fatty acids were detected compared to 17 in

the profiles with branched fatty acids. The amount of fatty acids was distributed in a similar way, when grown at 20 °C the amount of EPA detected was high while the fatty acid amount detected shifted to shorter chain fatty acids when grown at 27 °C in the FAME profiles with branched and unbranched fatty acids. When grown at 20 °C the detected amount of EPA in the FAME profiles without branched fatty acids was 39.27 % and grown at 27 °C it was 20.25 % eicosapentaenoic acid of total fatty acids. Higher amounts of long chain fatty acids were produced when grown at 20 °C while more fatty acids with shorter chains were detected at 27 °C.

Low amounts of dihomo- γ -linolenic acid (C20:3 ω 6), 0.16 %, and eruric acid (C22:1), 1.06 %, were found as well as a compound that was assigned to a fatty acid labelled as C22:3 ω 3 with 0.38 %. Stearidonic acid (C18:4 ω 3) was not detected in any of the samples.

These findings suggested the presence of a complete pathway for the de novo production of VLCPUFAs in the *Pythium dissotocum* strain P100.30.

The *Pythium dissotocum* strains grew, in comparison to the other isolates and especially *Phytophthora lacustris* strains, very fast. At 20 °C Celsius a petri dish with a diameter of six centimetres and Potato-dextrose-broth-V8-agar was fully colonized by P100.30 after three days with dense growing mycelium and lots of aerial hyphae. The mycelium grew densely and for any further analysis the mycelium could be pulled off of the agar almost, having only traces of agar in the sample that could be easily removed by washing.

The *Phytophthora lacustris* strains showed a different growth pattern, the six cm petri dish was fully colonized after 8-9 days at 20 °C with the mycelium showing a very fine and sparse growth pattern as shown in Figure 27.

Based on the fatty acid profile and the growth pattern the *Pythium dissotocum* isolate P100.30 was chosen for further analysis including the sequencing of the genome and the transcriptome.

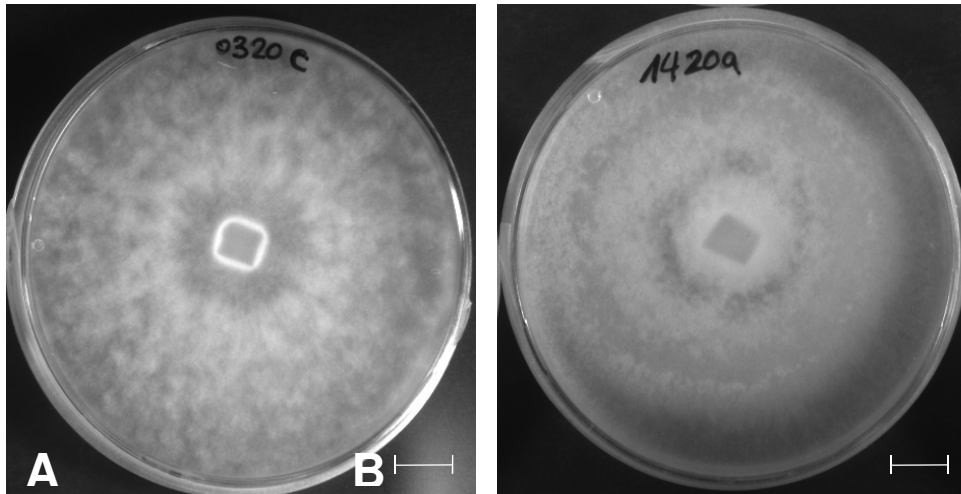


Figure 32: Growth on PDB-agar plates at 20 °C. A is *Pythium dissotocum* P100.30 and B is EMTS 1.2.1 from the *Phytophthora lacustris* strains. Picture A was taken after three days, picture B after eight days. Scale bar = 0.75 cm in all pictures

3.4. Characterisation of enzymes involved in long-chain fatty acid synthesis in *Pythium dissotocum* P100.30

In order to identify the enzymes and verify the findings of the genomic and transcriptomic data oligonucleotides were designed.

In the gene ontology table 18019 protein coding genes were annotated. Protein domains were searched in the gene ontology table and revealed multiple putative enzymes possibly involved in the fatty acid synthesis. Search for the $\Delta 6$ -elongase gave 21 hits, for the $\Delta 12$ -desaturase 16 hits, for the $\Delta 5$ -desaturase seven hits, for the $\Delta 6$ -desaturase 15 hits, for the $\Delta 15$ -desaturase 17 hits and for the $\Delta 4$ -desaturase six hits. The sequences of the hits were extracted from the genomic data and searched in the public database NCBI. Because the quality of the genome assembly was not sufficient to resolve the sequences, sequences of similar enzymes were taken from the public databases Ncbi (Clark *et al.*, 2016), and based on highly conserved regions of each

corresponding enzyme oligonucleotides were designed using Primer3 (Untergasser *et al.*, 2012). Genomic DNA from the *Pythium dissotocum* strain P100.30 was used as the template for DNA amplification.

In total 226 oligonucleotides were designed to verify the sequences from enzymes involved in the synthesis of long chain fatty acids. 48 oligonucleotides verified the sequences of six enzymes, five desaturases and one elongase, by producing DNA fragments. Blasting the obtained sequences against the public database NCBI (Clark *et al.*, 2016) and against the transcriptomic data of P100.30 helped to clearly identify the open reading frame and to verify the expression of said enzymes.

To classify the protein families the sequences were translated into the protein sequence and with Interproscan (Jones *et al.*, 2014) domains and protein families were clarified.

Motifs were searched in the protein sequences with Geneious 9.1.8 (www.geneious.com) and multiple protein alignments were used to compare existing motifs and conserved regions of similar enzymes from different oomycetes, namely from organisms belonging to the *Saprolegniomycetes* and the *Peronosporomycetes*.

To visualize the structure and localization of the enzymes in the organelle wall structure figures were created.

3.5. Elongase of P100.30

Elongases are the rate-limiting enzymes responsible for the synthesis of fatty acids with a longer carboxylic chain than C14:0. The elongation is a condensation step in which two carbon atoms are added to the carbon-chain by elongases. Elongases either belong to the ELO-family for long chain fatty acids or to the ELOVL-family for very long chain fatty acids. (Monroig and Kabeya, 2018)

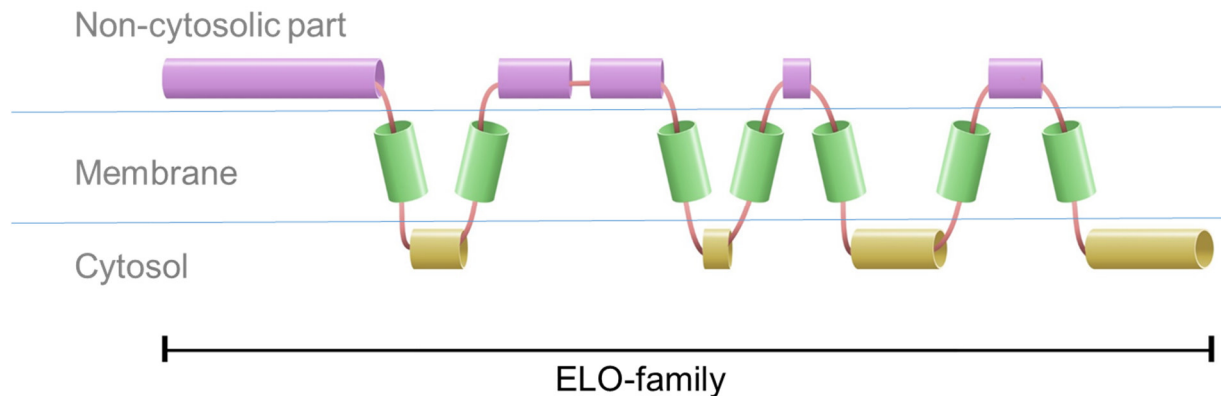


Figure 33: Protein domains of the elongase of P100.30. Non-cytosolic parts are purple, transmembrane helices are green and cytosolic domains are yellow.

The sequences derived from genome and transcriptome sequencing revealed the open reading frame consisted of 831 bp, translated into a protein with 276 amino acids. Annotation of the domains present in the protein sequence of the elongase was done with Interproscan. The annotation revealed that the elongase has 16 annotated domains, five in the non-cytosolic part, seven transmembrane helices who span the membrane and four domains located in the cytosol of the cell, visualized in Figure 33. The enzyme, belonging to the integral membrane proteins, consisted of three regions with a molecular weight of 32.06 kDa.

In the N-terminal region two transmembrane domains were found and in the C-terminal region two transmembrane domains together with an ER-retention signal (KKXX) and a central part with a hydrophilic loop region were found.

Comparison of the amino acid sequences with the Blosum90 matrix (threshold=1) revealed that the *Pythium dissotocum* $\Delta 6$ -elongase had 20.4 % similarity to the elongase from *Aphanomyces astaci* and *Saprolegnia diclina*, 20 % similarity to the elongase from *Saprolegnia parasitica* and 20.1 % *Aphanomyces euteiches*. Similarity to the *Peronosporomycete* elongases was much higher with 92.4 % to *Pythium aphanidermatum* and 86.9 % to *Phytophthora parasitica*.

Elongases are involved in the elongation of the carbon-chain in the fatty acid synthesis of long chain fatty acids which is predicted to be located in the endoplasmatic reticulum. The substrates for elongation would be C18 and C20 fatty acids.

ELO family domains are highly conserved in eukaryotes. They share similar biochemical features like a minimum of five membrane spanning domains and a histidine box. In the elongase of *Pythium dissotocum* one histidine box was found accompanied by two ER-retention signals. Comparing the aligned protein sequences in Figure 34 revealed that the elongases from the *Peronosporomycetes* had similar structures in regard to the position and number of their histidine box as well as the ER-retention signal. The elongases belonging to organisms from the *Saprolegniomycetes* had up to five additional histidine boxes but no ER-retention signal.

The C-terminal part of the *Peronosporacean* protein sequence was highly similar whereas this part of the protein sequence in the *Saprolegniomycetes* did not exist. These factors clearly distinguished the *Peronosporomycetic* elongases from the *Saprolegniomycetic* elongases.



Figure 34: Protein alignment of the elongase of *Pythium dissotocum* and elongases from other oomycetes. Thick arrows mark histidine boxes and the smaller arrows mark the ER-retention signal. The first four sequences belong to members of the *Saprolegniomycetes*, the last four belong to the *Peronosporomycetes*.

In many organisms two separate elongases are involved in the synthesis of polyunsaturated fatty acids, one $\Delta 5$ - and a $\Delta 6$ -elongase while in others one elongase elongates both, C18 substrates as well as C20 substrates.

In the P100.30 genome only one sequence coding for a $\Delta 6$ -elongase could be found, indicating that this elongase could work on both substrates.

3.6. Desaturases of P 100.30

Desaturases play an important part in the synthesis of polyunsaturated fatty acids as they introduce C=C double bonds in existing fatty acids and convert saturated fatty acids into unsaturated fatty acids or insert double bonds into already saturated ones. These enzymes exist in all living organisms but their distinct role differs as well as their structural features. The differences in their structure display the different tasks and substrates they can act on. Well known eukaryotic desaturases are $\Delta 6$ -desaturases, $\Delta 5$ -desaturases, $\Delta 12$ -desaturases and $\Delta 15$ -desaturases and lots of the knowledge existing about eukaryotic desaturases comes from studying desaturases from microorganisms.

Many desaturases share similar structural motifs that are highly conserved. Common shared motifs are for example a cytochrome b5 domain in the N-terminal part of the protein and seven histidine boxes in the C-terminal part forming the His box and even more specific, in carboxyl-end desaturases a substitution of histidine with a glutamine in the third motif. These structural similarities are said to be crucial for the catalytic activity.

3.7. $\Delta 4$ -desaturase

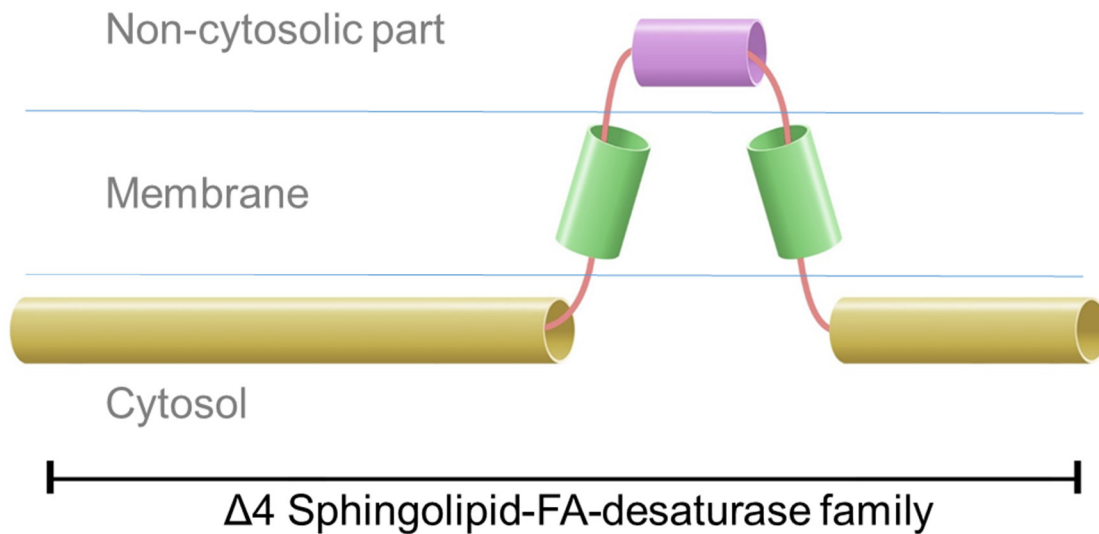


Figure 35: Protein domains of the elongase of P100.30. Non-cytosolic parts are purple, transmembrane helices are green and cytosolic domains are yellow.

The $\Delta 4$ -desaturase sequence of *Pythium dissotocum* strain P100.30 had 1011 bp encoding for 336 amino acids resulting in a molecular weight of 38.58 kDa.

In the protein two large cytosolic domains were connected to the non-cytosolic domain with two transmembrane domains, as shown in Figure 35. The N-terminal and the C-terminal part were both located in the cytosolic part of the cell. More than 95 % of the protein sequence matched to a family annotated as the $\Delta 4$ -sphingolipid-desaturase-family, implying that the protein sequence of the $\Delta 4$ -desaturase was a homolog to the $\Delta 4$ -sphingolipid-desaturase.

The $\Delta 4$ -desaturase is an integral membrane protein required for the aerobic synthesis of docosahexaenoic acid by the introduction of a cis double bond at the $\Delta 4$ -position of fatty acids. Fatty acid desaturases are enzymes that catalyse the insertion of a double bond at the Δ -position of fatty acids. There seem to be two distinct families of fatty acid desaturases which do not seem to be evolutionary related.

In the first family Stearoyl-CoA desaturases can be found while in the second family bacterial fatty acid desaturases, Plant-stearoyl-acyl-carrier-protein desaturases and cyanobacterial desaturases can be found. The desaturase can introduce a second cis double bond at the $\Delta 12$ -position of fatty acids and is said to be involved in the chilling tolerance. If the temperature requires more unsaturated fatty acids of the membrane lipids, the desaturase can introduce them into membrane bound fatty acids.

The sequence alignment shown in Figure 36 visualizes how similar and conserved the $\Delta 4$ -desaturases are. Two histidine boxes were found in all examined sequences as well as ER-retention signals. The ER-retention signal positions varied, in the *Saprolegniomycetes*, *Pythium insidiosum* and *Pythium dissotocum* only one ER-retention signal was present while the other *Peronosporomycetes* two ER-retention signals were found.

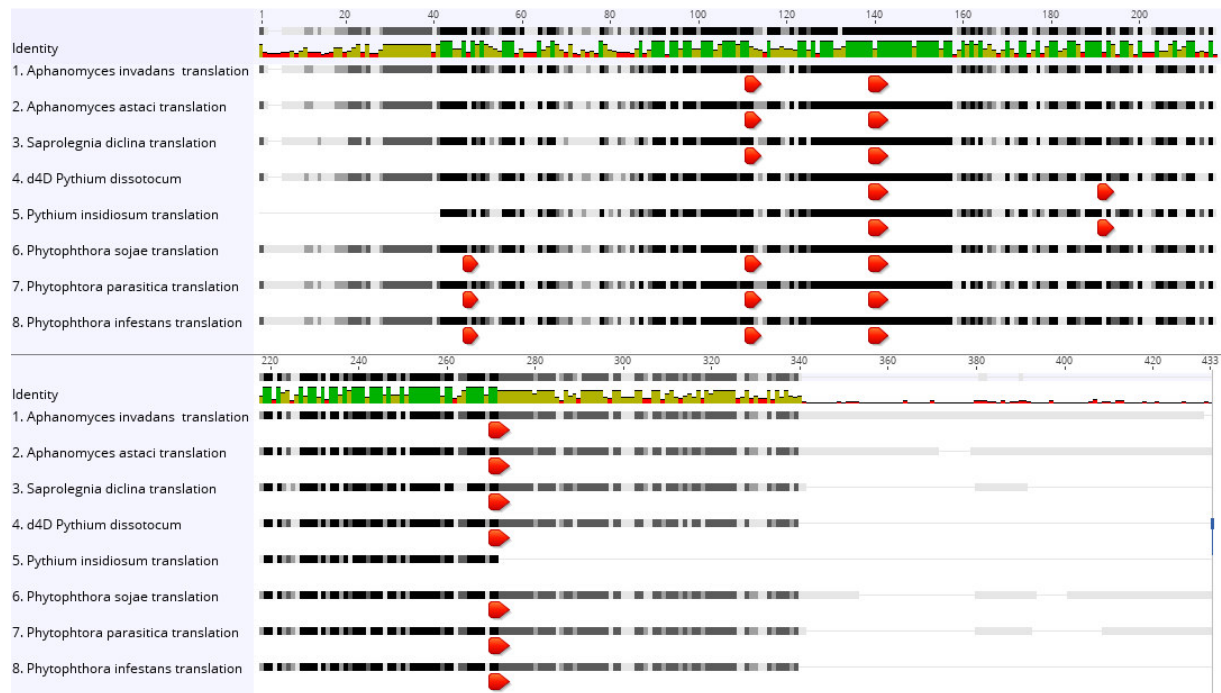


Figure 36: Protein alignment of the $\Delta 4$ -desaturase protein sequences from different oomycetes. Thick arrows mark histidine boxes, smaller arrows mark ER-retention signals. Similarity is shown in shades of black, black meaning 100 % similarity.

Comparison of the amino acid sequences (Blosum90, threshold=1) revealed that the $\Delta 4$ -desaturases from *Pythium dissotocum* shared 57.9 % similarity with *Aphanomyces invadans*, 58.6 % with *Aphanomyces astaci*, 66.9 % with *Saprolegnia diclina*, 58 % with *Pythium insidiosum*, 67 % with *Phytophthora sojae*, 69.9 % with *Phytophthora parasitica* and 80.8 % with *Phytophthora infestans*.

3.8. $\Delta 5$ -desaturase

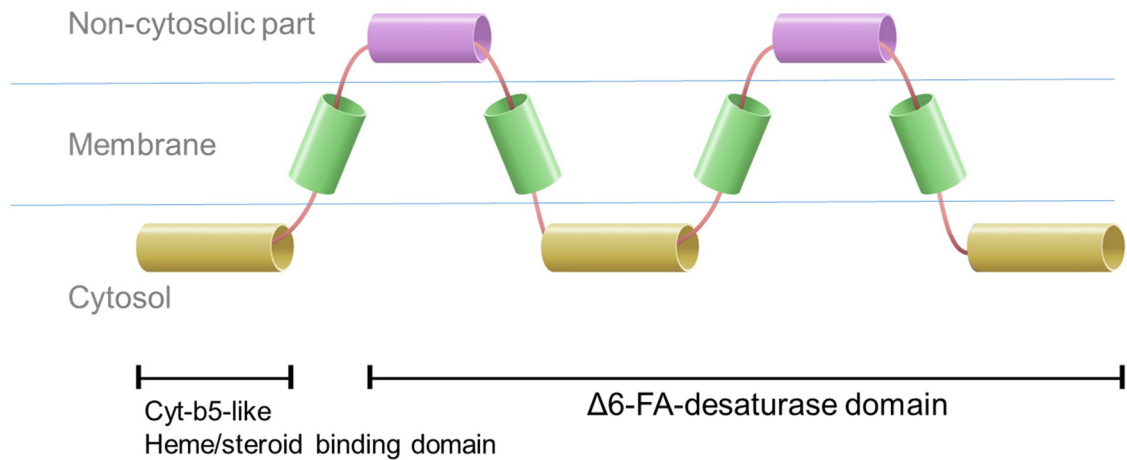


Figure 37: Protein domains of the $\Delta 5$ -desaturase of P100.30. Non-cytosolic parts are purple, transmembrane helices are green and cytosolic domains are yellow.

The $\Delta 5$ -desaturase and the $\Delta 6$ -desaturase appeared to be paralogs. In the N-terminal region of the $\Delta 5$ -desaturase a cytochrome b5-like-heme/steroid-binding domain was found as well as a $\Delta 6$ -fatty acid-desaturase domain, shown in Figure 37. The sequence of the $\Delta 5$ -desaturase seemed to belong to the family of the $\Delta 5$ -desaturases.

In the C-terminal region multiple membrane spanning helices were found. In total nine domains were identified, starting in the cytosolic part of the cell and spanning four times through the membrane with two domains located in the non-cytosolic part and the C-terminal region located in the cytosol. The protein sequence consisted of 488 amino acids encoded for by 1467 bp resulting in a molecular weight of 54.51 kDa.

The cytochrome b5-like heme/steroid binding domain is thought to be important as it supposed to ensure and enhance catalytic activity. The $\Delta 5$ -desaturase desaturates either dihomo- γ -Linolenic acid (C20:3 ω 6) to arachidonic acid (C20:4 ω 6) or of eicosatetraenoic acid (C20:4 ω 3) to eicosapentaenoic acid (C20:5 ω 3). The substrates have a chain length of 20 carbon atoms while the position of the already existing double bond varies and $\Delta 5$ -desaturases belong to the front-end desaturases.

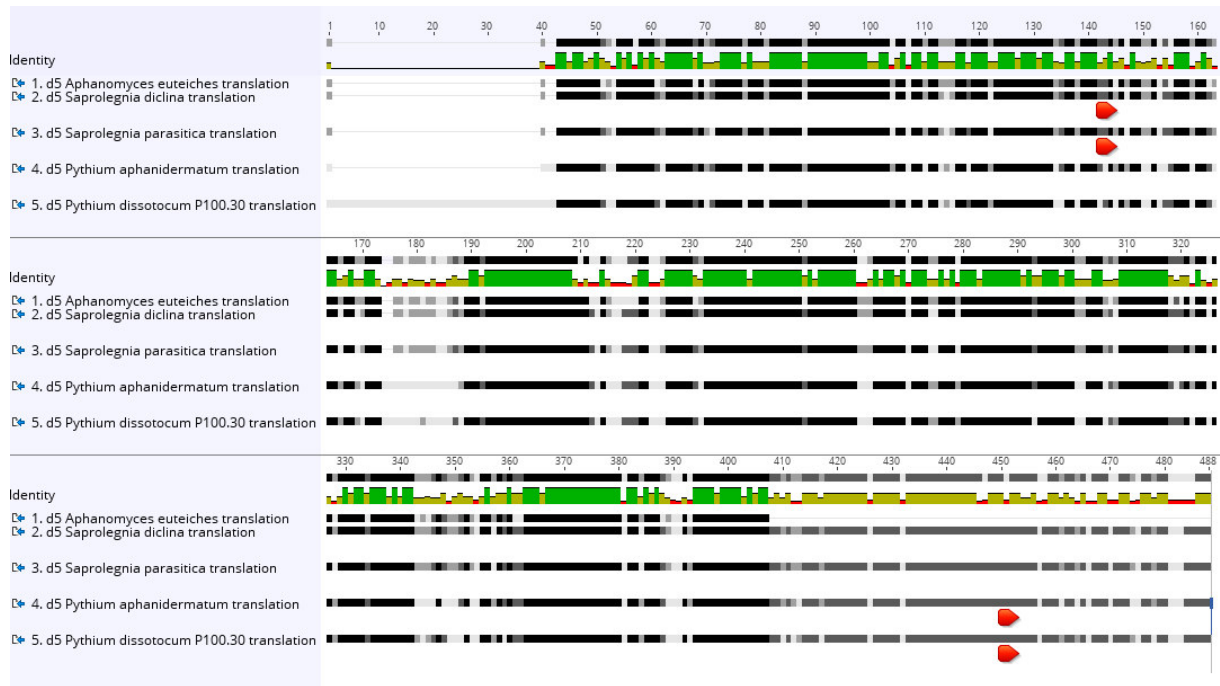


Figure 38: Protein alignment of the delta5-desaturase of different oomycetes. Red arrows indicate ER-retention signals, similarity is shown in shades of black while black stands for 100 % similarity.

In Figure 38 the alignment of the deduced amino acid sequences is shown. No histidine boxes were found but the red arrows show the positions of the ER-retention-signal motifs (KKXX). While the *Aphanomyces euteiches* sequence had no ER-retention signal motif at all, the two sequences of the *Saprolegnia* strains had the ER-retention-signal at the same position in the N-terminal part of the sequence. Both sequences of the *Pythium* strains share the same position of the ER-retention signal, located in the C-terminal part of the protein. The sequences of the *Pythium* strains shared more similarities than they did with the sequences belonging to the *Saprolegniomycetes*. The C-terminal part of the protein sequence was more variable while the N-terminal part and the middle part were, with short interruptions, highly conserved. Similarities of sequences, calculated by the Blosum90 matrix (threshold=1), to the $\Delta 5$ -desaturase from *Pythium dissotocum* were to *Aphanomyces euteiches* 55.9 %, to *Saprolegnia diclina* 71.1 %, to *Saprolegnia parasitica* 71.1 % and to *Pythium aphanidermatum* 84.4 %.

3.9. $\Delta 6$ -desaturase

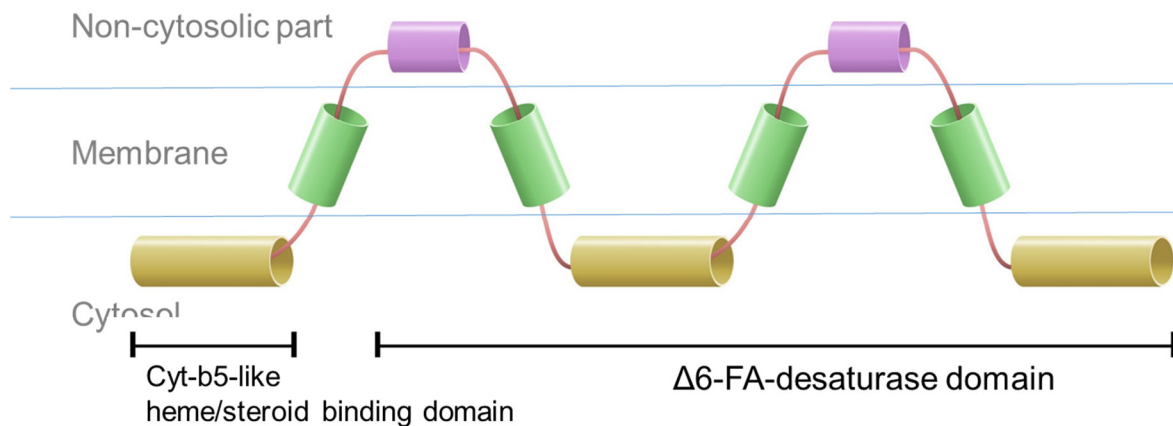


Figure 39: Protein domains and families of the elongase of P100.30. Non-cytosolic parts are purple, transmembrane helices are green and cytosolic domains are yellow.

The protein sequence of the $\Delta 6$ -desaturase consisted of 457 amino acids, coded for by 1374 bp. The $\Delta 6$ -desaturase had, as well as the $\Delta 5$ -desaturase, a cytochrome b5-like-heme/steroid-binding domain fused at the N-terminal part of the main fatty-acid-desaturase domain and in the C-terminal region multiple helices were spanning through the membrane, shown in Figure 39. Multiple fatty acid desaturase domains were identified in the sequence as well as the sequence was recognized to be part of the $\Delta 5$ -fatty acid-desaturase family.

Nine protein domains were found in the sequence of the protein, just like in the $\Delta 5$ -desaturase and the pattern of how the domains were located in the cytosolic and non-cytosolic part and spanned the membrane are similar. The domains located in the non-cytosolic part of the cell were shorter than the domains of the $\Delta 5$ -desaturase.

Similarity to $\Delta 6$ -desaturases of other oomycetes was 35.7 % in *Aphanomyces astaci*, 70.3 % in *Saprolegnia parasitica* and 94.5 % in *Pythium aphanidermatum*.

The action of the $\Delta 6$ -desaturase is thought to be the rate limiting step in the PUFA synthesis, responsible for introducing a double bond into either linoleic acid (C18:2 ω 6) or α -linolenic acid (18:2 ω 3).

The $\Delta 5$ -desaturase and the $\Delta 6$ -desaturase both belong to the front-end-desaturases, introducing a double bond between a pre-existing one and the carboxyl end of the substrate.

The sequence alignment of the $\Delta 6$ -desaturase of *Pythium dissotocum* with *Aphanomyces astaci*, *Saprolegnia parasitica*, *Pythium aphanidermatum*, *Pythium irregulare* and *Pythium splendens* is shown in Figure 40.

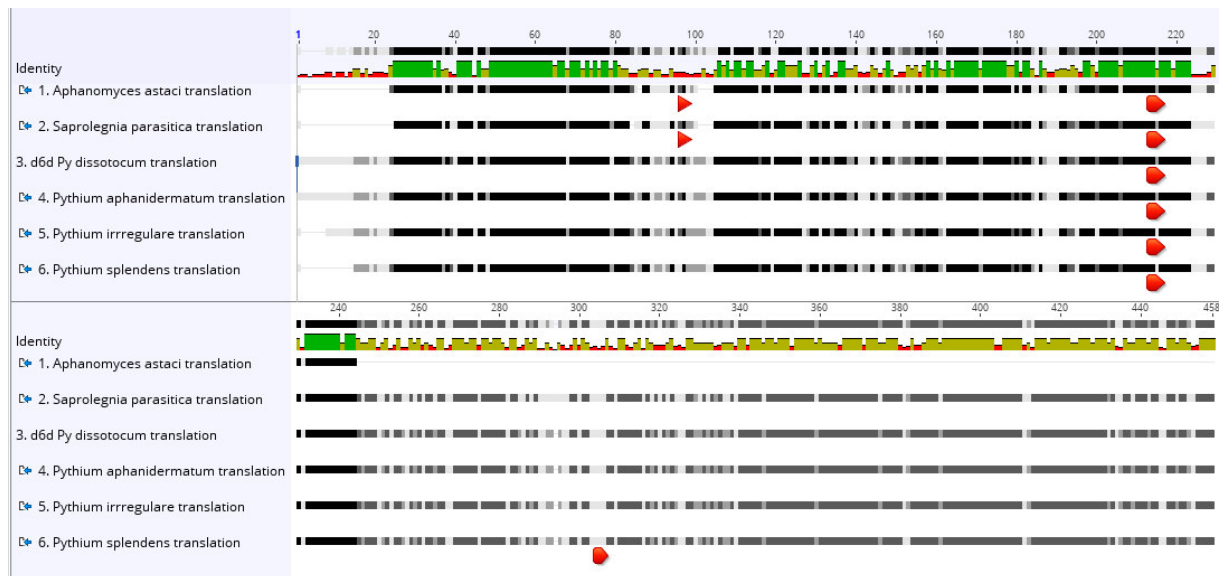


Figure 40: Protein alignment of the delta5-desaturase of different oomycetes. Red pointy arrows indicate ER-retention signals, thick red arrows mark histidine-boxes, and similarity is shown in shades of black while black stands for 100 % similarity.

The protein sequences from the *Peronosporomycetes* were longer than the *Saprolegniomycete* sequences and had conserved parts in the additional part of the C-terminal sequence in common. The C-terminal part otherwise was highly similar, interrupted by more dissimilar parts whereas the N-terminal part of the protein sequence was less similar.

Highly conserved were the locations of the histidine boxes whereas the ER-retention signal only seemed to be conserved in the two sequences from the *Saprolegniomycetes*.

The similarities, calculated by the Blosum90 matrix (threshold=1), to the $\Delta 6$ -desaturase from *Pythium dissotocum* were to *Aphanomyces astaci* 73.4 %, to *Saprolegnia parasitica* 74.3 %, to *Pythium irregulare* 82.7 % and to *Pythium aphanidermatum* 94.5 %.

3.10. Δ 12-desaturase

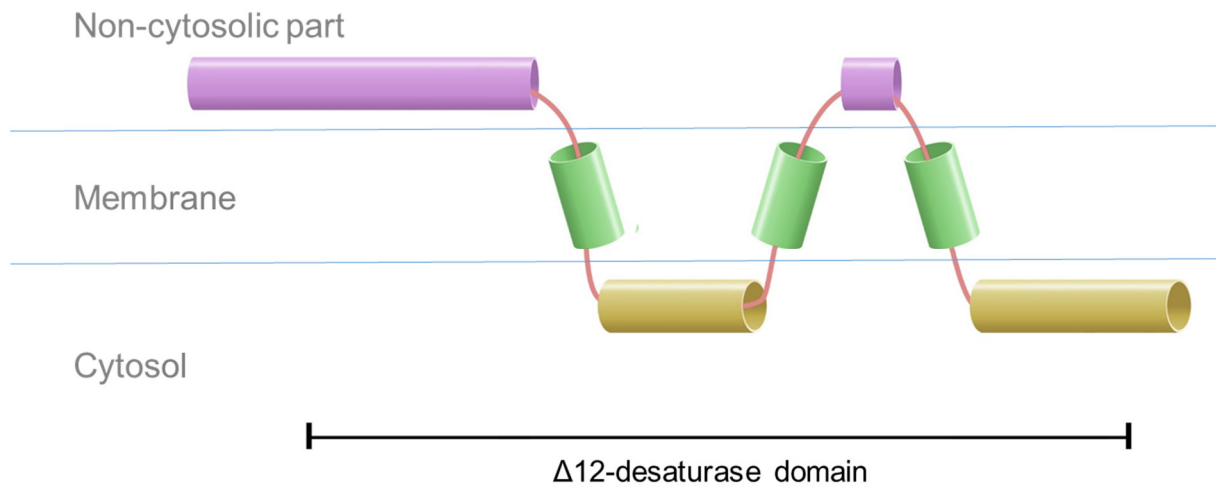


Figure 41: Protein domains of the desaturase of P100.30. Non-cytosolic parts are purple, transmembrane helices are green and cytosolic domains are yellow.

The Δ 12-desaturase protein-sequence had 1197 bp coding for 398 amino acids.

In the protein sequence a Δ 12-desaturase domain was found as well as different families were recognized. The sequence belonged to a fatty acid-desaturase family and a ω -6 fatty acid-desaturase family. An important part of the protein was its extensive hydrophobic regions that were spanning the membrane. In total two non-cytosolic domains were found, three transmembrane domains and two domains located in the cytosol, as shown in Figure 41.

The N-terminal part of the protein was located in the non-cytosolic part, transmembrane helices spanned the membrane and led the protein into the cytosolic part, back to the non-cytosolic part for the C-terminal part to end in the cytosol of the cell.

In the highly conserved parts of the protein sequence three histidine cluster motifs with eight histidine residues existed that were reported to be catalytically essential.

The Δ 12-desaturase is responsible for the synthesis of C18:2 ω 6 linoleic acid with C18:1 oleic acid being the desaturated substrate. It is the first double bond introduced in the pathway of the long chain polyunsaturated fatty acids.

Δ 12-desaturases are commonly found to be membrane bound and belong to the methyl-end desaturases and are widespread in plants and microorganisms while front-end desaturases are commonly found in animals and microorganisms.

The desaturase can introduce a second cis double bond at the Δ 12-position of fatty acids and is said to be involved in the chilling tolerance. If the temperature requires

more unsaturated fatty acids of the membrane lipids, the desaturase can introduce them into membrane bound fatty acids.

Sequence similarities between *Pythium dissotocum* and $\Delta 12$ -desaturases from other oomycetes were 75.5 % to *Aphanomyces euteiches*, 84.7 % to *Phytophthora parasitica* and 91.5 % to *Pythium aphanidermatum*.

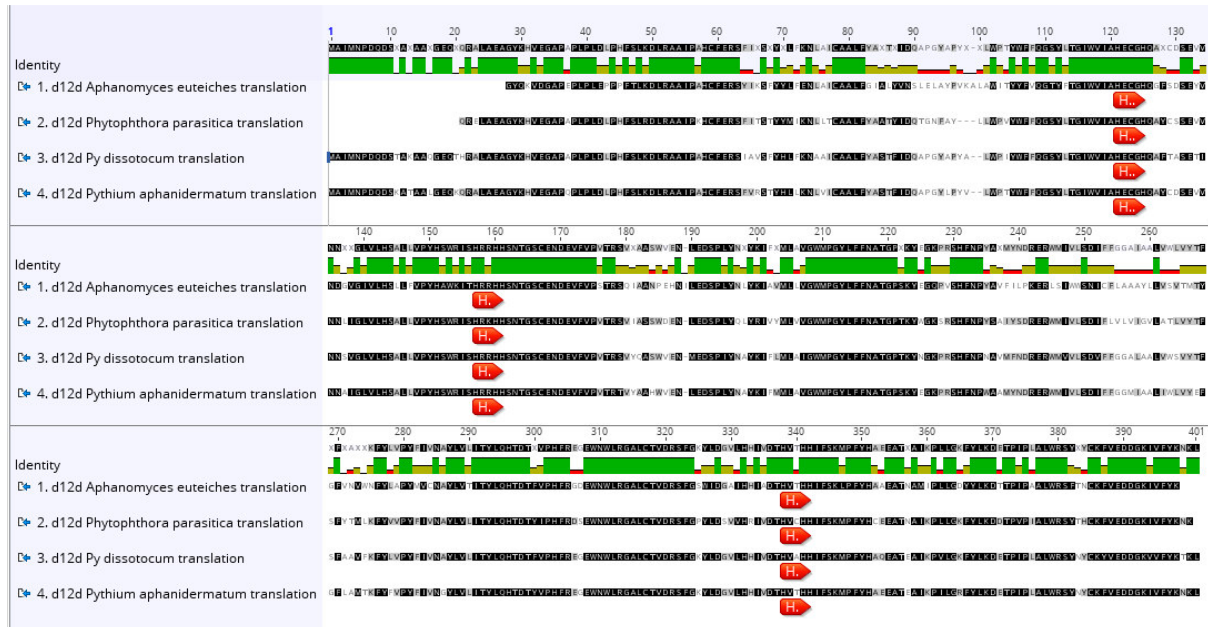


Figure 42: MAFFT alignment of the protein sequences of the delta 12-desaturase of different oomycetes. The purple arrows highlight HXXXH-motifs.

As shown in Figure 42 the three histidine-rich HXXXH motifs were highly conserved within the analysed oomycetes from both classes, the *Saprolegniomycetes* and the *Peronosporomycetes*. The majority of the sequence was highly conserved among the isolates from the *Saprolegniomycetes* and *Peronosporomycetes*, except the beginning of the protein sequence showed a bit variance in lengths with the sequences of the *Pythium* species being longer than the other sequences.

The $\Delta 12$ -desaturase and the $\Delta 15$ -desaturase belonged to the methyl-end-desaturases introducing double bonds between an existing unsaturation and the methyl-terminus of the fatty acid.

3.11. $\Delta 15$ -desaturase

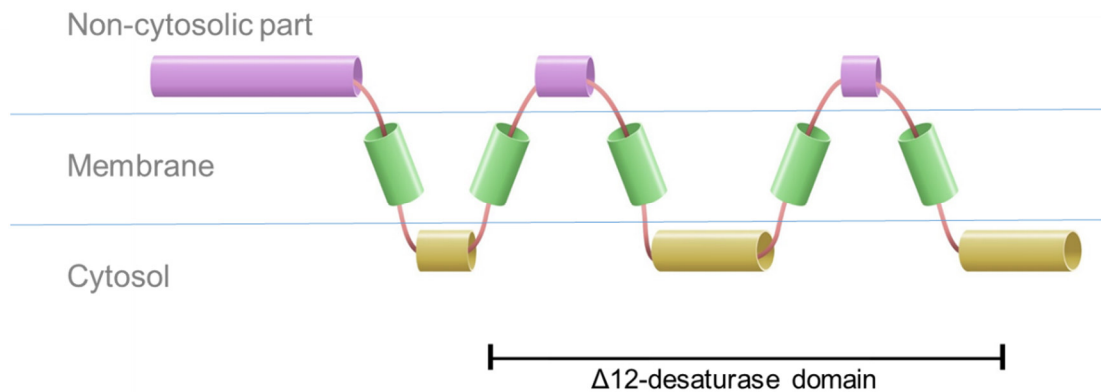


Figure 43: Protein domains of the elongase of P100.30. Non-cytosolic parts are purple, transmembrane helices are green and cytosolic domains are yellow

The $\Delta 15$ -desaturase protein sequence consisted of 367 amino acids coded for by 1104 bp.

Like in the $\Delta 12$ -desaturase a $\Delta 12$ -desaturase-domain was matched to the sequence and the sequence was recognized to be part of the ω -6 fatty acid desaturase-family. Compared to the domain prediction of the $\Delta 12$ -desaturase structural similarities were observed, even though the $\Delta 15$ -desaturase had more membrane spanning domains. In total three non-cytosolic domains were found, five transmembrane domains and three cytosolic domains, shown in Figure 43.

The $\Delta 12$ -desaturase and the $\Delta 15$ -desaturase belonged to the methyl-end-desaturases introducing double bonds between an existing unsaturation and the methyl-terminus of the fatty acid.

The $\Delta 15$ desaturase is supposed to desaturate linoleic acid (C18:2 ω 6) to α -linolenic acid (C18:2 ω 3) and to turn the C18-molecule from a ω -6 fatty acid into a ω -3 fatty acid. Higher animals, including humans, are lacking the $\Delta 12$ - and $\Delta 15$ -desaturases. With α -linolenic acid the first essential nutrient was produced in the pathway.

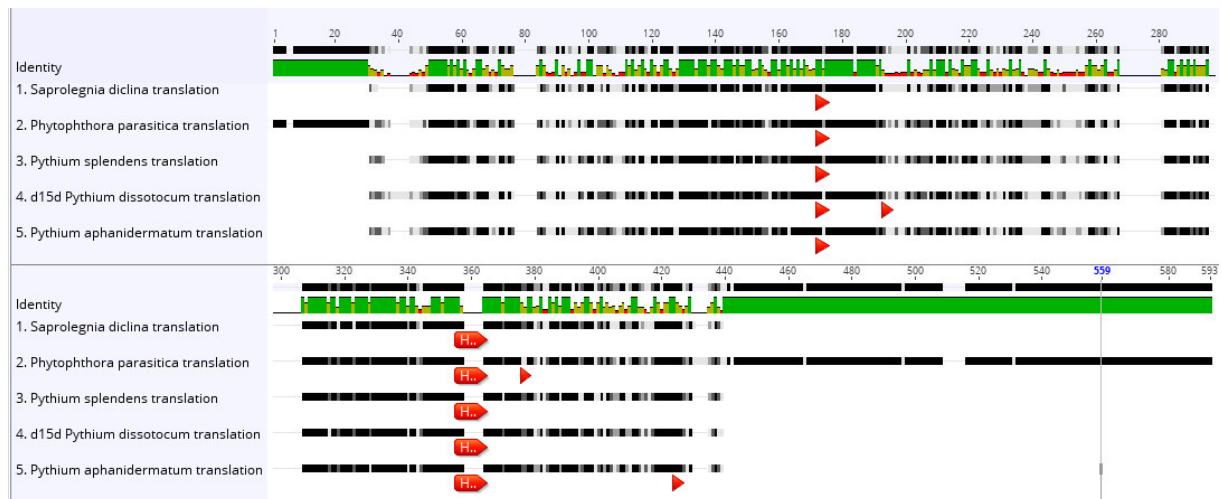


Figure 44: Protein alignment of the delta 15 desaturase from different oomycetes. ER-retention signals are the pointy arrows in red and the thicker arrows are Histidine boxes

As the protein alignment in Figure 44 shows the sequences were highly conserved. All of the sequences had an ER-retention signal as well as conserved histidine boxes at the same location. The similarity, calculated by the BLSM90 matrix (threshold=1) was from *Pythium dissotocum* to *Phytophthora parasitica* 71.2 %, to *Pythium splendens* 70.6 %, to *Saprolegnia diclina* 64.1 % and to *Pythium aphanidermatum* 88.3 %.

3.12. Pathway of long chain fatty acid synthesis in the *Pythium dissotocum* strain P 100.30

The pathway of the production of long chain fatty acids is of high interest. To elucidate which route the enzymes chose to produce the fatty acids was a step further in the understanding of the fatty acid synthesis.

For the elucidation only the fatty acid profiles from the *Pythium dissotocum* strain P100.30 without the branched fatty acids were used.

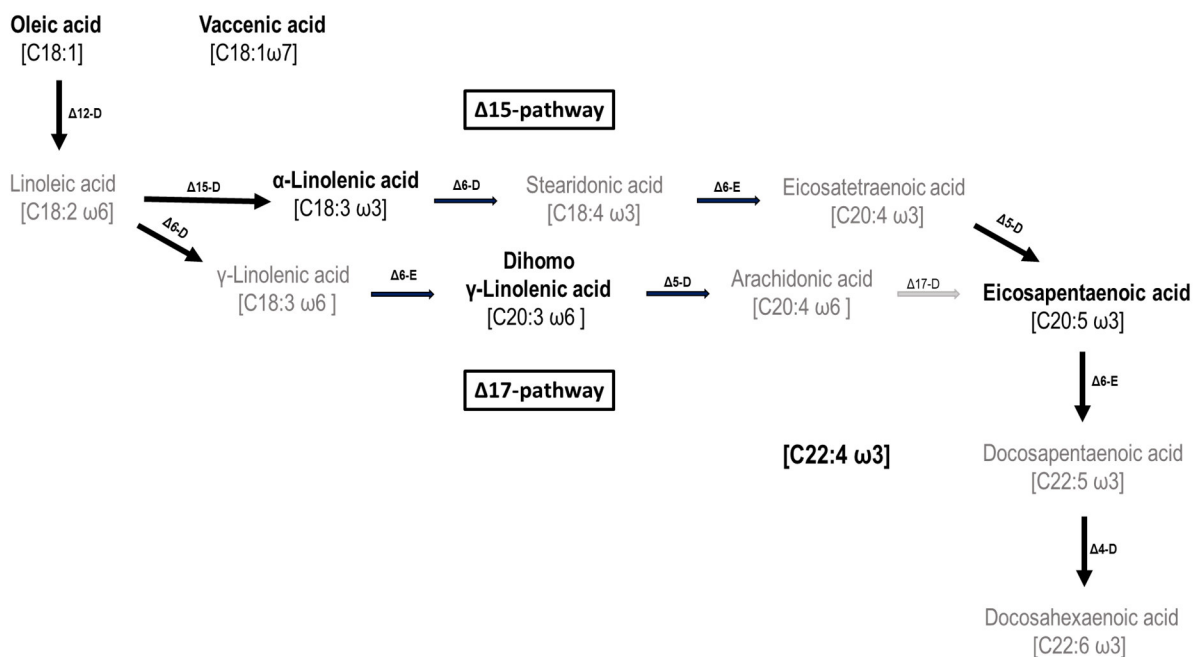


Figure 45: Combined results based on the fatty acids profiles of P100.30 and the genomic and transcriptomic data to identify the enzymes. Detected fatty acids and enzymes are marked with bold black letters, the fatty acids and enzyme that are not found are grey.

Combining the results from the FAME-analysis, the annotated genes found in the genome and the transcriptome of P100.30, the pathway of the VLCPUFA-synthesis could be elucidated.

As shown in Figure 45 between linoleic acid and eicosapentaenoic acid the route could either go through the $\Delta 15$ -desaturase-pathway or the $\Delta 17$ -desaturase pathway. The difference between the pathways was the name-giving desaturase and the fatty acid with the first introduced ω -3 desaturation.

The first fatty acid from the pathway found in the FAME profiles was oleic acid (C18:1), a fatty acid without any desaturation. The sequence of the first enzyme, a $\Delta 12$ -desaturase, using oleic acid as its substrate, was verified via PCR and the transcriptomic data.

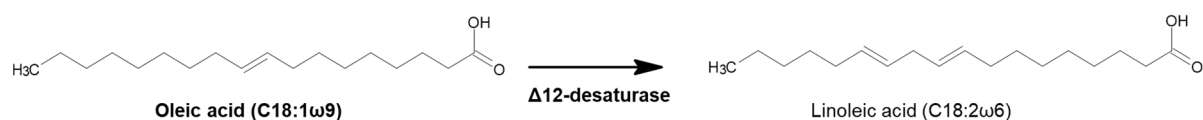


Figure 46: Desaturation of oleic acid by the $\Delta 12$ -desaturase leads to linoleic acid by the introduction of the double bond at the sixth carbon atom from the methyl-end. Fatty acids and enzymes with bold letters were detected/verified by FAME-analysis or PCR and genomic/transcriptomic data.

The product of the desaturation of oleic acid by the $\Delta 12$ -desaturase, shown in figure 46, would be linoleic acid (C18:2 ω 6) but it was not detected in the FAME analysis.

Consecutively either a $\Delta 6$ - or a $\Delta 15$ -desaturase would follow the first desaturation, resulting in the next product. The sequences of both enzymes, the elongase as well as the $\Delta 15$ -desaturase, were found and verified via polymerase chain reaction and the transcriptomic data.

The next desaturation step led to the intermediate product α -linolenic acid, the first ω -3 fatty acid in the pathway. This desaturation, as shown in figure 47, was thought to be done by a $\Delta 15$ -desaturase. The $\Delta 15$ -desaturase was verified via PCR and the genomic and transcriptomic data as well as the product, α -linolenic acid, was detected in the FAME analysis.

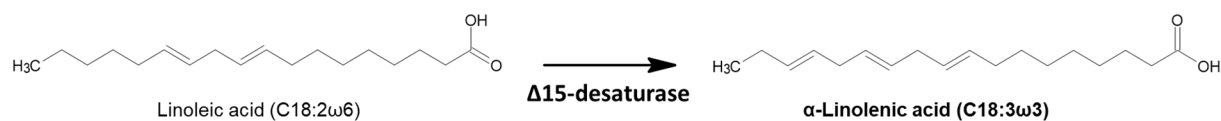


Figure 47: Assumed introduction of the double bond at the ω -3 position by the $\Delta 15$ -desaturase, turning linoleic acid into α -linolenic acid. Fatty acids and enzymes with bold letters were detected/verified by FAME-analysis or PCR and genomic/transcriptomic data.

The next desaturation step on α -linolenic acid is thought to be done by a $\Delta 6$ -desaturase resulting in stearidonic acid, C18:4 ω 3 (Figure 48). Stearidonic acid could not be detected in the FAME profile but the sequence of the $\Delta 6$ -desaturase was found in the genomic and transcriptomic data and verified with PCR.

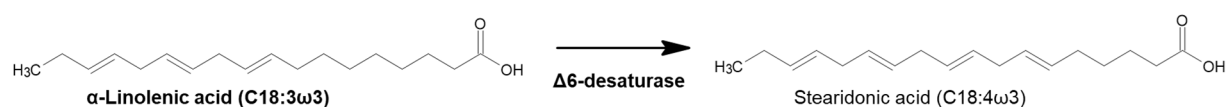


Figure 48: The desaturation of α -linolenic acid (C18:3 ω 3) led to the formation of stearidonic acid (C18:4 ω 3). The enzymatic reaction was thought to be catalyzed by the $\Delta 6$ -desaturase. Fatty acids and enzymes with bold letters were detected/verified by FAME-analysis or PCR and genomic/transcriptomic data.

The next fatty acid detected in the FAME profiles was dihomo- γ -linolenic acid, a ω -6 fatty acid.

The reaction needed for the formation of dihomo- γ -linolenic is shown in figure 49 and figure 50.

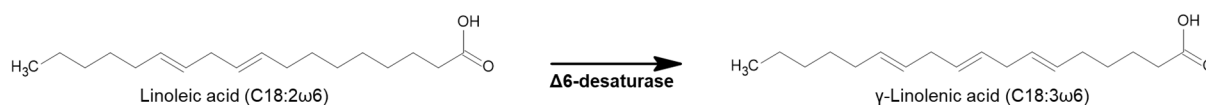


Figure 49: γ -linolenic acid (C18:3 ω 6) is the assumed product of the enzymatic reaction of the Δ 6-desaturase with linoleic acid (C18:2 ω 6). Fatty acids and enzymes with bold letters were detected/verified by FAME-analysis or PCR and genomic/transcriptomic data.

The synthesis would have gone a different route starting from linolenic acid. Instead of the introduction of the first ω -3 double bond and the formation of stearidonic acid, γ -linolenic acid, a ω -6 fatty acid, would have been synthesized with the help of the Δ 6-desaturase. Neither linoleic acid, nor γ -linolenic acid could be detected in the FAME analysis. The Δ 6-desaturase could be verified with the PCR-approach as well as with the genomic and transcriptomic data. This desaturase can catalyse the introduction of a double bond on both, ω -3 and ω -6 substrates.

The Δ 6-elongase elongates γ -linolenic acid by two carbon atoms and the resulting ω -6 fatty acid is dihomogamma-linolenic acid. Dihomogamma-linolenic acid could be, even though only in small amounts, found in the FAME-analysis as well as the Δ 6-elongase could be verified.

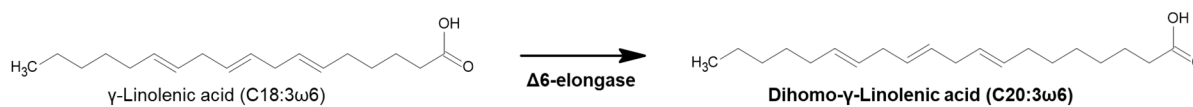


Figure 50: The elongation of γ -linolenic acid (C18:3 ω 6) would lead to the production of dihomogamma-linolenic acid (C20:3 ω 6) catalysed by the Δ 6-elongase. Fatty acids and enzymes with bold letters were detected/verified by FAME-analysis or PCR and genomic/transcriptomic data.

The Δ 6-elongase was the only elongase found in the genomic and transcriptomic data, indicating that this elongase can work on two substrates, a C18 fatty acid and a C20 fatty acid.

After the addition of two carbon atoms on the C18 product, either stearidonic acid (C18:4 ω 3) or γ -linolenic acid (C18:3 ω 3) a C20 fatty acid emerges, either dihomogamma-linolenic acid (C20:3 ω 6), the ω -6 version of the C20 fatty acid, or eicosatetraenoic acid (C20:4 ω 3), the ω -3 version.



Figure 51: Enzymatic reaction of the Δ 6-elongase with the ω -3 substrate stearidonic acid (C18:4 ω 3) resulting in the formation of eicosatetraenoic acid (C20:4 ω 3). Fatty acids and enzymes with bold letters were detected/verified by FAME-analysis or PCR and genomic/transcriptomic data.

Neither stearidonic acid (C18:4 ω 3), nor eicosatetraenoic acid (C20:4 ω 3) could be detected in the FAME-analysis, unlike the Δ 6-elongase. The putative synthesis of eicosatetraenoic acid is shown in Figure 51.

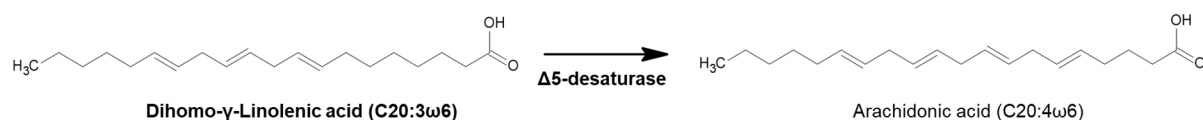


Figure 52: The $\Delta 5$ -desaturase catalyses the formation of arachidonic acid (C20:4 ω 6) as it introduces a double bond into dihomo- γ -linolenic acid. Fatty acids and enzymes with bold letters were detected/verified by FAME-analysis or PCR and genomic/transcriptomic data.

In Figure 52 the introduction of a double bond into dihomo- γ -linolenic acid (C20:3 ω 6) by the $\Delta 5$ -desaturase is shown, resulting in arachidonic acid (C20:4 ω 6). Dihomo- γ -linolenic acid was detected as well as the $\Delta 5$ -desaturase was verified but arachidonic acid could not be detected.

No C20:4 fatty acid could be detected in the FAME profiles but, as it can be seen in Figure 53, the enzyme responsible for the introduction of a double bond to turn arachidonic acid into a ω -3 fatty acid, a $\Delta 17$ -desaturase, could neither be found in the genomic or transcriptomic data.

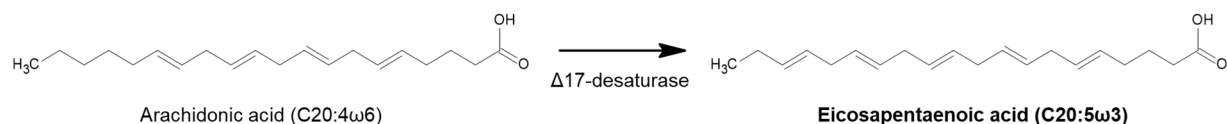


Figure 53: Synthesis of eicosapentaenoic acid (C20:5 ω 3), catalysed by the introduction of a double bond at the ω -3 position by a $\Delta 17$ -desaturase, starting from arachidonic acid (C20:4 ω 6). Fatty acids and enzymes with bold letters were detected/verified by FAME-analysis or PCR and genomic/transcriptomic data.

The $\Delta 17$ -desaturase is the characterizing enzyme for the $\Delta 17$ -pathway while the other pathway, to synthesize eicosapentaenoic acid, is characterised by the presence of the $\Delta 15$ -desaturase.

The reaction from eicosatetraenoic acid (C20:4 ω 3) to eicosapentaenoic acid (C20:5 ω 3) is catalysed by the $\Delta 5$ -desaturase and shown in Figure 54.

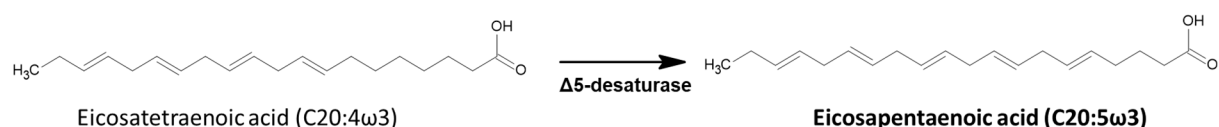


Figure 54: Desaturation of eicosatetraenoic acid (C20:4 ω 3) by the $\Delta 5$ -desaturase led to the formation of eicosapentaenoic acid (C20:5 ω 3) by the introduction of the double bond. Fatty acids and enzymes with bold letters were detected/verified by FAME-analysis or PCR and genomic/transcriptomic data.

The only detected C20 fatty acid in the FAME-analysis was eicosapentaenoic acid (C20:5 ω 3), but no intermediate product, like a C20:4 fatty acid, could be detected.

Eicosapentaenoic acid was found in huge amounts. The C20:5 ω 3 fatty acid is one of the long chain fatty acid with a strongly increasing demand, next to docosahexaenoic acid.

After the last desaturation-step the eicosapentaenoic acid will be elongated and turned in a fatty acid with 22 carbon atoms. The elongase found in the genomic data was thought to act on C18 substrates as well as on C20 substrates, elongating them to be C22 fatty acids. Docosapentaenoic acid was not detected in the FAME profiles and neither was docosahexaenoic acid.

The desaturase, acting on docosapentaenoic acid and catalysing the formation of docosahexaenoic acid is called a Δ 4-desaturase.

The sequence of such Δ 4-desaturase was found and verified as described in Figure 35.

The fatty acid with 22 carbon atoms found was labelled as C22:4 ω 3, even though the amounts of the fatty acid detected were low.

Another rare fatty acid found in the FAME analysis is vaccenic acid, a C18:1 ω 7 fatty acid. This unsaturated ω -7 fatty acid does not interfere with the pathway of long chain polyunsaturated fatty acids.

4. Discussion

4.1. Fatty acids in oomycetes

The aim of this study was to widen the current knowledge on oomycetes and their fatty acids, as well as their de novo synthesis.

In this study, 192 FAME profiles of 23 oomycetes belonging to the *Peronosporomycetes* were produced and analysed. For one of these, the *Pythium dissotocum* strain P100.30, genomic and transcriptomic data were generated and the enzymes involved in the de novo synthesis of long chain polyunsaturated fatty acids were identified and characterised. The combination of the FAME profiles produced and the enzymes identified led to the elucidation of the pathway of the long chain polyunsaturated fatty acids, as well as an overview of the fatty acid profiles of many members of the *Peronosporomycetes*.

The FAME profiles from the *Peronosporomycetes* revealed that, except for *Globisporangium ultimum* (formerly *Pythium ultimum*), the oomycetes produce high amounts of long chain polyunsaturated fatty acids. This finding, that the FAME profile of *Globisporangium ultimum* differed from the rest of the analysed *Pythium* species, supports the separation of *Globisporangium ultimum* from the *Pythium* species complex (Uzuhashi *et al.*, 2010). Not only did the detected fatty acids from *Globisporangium ultimum* differ from the rest of the *Pythium* species, but the growth rate and the phylogenetic distance of *Globisporangium ultimum* also support this separation.

All of the oomycetes profiled produced significant amounts of eicosapentaenoic acid (EPA). While the amounts of EPA produced differed among the oomycetes, it was notable that for all analysed strains the amount of EPA decreased with an increase in temperature.

The oomycetes were grown at 2 different temperatures, 20 °C and 27 °C, however, not all of the isolates fatty acid profiles could be obtained. Fatty acid synthesis in oomycetes is said to be mainly dependent on the temperature and the salinity at which they are grown (Tocher *et al.*, 1995; John E. Cronan and Jacob Thomas, 2009, xue; Xue *et al.*, 2013; Cronan and Thomas, 2009). Candidates especially from colder climates or from environments with high salinity produce high levels of EPA and docosahexaenoic acid (DHA) as these fatty acids ensure the integrity of the membranes (Devanadera *et al.*, 2019). All of the isolates used in this study, except for

LT7204, V2.4 and V21.2, were isolated in Frankfurt, Germany. These have adapted to the temperate climate which has an average temperature of 10.7 °C and this adaptation may be the reason for the poor growth at higher temperatures.

The dependency of the organisms on their fatty acid composition with respect to the temperature was shown in the study of Sun *et al.* (2013). When in cold shock, or generally if the temperature drops or rises, several desaturases, for example, the $\Delta 4$ -desaturase, can act directly on membrane-bound fatty acids to desaturate the fatty acid chain. The added double bond to the fatty acid chain hinders the fatty acids from becoming solid with decreasing temperatures, hence maintaining the function, stability and, especially, the fluidity of the membrane (Tocher *et al.*, 1995). Membrane-bound saturated fatty acids become pressed together tightly when the temperatures decrease because of their straight tails. The double bonds in natural unsaturated fatty acids introduce cis-“kinks” in the tails, resulting in a less dense packing structure and, thus, ensuring the integrity of the fluidity of the membrane even with decreasing temperatures (Arild C Rustan and Christian A Drevon, 2001; Rustan and Drevon, 2001). The regulation of the reaction to a cold shock is controlled at the gene expression level of the enzymes involved (Pe´gorier *et al.*, 2004; Cecile Clavaud *et al.*, 2009).

A study from Avis *et al.* (2007) demonstrated the importance of the unsaturated fatty acids in membrane integrity. Pathogens with high unsaturation levels in their fatty acid profiles were more sensitive to a treatment with aluminium chloride and sodium metabisulfate. The susceptibility to these salts, especially of *Phytophthora infestans*, was attributed to the high amounts of arachidonic acid in the bilayer of their membranes. When in contact with the salts, the organisms were found to lose a degree of their unsaturation and, as the authors concluded, the integrity of their membranes (Cecile Clavaud *et al.*, 2009; Avis *et al.*, 2007).

In a different study, Lerksuthirat *et al.* (2017) showed that the insensitivity to most antifungal drugs by the pathogen *Pythium insidiosum* is caused by its inability to produce sterols de novo. This study on linking the missing enzymes in the sterol biosynthesis as being the targets of the antifungal drugs analysed, demonstrates the importance of research on oomycetes.

Oomycetes are known for their ability to gain resistance rapidly against fungicides with devastating results for crop production. Developing new, powerful fungicides to minimise crop losses is needed as well as identifying the potential targets for such

fungicides (Pasteris *et al.*, 2016; Binyam Tsedaley, 2014). This thesis contributes to the knowledge about oomycetic fatty acids as highlighted in the studies of Pasteris *et al.* (2016) and Avis *et al.* (2007).

The fatty acid profiles shown in this study proved that with a higher temperature, in this case 27 °C, the fatty acid composition in the organisms changed from a fatty acid profile that was mainly composed of long chain fatty acids at 20 °C to a profile with shorter chain fatty acids at 27 °C. A possible reason for this shift in fatty acid composition could be that shorter chain fatty acids are less expensive to synthesise for the organism. At 20 °C, shorter chain fatty acids are solid because of their structure while unsaturated long chain fatty acids remain liquid due to their structure and the kinks in the chain caused by the double bonds (Ahmad, 2017; Arild C Rustan and Christian A Drevon, 2001).

The production of such high levels of long chain and very long chain polyunsaturated fatty acids (VLCPUFAs) in the *Peronosporomycetes* appears to be an additional step in the compensation for sterol auxotrophy in order to ensure membrane integrity, even when the amounts of exogenous sterols are low. This assumption is supported by the fatty acid profiles from *Saprolegniomycetes* which rarely produce longer fatty acids than EPA. In the fatty acid profiles of *Saprolegniomycetes* reported in the study of Kendrick *et al.* (1992), eicosapentaenoic acid was the longest polyunsaturated fatty acid to be produced in significant amounts (Andrew Kendrick and Colin Ratledge, 1992).

It is commonly known that higher organisms are not able to produce a sufficient amount of VLCPUFAs themselves, but acquire them through their diet (Salem and Eggersdorfer, 2015). Therefore, besides finding organisms which produce high amounts of certain long chain fatty acids, it is of great interest to decipher how these organisms produce them. By assuming that the produced amounts of fatty acids can be traced back to highly active enzymes and a very efficient pathway, the enzymes of the *Pythium dissotocum* strain P100.30 were identified and characterised. Based on the enzymes found, the route that the enzymes follow in the synthesis of the fatty acids could then be elucidated. The sequences of the enzymes found in this study are of special interest for the development of transgenic organisms yielding high levels of the highly sought after eicosapentaenoic acid (Food and Agriculture Organization of the United Nations, 2010). Efforts to engineer transgenic microorganisms producing eicosapentaenoic acid, as well as docosahexaenoic acid, are ongoing as the demand

for these essential nutrients is rising (Salem and Eggersdorfer, 2015; Food and Agriculture Organization of the United Nations, 2010; Flynn *et al.*, 2012).

Fatty acids have been widely investigated due to the growing demand for nutritional supplements. The health benefits of EPA and DHA consumption have been proven in multiple preclinical and clinical studies, therefore, they are increasingly being regarded as vital factors and top priority nutrients in the growing demand and needs for a healthy human diet. The converging estimations among experts, professional organisations and health professionals are that the annual human consumption of EPA and DHA, following the recommended intake of 500 mg, adds up to 1.3 million metric tons of EPA/DHA globally. At present, only a fraction of this amount is consumed. The core problem is that the fatty acids are mainly derived from seafood and fish, thus, the growing demand cannot be met. Current solutions to meet this demand are both inefficient and insufficient: aquacultures are not profitable, fish catch is not sustainable, α -linolenic acid as an ω -3 fatty acid from plants is merely converted to EPA/DHA and transgenic plants producing EPA and DHA are not commercially available at the moment (Salem and Eggersdorfer, 2015; Food and Agriculture Organization of the United Nations, 2010; Flynn *et al.*, 2012; Monroig and Kabeya, 2018). This illustrates how important a new, environmentally friendly and sustainable source of ω 3-fatty acids is needed.

Six enzymes were identified in this study that are responsible for the synthesis of long chain polyunsaturated fatty acids by using oleic acid (C18:1) as a source. This starting point was chosen because most organisms are able to produce oleic acid by themselves (Xue *et al.*, 2013), however, the enzymes from the oomycetes are not ubiquitously present (Sun *et al.*, 2013).

Oomycetes form part of the group of microorganisms that produce VLCPUFAs (Xue *et al.*, 2013). Since some oomycetes are easily cultivable, grow rapidly and do not require expensive media for axenical cultivation, they represent a new and environmentally friendly source of ω -3 fatty acids (Sun *et al.*, 2013). Exploitation of such oomycetes could provide a significant contribution to the environment, mostly with the exploitation of the enzymes responsible for fatty acid production, although oomycetes cannot be efficiently cultivated as well as yeast or bacteria. Cultivation of oomycetes on a commercial scale, such as yeast, bacteria or microalgae (Zhu *et al.*, 2017), is not possible as they do not grow as fast in liquid culture as yeast or bacteria. However, the enzymes can be used to produce the fatty acids in lipophilic yeasts, for example. In

this case, the enzymes which act on fatty acids with a carbon chain length of 18 are of special interest because most yeasts produce C18-fatty acids (Wang *et al.*, 2013). An elongase was found and characterised which works on C18- and C20-substrates. Five desaturases were found and characterised and among these desaturases was a Δ 15-desaturase. The enzymes were compared to enzymes from the closely related *Peronosporomycetes* and to enzymes from *Saprolegniomycetes*. All of the enzymes, especially the Δ 4-desaturase responsible for the production of DHA, were also present in the *Saprolegniomycetes*.

By comparing the sequences coding for the enzymes involved in fatty acid synthesis from the *Pythium dissotocum* genome with different *Aphanomyces* genomes available, the existence of a similar enzymatic set was revealed in this study.

The *Aphanomyces* and *Saprolegnia* species analysed possess the enzymatic equipment required to synthesise DHA, however, no published FAME profiles have detected docosahexaenoic acid or other long chain polyunsaturated fatty acids. A possible reason for this could be the fast metabolism of DHA, similar to stearidonic acid (C18:4 ω 3), that is difficult to detect due to the fast processing of the elongase. Another reason could be that they do not produce DHA as they have the ability to produce sterols *de novo* and, thus, there is no need to synthesise DHA (Larsen *et al.*, 2000; Dahlin *et al.*, 2017; Gaulin *et al.*, 2010). It may also be possible that VLCPUFAs do not have the same importance for the *Saprolegniomycetes* as they do for the *Peronosporomycetes*.

4.2. Endosymbiosis

The results of the FAME measurements were not as expected. However, a feasible explanation for the high quantities of branched fatty acids detected in almost all of the FAME profiles obtained, could be that the isolates carry endosymbiotic bacteria.

Branched fatty acids are not known to occur naturally in oomycetes but are a common fatty acid form found in bacteria (Cronan and Thomas, 2009)(John E. Cronan and Jacob Thomas, 2009).

In general, bacteria have a similar fatty acid composition as other species, such as oomycetes, for example, but they tend to have shorter fatty acids, lack polyunsaturated

fatty acids and have different double bond positions in their C18-fatty acids (John E. Cronan and Jacob Thomas, 2009; Cronan and Thomas, 2009).

After the first batch of FAME profiles revealed the presence of branched fatty acids, the assumption of bacterial contamination was obvious. However, from the outset, multiple measures were taken to remove the risk of any bacterial contamination in this study. As mentioned in the Methods, from the commencement of the study, the rifampicin concentration was raised to 50 µg/ml, Rapers rings were placed around the inoculation agar plug and the inoculation itself was performed under a microscope with a scalpel, making sure only to transfer hyphae without any contamination. The aim of these actions was to avoid potential contaminations, even so, branched fatty acids were still detected.

There are several possible explanations for this result. One plausible explanation may be a potential endosymbiosis with bacteria.

For many *Zygomycetes*, for example *Rhizopus oryzae*, eukaryotic endosymbiosis with bacteria has been described (Ibrahim *et al.*, 2008). Due to the physical size of the organisms, the unicellular bacteria in this combination is always the endosymbiont and the fungal-like organism the host. It is believed that the bacterial endosymbiotic genes benefit the fungal-like host by facilitating nutrient acquisition and, thus, improve the overall fitness of the host (Ibrahim *et al.*, 2008).

The endosymbionts, living inside the oomycete hyphae, would be protected from antibiotics, the transfer-methods used and the utilisation of Raper rings. This could, therefore, be a plausible explanation for why the branched fatty acids constantly appeared in the fatty acid profiles.

4.3. Pathway

The FAME profiles of the *Pythium dissotocum* strain P100.30 were not sufficient to trace the pathway of the fatty acid synthesis, however, in combination with the enzymes found in the genome, the pathway could still be described.

The combined results found in this study suggest that the long chain fatty acids produced in the *Pythium dissotocum* strain P100.30 followed the $\Delta 15$ -desaturase-route. The presence of a $\Delta 15$ -desaturase which converts linoleic acid into α -linolenic acid, the first ω -3 fatty acid in the pathway, strongly indicates the usage of the ω -3/ $\Delta 15$ -

pathway. The usage of either the $\Delta 15$ - or the $\Delta 17$ -desaturase determines the route that the organisms use for the production of VLCPUFAs, because in either way the other enzymes are identical.

Besides the enzymes found in the genome, the presence of the fatty acids stearidonic acid C18:4 ω 3 (STA) or dihomo- γ -linolenic acid C20:3 ω 6 (DGLA) are important for identifying the steps taken in the synthesis. The presence of STA hints towards the usage of the ω -3 pathway, whilst the presence of DGLA indicates the use of the ω -6 pathway.

Despite the fact that in many of the fatty acid profiles branched fatty acids were detected, profiles without branched fatty acids were also obtained. Only the latter fatty acid profiles were used to determine the synthesis pathway followed in the *Pythium dissotocum* strain P100.30.

In the fatty acid profiles of P100.30 (devoid of branched fatty acids), no stearic acid C18:4 ω 3 could be detected. As the elongase found in the genome is known to have a strong preference for C18-substrates, STA is rarely available in a free form as it gets converted rapidly into eicosatetraenoic acid (C20:4 ω 3) by the elongase and is, thus, rarely detected (Meyer *et al.*, 2004).

Dihomo- γ -linolenic acid was detected in very small quantities of 0.16 %. This finding suggests the usage of the ω 6/ Δ 17-pathway for the production of long chain fatty acids in P100.30.

In some oomycetes, such as *Phytophthora*, *Salisapilia*, *Halophytophthora* and *Pythium ultimum*, traces of DGLA were also found, indicating a different pathway for the production of VLCPUFAs, the ω -6/ Δ 17-pathway.

Furthermore, some *Phytophthora* species only had detectable DGLA-amounts when grown at higher temperatures (27 °C). In contrast, the *Salisapilia tartarea* strain only had DGLA present in its fatty acid profile at 20 °C; at 27 °C no DGLA was detected although C22:4 was produced in much higher quantities than at the lower temperature. Depending on the temperature optimum of the strain in question, these findings could hint towards a change of pathway or a different substrate specificity for the desaturases and elongases involved. This seems to be plausible as the fatty acid composition of each organism is regulated at the gene expression level (Pe'gorier *et al.*, 2004).

The detection of fatty acids using GC-MS-MS is very accurate and sensitive, capable of detecting the smallest quantities precisely. The resulting retention times were compared to an internal library and, thus, the fatty acids were identified. In none of the

measurements were internal or surrogate standards used. The reason for these rather contradictory results is still not entirely clear, but the enzymes present in the genome of P100.30 hint towards the ω -3 fatty acid pathway.

These findings, even though the fatty acid profiles were not as distinct, confirm the usefulness of oomycetes, in particular *Pythium dissotocum*, as potential organisms for exploiting their enzymes in the production of high amounts of eicosapentaenoic acid in transgenic organisms.

4.4. Sterols

Sterols and VLCPUFAs are important factors in maintaining the integrity of membranes by regulating the membranes' fluidity and permeability. They can also act as buffers for the rigidity of the membranes over a great temperature and salinity range, similar to fatty acids (Gaulin *et al.*, 2010).

The *Saprolegniomycetes* are sterol prototrophs that are able to synthesise fucosterol de novo, while the *Peronosporomycetes* are sterol auxotrophs that can modify certain sterols that they acquire but are unable to produce them de novo as they lack the SqE-genes coding for the squalene-monooxygenase enzyme (Dahlin *et al.*, 2017). In *Aphanomyces euteiches*, genes predicted to be involved in sterol synthesis were found and, furthermore, in an experimental approach the organisms could be grown on sterol-free medium. These genes were found in other members of the *Saprolegniomycetes* but not in *Peronosporomycetes* (Gaulin *et al.*, 2010; Lerksuthirat *et al.*, 2017; Dahlin *et al.*, 2017).

The comparison of FAME profiles from previous studies of different oomycete orders has revealed that *Aphanomyces euteiches*, *Aphanomyces astaci*, *Saprolegnia diclina* and *Saprolegnia parasitica* (all members of the *Saprolegniomycetes*) do not produce docosahexaenoic acid (C22:6 ω 3) or fatty acids with a longer chain length than 20 (Larsen *et al.*, 2000). The loss of the ability to produce sterols is said to be linked to an expansion of the elicitin family in the *Peronosporomycetes* and, furthermore, no elicitin coding genes could be found in the *Pythium* species (Gaulin *et al.*, 2010). Elicitins can work as sterol carriers and facilitate the uptake of free sterols. If no free sterols are available, the long chain polyunsaturated fatty acids could work in a compensatory role for the missing sterols (Gaulin *et al.*, 2010).

In another experiment analysing the fatty acids produced in *Aphanomyces euteiches*, the VLCPUFAs detected only extended to C20:5 ω 3, eicosapentaenoic acid; C22:6 ω 3 docosahexaenoic acid (DHA), or its precursors, were not detectable, in contrast to other oomycetes, especially the *Peronosporomycetes* (Larsen *et al.*, 2000). The production of EPA for energy storage, membrane components and normal biochemical processes appears to be sufficient for the *Saprolegniomycetes* as they can rely on their own synthesis of sterols to keep their membranes intact (Larsen *et al.*, 2000; Dahlin *et al.*, 2017; Gaulin *et al.*, 2010).

Regarding the use of long chain fatty acids as integral membrane components in the sterol auxotrophic *Peronosporomycetes*, it was determined that all of the analysed organisms in this study produced long chain polyunsaturated fatty acids. Even though sterols are essential components of membranes and contribute significantly to their integrity, the lack of the ability to produce sterols *de novo* in the *Peronosporomycetes* may partly be compensated by the heightened production of long chain polyunsaturated fatty acids. This is supported by the findings of Dahlin *et al.* (2017) and Larsen *et al.* (2000). Both groups came to the same conclusion that the loss of the sterol synthesis genes may be compensated by the heightened production of VLCPUFAs, whereas in *Aphanomyces euteiches*, a member of the *Saprolegniomycetes*, because of its ability to produce sterols *de novo*, this is not necessary (Dahlin *et al.*, 2017; Larsen *et al.*, 2000). This finding is also confirmed by previous findings in the literature from Devandera *et al.* (2019). They discovered sterol auxotrophic oomycetes in highly salinic environments, in their case *Halophytophthora* from the Philippines; it is also very likely that these oomycetes use VLCPUFAs to control the membrane rigidity and salinity intake in such environments (Devanadera *et al.*, 2019).

Studies on fish cells have shown that with rising salinity the level of polyunsaturated fatty acids (PUFAs) rises, concluding that they play an important role in osmoregulation. Changes in the membrane fatty acid concentration can have important effects on the activity of membrane-bound enzymes, for example, Na⁺-K⁺-ATPase, which are involved in the maintenance of the ion concentration levels and osmotic regulation in cells (Tocher *et al.*, 1995).

Another approach to compensate for the sterol auxotrophy was revealed by Lerksuthirat *et al.* (2017). Some oomycetes have a heightened capacity to bind exogenous sterols due to an increased number of genes (the elicitors) encoding for

sterol-binding and sterol-uptake proteins. This elevated number of genes, to this extent, is only present in the *Peronosporomycetes* and is not as pronounced in the *Saprolegniomycetes* (Lerksuthirat *et al.*, 2017). These findings are in line with many of the *Peronosporomycetes* which are the initial colonisers of debris and outcompete other pathogens easily by their growing pace. Thus, being among the initial composters, the availability of sterol precursors is high and they can use these precursors to synthesise the sterols they need (Beakes and Thines, 2017).

The evolution of sterol synthesis is considered to be one of the keys to eukaryotic evolution. Sterol self-sufficiency appears to be spread throughout the order of the *Saprolegniomycetes* but, as it is lacking in the *Peronosporomycetes*, then it is probable that these organisms have lost this ability (Kendrick and Ratledge, 1992).

In the study of Ah-Fong *et al.* (2019) they state that the incomplete sterol biosynthetic pathway not only makes the affected organisms dependent on exogenous sterol acquisition for their basic metabolism, but also leads to them being resistant to several drugs. This is an advantage for many of the *Peronosporomycetes* and complicates infections, for example, caused by *Pythium insidiosum*, tremendously (Ah-Fong *et al.*, 2019).

One of the main issues concerning our knowledge of oomycetes is the lack of understanding of how the different metabolic pathways work. The understanding of the metabolic pathways and how they interact is vitally important in order to develop fungicides to combat pathogenic oomycetes.

As many of the drugs used to treat diseases caused by oomycetes, for example pythiosis, are targeted at the sterol synthesising enzymes, these drugs are largely ineffective. Thus, the "downside" of losing the SqE-genes actually provides an advantage for some of the most destructive pathogens among the *Oomycota*. Therefore, acquiring more knowledge about the metabolic pathways will not only help to develop new drugs against the pathogens, but might help to understand why certain oomycetes are more resistant to already existing drugs than others (Ah-Fong *et al.*, 2019; Lerksuthirat *et al.*, 2017).

In addition, the *Saprolegnia* and *Aphanomyces* strains do not grow nearly as fast as the *Peronosporomycetes*; the difference can be found in the way that they colonise their hosts. *Pythium* strains are often among the first colonisers or pioneer colonisers of debris and, as such, outcompete other microorganisms by growing rapidly, although not necessarily efficiently (Lerksuthirat *et al.*, 2017).

Sterols are more rigid and durable as they are not as prone to oxidation and degradation as long chain polyunsaturated fatty acids; fatty acids need to be protected from premature degradation and oxidation, while the synthesis of long chain fatty acids is more expensive. The production of sterols, in comparison, is easier and energy-wise cheaper than the synthesis of VLCPUFAs, especially DHA (Arild C Rustan and Christian A Drevon, 2001; Müller-Esterl and Brandt, 2009; Rustan and Drevon, 2001). The loss of the ability to produce sterols de novo can be compensated by the synthesis of long chain fatty acids, but this is more expensive for the organism (Müller-Esterl and Brandt, 2009; Nes, 1987).

4.5. Reliability of FAME profiles and the possible fingerprinting of microorganisms

FAME profiles are believed to provide a precise method for identifying isolates if certain factors, such as growth medium, cultivation temperature, cultivation time and age of the culture, are kept consistent.

Although FAME profiles may provide an elegant solution to the problem of identifying bacteria, due to their distinct fatty acid profiles, the number of screened oomycetes for their specific FAME profiles remains low (John E. Cronan and Jacob Thomas, 2009; Cronan and Thomas, 2009).

One of the major drawbacks of this method is the variation in FAME profiles produced from isolates of prolonged storage on agar media. In culture collections, the age of a culture varies and for such situations the polymerase chain reaction (PCR) approach, rather than a phylogenetic analysis, may be a preferable solution.

The fatty acid profiles obtained during this study showed great variation in the amount of fatty acids detected. A possible reason for this may be the prolonged storage time of the isolates on the agar plates. For every organism, multiple fatty acid profiles were prepared. While the medium, temperature, growth time and the sampling of the mycelium, as well as the method of the sampling, were kept consistent, the age of the organisms differed as well as they would continue to age during the process of preparing multiple FAME profiles.

In between the samplings, the isolates were kept on agar plates at 4 °C in order to slow down their growth. When they were to be sampled again, they were inoculated onto

fresh media plates at room temperature, grown for five days and, from those plates, the agar plugs to be used for the inoculation were cut out to ensure that the mycelium was actively growing. This method was kept consistent throughout the study.

Direct comparability to existing profiles from the literature was not possible as multiple factors, such as the cultivation medium, cultivation temperature, age of the cultures, as well as the sampling method, all played a major role in order to keep the profiles in this study comparable and consistent. A key problem with much of the literature on FAME profiles from oomycetes is that neither the sampling method, cultivation method, cultivation time, cultivation temperature, salinity of the medium nor the age of the cultures are consistent or even mentioned in the literature. Therefore, because of these inconsistencies, the FAME profiles cannot be compared in the same way as, for example, the sequences that are derived from PCRs which can be compared directly. Since the growth pattern, or growth rate, for P100.30 was consistent, a form could be used to exclude the newest and oldest mycelium from the cultures. This was possible because the agar plug used to inoculate the medium usually had a similar diameter. For other oomycetes, naturally having different growth patterns and rates, forms varied and were used to keep the sampled mycelium comparable. This approach to consistency has not been mentioned in any of the literature, but needs to be taken into consideration.

For the detection and precise identification of unknown oomycetes, FAME profiles are said to be an interesting and powerful tool, although identification is not always possible and the technique is labour intensive. In addition, as FAME profiles of isolates can differ, previous studies have suggested to take 8-10 samples to clearly identify the isolate. Thus, this also needs to be taken into consideration because the workload can become extremely high compared to the work that is involved in the construction of a phylogenetic tree (Robert P. Larkin and Carol L. Groves). Extracting genomic DNA for use in the PCR, with subsequent sequencing of the amplicons, is a much quicker and precise way to identify unknown organisms, even though the sequences in the databases need to be viewed with caution; considerable care must be taken when using sequences from a database to check the identity of one's isolates. As can be seen in the phylogenetic analysis in Figure 7, the *Saprolegnia bulbosa* sequence was "matched" to one of the *Pythium* strains after BLAST analysis and has clearly been misidentified. A BLAST search of the sequence back to the database revealed a close

resemblance to sequences from *Pythium sp.* and *Pythium insidiosum*, both members of the *Peronosporomycetes*.

The benefits of using PCR, especially when sequencing multiple loci, or with the advances in technology the sequencing of whole genomes, are that it can lead, in combination with a phylogenetic analysis, to a high resolution of phylogenetic relationships and identification (Fiore-Donno and Bonkowski, 2021). When choosing this route to identify unknown organisms, the editing should be executed in a responsible and conservative way while always keeping in mind that the sequences deposited in databases may be flawed. Nevertheless, for a skilled person, this procedure takes less time than the production of multiple FAME profiles. Thus, in a laboratory or a culture collection, where the storage time of the isolates vary and the identification check is carried out on a regular basis, FAME profiles are not likely to replace molecular identification.

Nevertheless, when FAME profiles are obtained from axenically grown cultures, it is easy to discard the oldest and youngest mycelium and, thus, achieve consistency from the source. In a liquid culture this is not possible as mycelia of all growing stages are present in the liquid; resulting FAME profiles would vary greatly and would not be comparable. Naturally, in growing and developing hyphae, more fatty acids would be detectable since they are an integral part of the membranes, while in older hyphae those fatty acids may already have been broken down or different fatty acids compositions may be detected due to the organisms using them as energy storage.

The age of the mycelium is an important factor if FAME profiles are to be assumed to be comparable and consistent. What might be comparable and used for the identification of cultures grown at the same temperature, even though the produced amounts may differ, are the predominantly produced fatty acids (Robert P. Larkin and Carol L. Groves).

This study has not confirmed the previous research on FAME profiles used for the characterisation of oomycetes, however, it does serve to expand the knowledge on the usage of FAME profiles. FAME profiles provide a great opportunity to expand the toolkit for the identification of oomycetes, however, they are not able to replace the use of the PCR. PCR, combined with sequencing, is a very easy, cheap and reliable method used to identify organisms (Telle and Thines, 2008).

The analysis of fatty acids, in the form of derivatised fatty acids, provides a more robust analysis than the analysis of free fatty acids directly as the esterified fatty acids are not prone to oxidation or degradation (Eder, 1995).

Nevertheless, the retention times for unsaturated and saturated fatty acids can sometimes be very similar (Eder, 1995) as the double bonds render the compounds more polar, while some compounds are more difficult to distinguish than others when no internal standard is used.

In the FAME profiles obtained in this study, two compounds were found having no previous biological characterisation: C18:2 ω 3 and C22:4 ω 3. Not a single mention of C18:2 ω 3 or C22:4 ω 3 could be discovered in the databases or literature and it is possible that they have been attributed to be C18:2 ω 3 and C22:4 ω 3 by mistake. Following the putative pathway, it would be more plausible for C22:4 ω 3 to be C22:5 ω 3 or C22:6 ω 3 and for C18:2 ω 3 to be either linoleic acid (C18:2 ω 6) or α -linolenic acid (C18:3 ω 3), especially since α -linolenic acid was not detected at all. Throughout the repeated FAME analyses, these two compounds called were detected constantly.

5. Conclusion

To sum up this study has expanded the knowledge about the fatty acid synthesis in oomycetes. In total 192 fatty acid profiles were obtained and analysed and in combination with the analysis of genomic and transcriptomic data the pathway of the fatty acid synthesis in oomycetes was elucidated. The synthesis of polyunsaturated long chain fatty acids follows the Δ 15-pathway. All of the analysed oomycetes belong to the *Peronosporomycetes* and the sequences of the enzymes involved in the pathway were compared to sequences from *Saprolegniomycetes*.

The comparison of the enzymatic set with the *Saprolegniomycetes*, sterol auxotrophs, revealed the existence of the same set, even though they are not known to produce very long chain polyunsaturated fatty acids. Although there are limitations due to unexpected branched fatty acids in the FAME-profiles the enzymes involved in the VLCPUFA-synthesis were analysed. Gaining more knowledge about oomycetes is important in order to efficiently combat pathogenic oomycetes who still are responsible for enormous losses in agriculture and to use the acquired knowledge to possibly generate a sustainable, environmental friendly source of ω -3 fatty acids in

the future. The enzymes found in this study have the potential to be the foundation of a new source of ω -3 fatty acids in the future while the discovery of the metabolic differences between the *Peronosporomycetes* and (John E. Cronan and Jacob Thomas, 2009) and the *Saprolegniomycetes* and the potential endosymbiosis are important discoveries to be resolved in future studies.

References

- Ah-Fong, A.M.V., Kagda, M.S., Abrahamian, M. and Judelson, H.S. (2019), "Niche-specific metabolic adaptation in biotrophic and necrotrophic oomycetes is manifested in differential use of nutrients, variation in gene content, and enzyme evolution", *PLoS pathogens*, Vol. 15 No. 4, e1007729.
- Ahmad, M.U. (Ed.) (2017), *Fatty acids: Chemistry, synthesis, and applications edited by Moghis U. Ahmad, Jina Pharmaceuticals, Inc., Libertyville, IL, United States*, Academic Press an imprint of Elsevier, London.
- Altschul, S.F., Gish, W., Miller, W., Myers, E.W. and Lipman, D.J. (1990), "Basic local alignment search tool", *Journal of molecular biology*, Vol. 215 No. 3, pp. 403–410.
- Andrew Kendrick and Colin Ratledge (1992), "Lipids of selected molds grown for production of ω -3 and ω -6 polyunsaturated fatty acids", *Lipids*, Vol. 27 No. 1, pp. 15–20.
- Arild C Rustan and Christian A Drevon (Ed.) (2001), *Fatty Acids: Structures and Properties*, John Wiley & Sons, Ltd, Chichester.
- Augustyn, O., Ferreira, D. and Kock, J. (1991), "Differentiation between Yeast Species, and Strains within a Species, by Cellular Fatty Acid Analysis", *Systematic and Applied Microbiology*, Vol. 14 No. 4, pp. 324–334.
- Avis, T.J., Michaud, M. and Tweddell, R.J. (2007), "Role of lipid composition and lipid peroxidation in the sensitivity of fungal plant pathogens to aluminum chloride and sodium metabisulfite", *Applied and environmental microbiology*, Vol. 73 No. 9, pp. 2820–2824.
- Beakes, G.W. and Thines, M. (2017), "Hyphochytriomycota and Oomycota", in Archibald, J.M. (Ed.), *Handbook of the protists, Springer reference*, 2nd ed., Springer, New York, pp. 435–505.
- Binyam Tsedaley (2014), "Late Blight of Potato (*Phytophthora infestans*) Biology, Economic Importance and its Management Approaches", *Journal of Biology, Agriculture and Healthcare*, Vol. 4 No. 25, pp. 215–225.

- Cecile Clavaud, Vishu Kumar Aimanianda and Jean-Paul Latge (2009), "Organization of Fungal, Oomycete and Lichen (1,3)- β -Glucans", *Chemistry, Biochemistry, and Biology of 1-3 Beta Glucans and Related Polysaccharides*.
- Clark, K., Karsch-Mizrachi, I., Lipman, D.J., Ostell, J. and Sayers, E.W. (2016), "GenBank", *Nucleic Acids Research*, Vol. 44 D1, D67-72.
- Cooke, D.E., Drenth, A., Duncan, J.M., Wagels, G. and Brasier, C.M. (2000), "A molecular phylogeny of Phytophthora and related oomycetes", *Fungal genetics and biology FG & B*, Vol. 30 No. 1, pp. 17–32.
- Cronan, J.E. and Thomas, J. (2009), "Chapter 17 Bacterial Fatty Acid Synthesis and its Relationships with Polyketide Synthetic Pathways", in John E. Cronan and Jacob Thomas (Ed.), *Bacterial Fatty Acid Synthesis and its Relationships with Polyketide Synthetic Pathways, Methods in Enzymology*, Vol. 459, Elsevier, pp. 395–433.
- Dahiya, A. (Ed.) (2020), *Bioenergy: Biomass to Biofuels and Waste to Energy*, Academic Press.
- Dahlin, P., Srivastava, V., Ekengren, S., McKee, L.S. and Bulone, V. (2017), "Comparative analysis of sterol acquisition in the oomycetes *Saprolegnia parasitica* and *Phytophthora infestans*", *PloS one*, Vol. 12 No. 2, e0170873.
- Derevnina, L., Petre, B., Kellner, R., Dagdas, Y.F., Sarowar, M.N., Giannakopoulou, A., La Concepcion, J.C. de, Chaparro-Garcia, A., Pennington, H.G., van West, P. and Kamoun, S. (2016), "Emerging oomycete threats to plants and animals", *Philosophical transactions of the Royal Society of London. Series B, Biological sciences*, Vol. 371 No. 1709.
- Devanadera, M.K.P., Bennett, R.M., Watanabe, K., Santiago, M.R., Ramos, M.C., Aki, T. and Dedeles, G.R. (2019), "Marine Oomycetes (*Halophytophthora* and *Salispina*): A Potential Source of Fatty Acids with Cytotoxic Activity Against Breast Adenocarcinoma Cells (MCF7)", *Journal of oleo science*, Vol. 68 No. 12, pp. 1163–1174.
- Eder, K. (1995), "Gas chromatographic analysis of fatty acid methyl esters", *Journal of Chromatography B*, pp. 113–131.
- Fawke, S., Doumane, M. and Schornack, S. (2015), "Oomycete interactions with plants: infection strategies and resistance principles", *Microbiology and molecular biology reviews MMBR*, Vol. 79 No. 3, pp. 263–280.

- Fiore-Donno, A.M. and Bonkowski, M. (2021), “Different community compositions between obligate and facultative oomycete plant parasites in a landscape-scale metabarcoding survey”, *Biology and Fertility of Soils*, Vol. 57 No. 2, pp. 245–256.
- Flynn, A., Martin, A., Przyrembel, H. and Strain, Sean (J.J.) (2012), “Scientific Opinion on the Tolerable Upper Intake Level of eicosapentaenoic acid (EPA), docosahexaenoic acid (DHA) and docosapentaenoic acid (DPA)”, *EFSA Journal*, Vol. 10 No. 7.
- Food and Agriculture Organization of the United Nations (2010), *Fats and fatty acids in human nutrition: Report of an expert consultation 10-14 November 2008, Geneva, FAO food and nutrition paper*, Vol. 91, Food and Agriculture Organization of the United Nations, Rome.
- Gaastra, W., Lipman, L.J.A., Cock, A.W.A.M. de, Exel, T.K., Pegge, R.B.G., Scheurwater, J., Vilela, R. and Mendoza, L. (2010), “Pythium insidiosum: an overview”, *Veterinary microbiology*, Vol. 146 1-2, pp. 1–16.
- Gaulin, E., Bottin, A. and Dumas, B. (2010), “Sterol biosynthesis in oomycete pathogens”, *Plant signaling & behavior*, Vol. 5 No. 3, pp. 258–260.
- Hein, I., Gilroy, E.M., Armstrong, M.R. and Birch, P.R.J. (2009), “The zig-zag-zig in oomycete-plant interactions”, *Molecular plant pathology*, Vol. 10 No. 4, pp. 547–562.
- Ho, H. (2018), “The Taxonomy and Biology of Phytophthora and Pythium”, *Journal of Bacteriology & Mycology: Open Access*, Vol. 6 No. 1.
- Ibrahim, A.S., Gebremariam, T., Liu, M., Chamilos, G., Kontoyiannis, D., Mink, R., Kwon-Chung, K.J., Fu, Y., Skory, C.D., Edwards, J.E. and Spellberg, B. (2008), “Bacterial endosymbiosis is widely present among zygomycetes but does not contribute to the pathogenesis of mucormycosis”, *The Journal of infectious diseases*, Vol. 198 No. 7, pp. 1083–1090.
- Javed, M.R., Abbasi, A.Z., Akhtar, M.J., Ghafoor, S., Afzal, M.A., Majeed, Z. and Umer, B. (2021), “Current trends and recent progress of genetic engineering in genus Phytophthora using CRISPR systems”, in *CRISPR and RNAi Systems*, Elsevier, pp. 183–209.
- Jennifer M. Davidson, Allison C. Wickland, Heather A. Patterson, Kristen R. Falk and David M. Rizzo (2005), “Transmission of Phytophthora ramorum in Mixed-Evergreen Forest in California”, *Phytopathology*, pp. 587–596.

- Jiang, R.H.Y. and Tyler, B.M. (2012), "Mechanisms and evolution of virulence in oomycetes", *Annual review of phytopathology*, Vol. 50, pp. 295–318.
- John E. Cronan and Jacob Thomas (Ed.) (2009), *Bacterial Fatty Acid Synthesis and its Relationships with Polyketide Synthetic Pathways, Methods in Enzymology*, Elsevier.
- Jones, P., Binns, D., Chang, H.-Y., Fraser, M., Li, W., McAnulla, C., McWilliam, H., Maslen, J., Mitchell, A., Nuka, G., Pesseat, S., Quinn, A.F., Sangrador-Vegas, A., Scheremetjew, M., Yong, S.-Y., Lopez, R. and Hunter, S. (2014), "InterProScan 5: genome-scale protein function classification", *Bioinformatics (Oxford, England)*, Vol. 30 No. 9, pp. 1236–1240.
- Judelson, H.S. (2009), "Sexual Reproduction in Oomycetes: Biology, Diversity, and Contributions to Fitness", in Lamour, K. and Kamoun, S. (Eds.), *Oomycete Genetics and Genomics*, John Wiley & Sons, Inc, Hoboken, NJ, USA, pp. 121–138.
- Judelson, H.S. and Ah-Fong, A.M.V. (2019), "Exchanges at the Plant-Oomycete Interface That Influence Disease", *Plant physiology*, Vol. 179 No. 4, pp. 1198–1211.
- Katoh, K., Misawa, K., Kuma, K. and Miyata, T. (2002), "MAFFT: a novel method for rapid multiple sequence alignment based on fast Fourier transform", *Nucleic Acids Research*, Vol. 30 No. 14, pp. 3059–3066.
- Kihara, A. (2012), "Very long-chain fatty acids: elongation, physiology and related disorders", *Journal of biochemistry*, Vol. 152 No. 5, pp. 387–395.
- Larkin, R.P. and Groves, C.L. (2003), "Identification and Characterization of Isolates of *Phytophthora infestans* Using Fatty Acid Methyl Ester (FAME) Profiles", *Plant disease*, Vol. 87 No. 10, pp. 1233–1243.
- Larsen, J., Mansfeld-Giese, K. and Bødker, L. (2000), "Quantification of *Aphanomyces euteiches* in pea roots using specific fatty acids", *Mycological Research*, Vol. 104 No. 7, pp. 858–864.
- Lerksuthirat, T., Sangcakul, A., Lohnoo, T., Yingyong, W., Rujirawat, T. and Krajaejun, T. (2017), "Evolution of the Sterol Biosynthetic Pathway of *Pythium insidiosum* and Related Oomycetes Contributes to Antifungal Drug Resistance", *Antimicrobial agents and chemotherapy*, Vol. 61 No. 4.
- Lücking, R., Aime, M.C., Robbertse, B., Miller, A.N., Ariyawansa, H.A., Aoki, T., Cardinali, G., Crous, P.W., Druzhinina, I.S., Geiser, D.M., Hawksworth, D.L., Hyde, K.D., Irinyi, L., Jeewon, R., Johnston, P.R., Kirk, P.M., Malosso, E., May, T.W., Meyer, W., Öpik, M., Robert, V., Stadler, M., Thines, M., Vu, D., Yurkov, A.M.,

- Zhang, N. and Schoch, C.L. (2020), “Unambiguous identification of fungi: where do we stand and how accurate and precise is fungal DNA barcoding?”, *IMA fungus*, Vol. 11, p. 14.
- Meesapyodsuk, D. and Qiu, X. (2012), “The front-end desaturase: structure, function, evolution and biotechnological use”, *Lipids*, Vol. 47 No. 3, pp. 227–237.
- Meyer, A., Kirsch, H., Domergue, F., Abbadi, A., Sperling, P., Bauer, J., Cirpus, P., Zank, T.K., Moreau, H., Roscoe, T.J., Zähringer, U. and Heinz, E. (2004), “Novel fatty acid elongases and their use for the reconstitution of docosaheptaenoic acid biosynthesis”, *Journal of lipid research*, Vol. 45 No. 10, pp. 1899–1909.
- Moncalvo, J.-M., Wang, H.-H. and Hseu, R.-S. (1995), “Phylogenetic relationships in *Ganoderma* inferred from the internal transcribed spacers and 25S ribosomal DNA sequences”, *Mycologia*, Vol. 87 No. 2, pp. 223–238.
- Monroig, Ó. and Kabeya, N. (2018), “Desaturases and elongases involved in polyunsaturated fatty acid biosynthesis in aquatic invertebrates: a comprehensive review”, *Fisheries Science*, Vol. 84 No. 6, pp. 911–928.
- Müller-Esterl, W. and Brandt, U. (2009), *Biochemie: Eine Einführung für Mediziner und Naturwissenschaftler*, Korrigierter Nachdr. 2009 der 1. Aufl. 2004, Spektrum, Akad. Verl., Heidelberg.
- Nes, W.D. (1987), “Biosynthesis and Requirement for Sterols in the Growth and Reproduction of Oomycetes”, in Fuller, G. and Nes, W.D. (Eds.), *Ecology and Metabolism of Plant Lipids, ACS Symposium Series*, Vol. 325, American Chemical Society, Washington, DC, pp. 304–328.
- Oliver, L., Dietrich, T., Marañón, I., Villarán, M.C. and Barrio, R.J. (2020), “Producing Omega-3 Polyunsaturated Fatty Acids: A Review of Sustainable Sources and Future Trends for the EPA and DHA Market”, *Resources*, Vol. 9 No. 12, p. 148.
- Pang, K.-L., Lin, H.-J., Lin, H.-Y., Huang, Y.-F. and Chen, Y.-M. (2015), “Production of arachidonic and eicosapentaenoic acids by the marine oomycete *Halophytophthora*”, *Marine biotechnology (New York, N.Y.)*, Vol. 17 No. 2, pp. 121–129.
- Pasteris, R.J., Hanagan, M.A., Bisaha, J.J., Finkelstein, B.L., Hoffman, L.E., Gregory, V., Andreassi, J.L., Sweigard, J.A., Klyashchitsky, B.A., Henry, Y.T. and Berger, R.A. (2016), “Discovery of oxathiapiprolin, a new oomycete fungicide that targets an oxysterol binding protein”, *Bioorganic & medicinal chemistry*, Vol. 24 No. 3, pp. 354–361.

- Pe'gorier, J.-P., Le May, C. and Girard, J. (2004), "Control of Gene Expression by Fatty Acids", *American Society for Nutritional Sciences*.
- Raper, J.R. (1937), "A method of freeing fungi from bacterial contaminations", *Science (New York, N.Y.)*, Vol. 85 No. 2205, p. 342.
- Rice, P., Longden, I. and Bleasby, A. (2000), "EMBOSS: The European Molecular Biology Open Software Suite", *The European Molecular Biology Open Software Suite*, Vol. 16 No. 6.
- Robert P. Larkin and Carol L. Groves, "Identification and Characterization of Isolates of *Phytophthora infestans* Using Fatty Acid Methyl Ester (FAME) Profiles".
- Rustan, A.C. and Drevon, C.A. (2001), "Fatty Acids: Structures and Properties", in Arild C Rustan and Christian A Drevon (Ed.), *Fatty Acids: Structures and Properties*, John Wiley & Sons, Ltd, Chichester.
- Salem, N. and Eggersdorfer, M. (2015), "Is the world supply of omega-3 fatty acids adequate for optimal human nutrition?", *Current opinion in clinical nutrition and metabolic care*, Vol. 18 No. 2, pp. 147–154.
- Schornack, S., Huitema, E., Cano, L.M., Bozkurt, T.O., Oliva, R., van Damme, M., Schwizer, S., Raffaele, S., Chaparro-Garcia, A., Farrer, R., Segretin, M.E., Bos, J., Haas, B.J., Zody, M.C., Nusbaum, C., Win, J., Thines, M. and Kamoun, S. (2009), "Ten things to know about oomycete effectors", *Molecular plant pathology*, Vol. 10 No. 6, pp. 795–803.
- Sun, Q., Jiang Liu, Qin Zhang, Xiaohe Qing, Gary Dobson, Xinzheng Li and Baoxiu Qi (2013), "Characterization of three novel desaturases involved in the delta-6 desaturation pathways for polyunsaturated fatty acid biosynthesis from *Phytophthora infestans*", *Applied microbiology and biotechnology* No. 97, pp. 7689–7697.
- Tamura, K., Peterson, D., Peterson, N., Stecher, G., Nei, M. and Kumar, S. (2011), "MEGA5: molecular evolutionary genetics analysis using maximum likelihood, evolutionary distance, and maximum parsimony methods", *Molecular biology and evolution*, Vol. 28 No. 10, pp. 2731–2739.
- Telle, S. and Thines, M. (2008), "Amplification of *cox2* (approximately 620 bp) from 2 mg of up to 129 years old herbarium specimens, comparing 19 extraction methods and 15 polymerases", *PloS one*, Vol. 3 No. 10, e3584.
- Thines, M. (2014), "Phylogeny and evolution of plant pathogenic oomycetes—a global overview", *European Journal of Plant Pathology*, Vol. 138 No. 3, pp. 431–447.

- Thines, M. (2018), "Oomycetes", *Current biology CB*, Vol. 28 No. 15, R812-R813.
- Timothy C. Paulitz & Richard R. Bélanger (2001), "Biological control in greenhouse systems", *Annual review of phytopathology*, Vol. 39, pp. 103–133.
- Tocher, D.R., Castell I, J.D., Dick, J.R. and Sargen, J.R. (1995), "Effects of salinity on the fatty acid compositions of total lipid and individual glycerophospholipid classes of Atlantic salmon (*Salmo salar*) and turbot (*Scophthalmus maximus*) cells in culture", *Fish Physiology and Biochemistry* No. 14, pp. 125–137.
- Tuffs, S. and Oidtmann, B. (2011), "A comparative study of molecular diagnostic methods designed to detect the crayfish plague pathogen, *Aphanomyces astaci*", *Veterinary microbiology*, Vol. 153 3-4, pp. 343–353.
- Untergasser, A., Cutcutache, I., Koressaar, T., Ye, J., Faircloth, B.C., Remm, M. and Rozen, S.G. (2012), "Primer3--new capabilities and interfaces", *Nucleic Acids Research*, Vol. 40 No. 15, e115.
- Uzuhashi, S., Kakishima, M. and Tojo, M. (2010), "Phylogeny of the genus *Pythium* and description of new genera", *Mycoscience*, Vol. 51 No. 5, pp. 337–365.
- Vallance, J., Le Floch, G., Déniel, F., Barbier, G., Lévesque, C.A. and Rey, P. (2009), "Influence of *Pythium oligandrum* biocontrol on fungal and oomycete population dynamics in the rhizosphere", *Applied and environmental microbiology*, Vol. 75 No. 14, pp. 4790–4800.
- Wang, M., Chen, H., Gu, Z., Zhang, H., Chen, W. and Chen, Y.Q. (2013), " ω 3 fatty acid desaturases from microorganisms: structure, function, evolution, and biotechnological use", *Applied microbiology and biotechnology*, Vol. 97 No. 24, pp. 10255–10262.
- Xue, Z., He, H., Hollerbach, D., Macool, D.J., Yadav, N.S., Zhang, H., Szostek, B. and Zhu, Q. (2013), "Identification and characterization of new Δ -17 fatty acid desaturases", *Applied microbiology and biotechnology*, Vol. 97 No. 5, pp. 1973–1985.
- Yoshida, K., Schuenemann, V.J., Cano, L.M., Pais, M., Mishra, B., Sharma, R., Lanz, C., Martin, F.N., Kamoun, S., Krause, J., Thines, M., Weigel, D. and Burbano, H.A. (2013), "The rise and fall of the *Phytophthora infestans* lineage that triggered the Irish potato famine", *eLife Sciences Publications, Ltd*, 28 May, available at: <https://elifesciences.org/articles/00731> (accessed 29 March 2021).

Zhu, A., Nowack, L. and Jeong, M.Y. (2017), "On the Production of High-Purity Docosahexaenoic Acid from Heterotrophic Microalgae", *Department of Chemical & Biomolecular Engineering*, pp. 1–387.

6. List of Figures

Figure 1: Overview of the phylogeny of the species used in this thesis.....	1
Figure 2: Example of short, medium, long and very long chain fatty acids	8
Figure 3: α -Linolenic acid C18:3 ω 3	9
Figure 4: the aerobic-synthesis pathway of ω -3 Fatty acids	13
Figure 5: Visualization of the mycelium used for the FAME analysis. All mycelium within the inner circle and outside of the outer circle were discarded.	26
Figure 6: Axenical growth pattern of the <i>Salisapilia tartarea</i> strain LT7204 on PDB-agar at 20 °C after 5 days.....	30
Figure 7: Phylogenetic tree inferred from Minimum Evolution analysis based on ITS sequences with 500 bootstraps. The numbers above the branches indicate the respective support, bootstrap values below 75 % are not shown. The spacer bar indicates the number of base substitutions per position. Isolates used in this study are marked with bold letters. Asterisks mark isolates belonging to the Peronosporomycetes, the degree sign marks the isolate belonging to the Saprolegniomycetes.	31
Figure 8: Fatty acid profile of the <i>Pythium dissotocum</i> strain P100.31 grown at 20 °C and 27 °C. Values shown are averages of all fatty acids methyl ester profiles obtained.....	33
Figure 9: Fatty acid profile of the <i>Pythium dissotocum</i> strain P100.30 grown at 20 °C and 27 °C. Values shown are averages of all fatty acids methyl ester profiles obtained.....	34
Figure 10: Fatty acid profile of the <i>Pythium dissotocum</i> strain P100.39 grown at 20 °C. Values shown are averages of all fatty acids methyl ester profiles obtained.	35
Figure 11: Fatty acid profile of the <i>Pythium dissotocum</i> strain P100.4 grown at 20 °C. Values shown are averages of all fatty acids methyl ester profiles obtained.	36
Figure 12: Fatty acid profile of the <i>Pythium dissotocum</i> strain P77.13 grown at 20 °C and 27 °C. Values shown are averages of all fatty acids methyl ester profiles obtained.....	36
Figure 13: Fatty acid profile of the <i>Pythium dissotocum</i> strain P101.2 grown at 20 °C. Values shown are averages of all fatty acids methyl ester profiles obtained.	37
Figure 14: Fatty acid profile of the <i>Pythium dissotocum</i> strain P101.3 grown at 20 °C. Values shown are averages of all fatty acids methyl ester profiles obtained.	38
Figure 15: Fatty acid profile of the <i>Pythium oopapillum</i> strain P76.3 grown at 20 °C and 27 °C. Values shown are averages of all fatty acids methyl ester profiles obtained.....	39
Figure 16: Fatty acid profile of the <i>Pythium kashmirensense</i> strain V2.4 grown at 20 °C. Values shown are averages of all fatty acids methyl ester profiles obtained.	40
Figure 17: Fatty acid profile of the <i>Pythium flavoense</i> strain V21.2 grown at 20 °C. Values shown are averages of all fatty acids methyl ester profiles obtained.	41
Figure 18: Fatty acid profile of the <i>Salisapilia tartarea</i> strain LT7204 grown at 20 °C and 27 °C. Values shown are averages of all fatty acids methyl ester profiles obtained.....	42
Figure 19: Fatty acid profile of the <i>Phytophthora lacustris</i> strain P2Z.2 grown at 20 °C and 27 °C. Values shown are averages of all fatty acids methyl ester profiles obtained.....	43
Figure 20: Fatty acid profile of the <i>Phytophthora lacustris</i> strain P2Z.3 grown at 20 °C and 27 °C. Values shown are averages of all fatty acids methyl ester profiles obtained.....	44

Figure 21: Fatty acid profile of <i>Phytophthora lacustris</i> strain P2Z.5 at 20 °C and 27 °C. Values shown are averages of all fatty acids methyl ester profiles obtained.	45
Figure 22: Fatty acid profile of <i>Phytophthora lacustris</i> strain P100.18 at 20 °C and 27 °C. Values shown are averages of all fatty acids methyl ester profiles obtained.	46
Figure 23: Fatty acid profile of <i>Phytophthora lacustris</i> strain EMTS1.2.1 at 20 °C and 27 °C. Values shown are averages of all fatty acids methyl ester profiles obtained.	47
Figure 24: Fatty acid profile of the <i>Phytophthora ramorum</i> strain 111 762 at 20 °C. Values shown are averages of all fatty acids methyl ester profiles obtained.	48
Figure 25: Fatty acid profile of the <i>Globisporangium ultimum</i> strain lev1805 grown at 20 °C and 27 °C. Values shown are averages of all fatty acids methyl ester profiles obtained.	49
Figure 26: Fatty acid profile of the <i>Phytophthora infestans</i> strain T30-4 grown at 20 °C. Values shown are averages of all fatty acids methyl ester profiles obtained.	50
Figure 27: Fatty acid profile of the <i>Halophytophthora</i> sp. strain EMTD 7 grown at 20 °C and 27 °C. Values shown are averages of all fatty acids methyl ester profiles obtained.	51
Figure 28: Fatty acid profile of the <i>Halophytophthora</i> sp. strain EMTS 23 grown at 20 °C and 27 °C. Values shown are averages of all fatty acids methyl ester profiles obtained.	52
Figure 29: Fatty acid profile of the <i>Halophytophthora</i> sp. strain EMTD 12 grown at 20 °C and 27 °C. Values shown are averages of all fatty acids methyl ester profiles obtained.	53
Figure 30: Comparison of ω 3 fatty acids of different oomycetes. Isolates with the letter a are <i>Pythium dissotocum</i> , b is <i>Pythium oopapillum</i> , c is <i>Pythium kashmirensis</i> , d is <i>Pythium ultimum</i> , e is <i>Salisapilia tartarea</i> , f is <i>Phytophthora lacustris</i> , g is <i>Phytophthora ramorum</i> and h is <i>Halophytophthora</i> sp.	54
Figure 31: Fatty acid profile of <i>Pythium dissotocum</i> strain P100.30 without FAME measurements that showed branched fatty acids.	58
Figure 32: Growth on PDB-agar plates at 20 °C. A is <i>Pythium dissotocum</i> P100.30 and B is EMTS 1.2.1 from the <i>Phytophthora lacustris</i> strains. Picture A was taken after three days, picture B after eight days. Scale bar = 0.75 cm in all pictures	60
Figure 33: Protein domains of the elongase of P100.30. Non-cytosolic parts are purple, transmembrane helices are green and cytosolic domains are yellow.	62
Figure 34: Protein alignment of the elongase of <i>Pythium dissotocum</i> and elongases from other oomycetes. Thick arrows mark histidine boxes and the smaller arrows mark the ER-retention signal. The first four sequences belong to members of the Saprolegniomycetes, the last four belong to the Peronosporomycetes.	63
Figure 35: Protein domains of the elongase of P100.30. Non-cytosolic parts are purple, transmembrane helices are green and cytosolic domains are yellow.	65
Figure 36: Protein alignment of the Δ 4-desaturase protein sequences from different oomycetes. Thick arrows mark histidine boxes, smaller arrows mark ER-retention signals. Similarity is shown in shades of black, black meaning 100 % similarity.	66
Figure 37: Protein domains of the Δ 5-desaturase of P100.30. Non-cytosolic parts are purple, transmembrane helices are green and cytosolic domains are yellow.	67
Figure 38: Protein alignment of the delta5-desaturase of different oomycetes. Red arrows indicate ER-retention signals, similarity is shown in shades of black while black stands for 100 % similarity.	68
Figure 39: Protein domains and families of the elongase of P100.30. Non-cytosolic parts are purple, transmembrane helices are green and cytosolic domains are yellow.	69

Figure 40: Protein alignment of the delta5-desaturase of different oomycetes. Red pointy arrows indicate ER-retention signals, thick red arrows mark histidine-boxes, and similarity is shown in shades of black while black stands for 100 % similarity... 70	70
Figure 41: Protein domains of the desaturase of P100.30. Non-cytosolic parts are purple, transmembrane helices are green and cytosolic domains are yellow. 71	71
Figure 42: MAFFT alignment of the protein sequences of the delta12-desaturase of different oomycetes. The purple arrows highlight HXXXH-motifs. 72	72
Figure 43: Protein domains of the elongase of P100.30. Non-cytosolic parts are purple, transmembrane helices are green and cytosolic domains are yellow. 73	73
Figure 44: Protein alignment of the delta 15 desaturase from different oomycetes. ER-retention signals are the pointy arrows in red and the thicker arrows are Histidine boxes. 74	74
Figure 45: Combined results based on the fatty acids profiles of P100.30 and the genomic and transcriptomic data to identify the enzymes. Detected fatty acids and enzymes are marked with bold black letters, the fatty acids and enzyme that are not found are grey. 75	75
Figure 46: Desaturation of oleic acid by the Δ 12-desaturase leads to linoleic acid by the introduction of the double bond at the sixth carbon atom from the methyl-end. Fatty acids and enzymes with bold letters were detected/verified by FAME-analysis or PCR and genomic/transcriptomic data. 76	76
Figure 47: Assumed introduction of the double bond at the ω -3 position by the Δ 15-desaturase, turning linoleic acid into α -linolenic acid. Fatty acids and enzymes with bold letters were detected/verified by FAME-analysis or PCR and genomic/transcriptomic data. 76	76
Figure 48: The desaturation of α -linolenic acid (C18:3 ω 3) led to the formation of stearidonic acid (C18:4 ω 3). The enzymatic reaction was thought to be catalyzed by the Δ 6-desaturase. Fatty acids and enzymes with bold letters were detected/verified by FAME-analysis or PCR and genomic/transcriptomic data. 76	76
Figure 49: γ -linolenic acid (C18:3 ω 6) is the assumed product of the enzymatic reaction of the Δ 6-desaturase with linoleic acid (C18:2 ω 6). Fatty acids and enzymes with bold letters were detected/verified by FAME-analysis or PCR and genomic/transcriptomic data. 77	77
Figure 50: The elongation of γ -linolenic acid (C18:3 ω 6) would lead to the production of dihomo- γ -linolenic acid (C20:3 ω 6) catalysed by the Δ 6-elongase. Fatty acids and enzymes with bold letters were detected/verified by FAME-analysis or PCR and genomic/transcriptomic data. 77	77
Figure 51: Enzymatic reaction of the Δ 6-elongase with the ω -3 substrate stearidonic acid (C18:4 ω 3) resulting in the formation of eicosatetraenoic acid (C20:4 ω 3). Fatty acids and enzymes with bold letters were detected/verified by FAME-analysis or PCR and genomic/transcriptomic data. 77	77
Figure 52: The Δ 5-desaturase catalyses the formation of arachidonic acid (C20:4 ω 6) as it introduces a double bond into dihomo- γ -linolenic acid. Fatty acids and enzymes with bold letters were detected/verified by FAME-analysis or PCR and genomic/transcriptomic data. 78	78
Figure 53: Synthesis of eicosapentaenoic acid (C20:5 ω 3), catalysed by the introduction of a double bond at the ω -3 position by a Δ 17-desaturase, starting from arachidonic acid (C20:4 ω 6). Fatty acids and enzymes with bold letters were detected/verified by FAME-analysis or PCR and genomic/transcriptomic data. 78	78
Figure 54: Desaturation of eicosatetraenoic acid (C20:4 ω 3) by the Δ 5-desaturase led to the formation of eicosapentaenoic acid (C20:5 ω 3) by the introduction of the double	

bond. Fatty acids and enzymes with bold letters were detected/verified by FAME-analysis or PCR and genomic/transcriptomic data. 78

7. Appendix

Pythium dissotocum

Number of FAME profiles

Fatty acids	11		1		12		6		3	
	P100.31 20 °C	STA	P 100.31 27 °C	P100.30 20 °C	STA	P100.30 27 °C	STA	P100.39 20°C	STA	
LP 12:0	0,31	0,43		0,26	0,22			0,48	0,09	
LP 14:0	8,44	7,56	28,43	15,77	5,51	1,59	1,83	16,68	1,13	
LP i14:0 ME	2,00	2,82	0,28							
LP 16:0 ME	12,15	16,34	11,62	14,59	12,21	13,05	15,07	14,18	8,40	
LP i16:0 MT	8,24	6,62	6,68	5,50	7,17	37,50	43,30	3,79	6,56	
LP 16:1				1,83	1,83			3,10	2,51	
LP 16:1w7c ME	2,17	2,08		2,07	1,71					
LP 16:1w9c ME										
LP 18:0				2,18	2,89			3,19	1,90	
LP 18:1	1,84	2,09		0,23	0,47					
LP 18:1w7c ME	1,19	1,49	4,24	8,63	5,16			12,11	5,92	
LP 18:1w9c ME	21,91	12,10	19,00	17,11	8,21			21,26		
LP 18:2w3 ME	1,44	1,44								
LP 18:2w6,9 ME	6,32	3,99	7,28	8,35	5,56	5,60	6,47	4,62	4,49	
LP 18:3w6,9,12 ME	0,01	0,02		1,56	3,32					
LP 18:4w3 ME	0,24	0,41		0,35	0,36			0,61	0,62	
LP 20:0 ME				0,26	0,07			0,66	0,11	
LP 20:1 ME	0,21	0,38	0,27	0,50	0,66			1,53	0,93	
LP i20:0 ME										
LP 20:3w6,9,12 ME				1,78	2,33			2,00	1,18	
LP 20:4w3,6,9,12 ME	0,34	0,65	0,55	0,65	0,70			1,46	0,89	
LP 20:4w6,9,12,15 ME	3,03	3,16		4,25	4,35			1,98	1,23	
LP 20:5w3,6,9,12,15 ME	1,18	1,27		0,84	0,79			1,33	0,65	
LP 22:0 ME	17,71	10,16	9,59	17,22	6,88	7,59	8,77	17,18	9,34	
LP 22:4w3 ME	0,01	0,01		0,03	0,04			0,19	0,11	
LP 22:4w6 ME	0,31	0,38	0,41	1,05	2,42			2,41	4,02	
LP 22:5 ME								0,07	0,06	
LP 22:5w3 ME				0,05	0,06			0,64	0,11	
LP 22:5w6 ME				0,09	0,06			0,27	0,03	

Number of FAME profiles	<i>Pythium dissotocum</i>							
	1		8		3		4	
	P100.4 20 °C	STA	P77.13 20 °C	STA	P77.13 27 °C	STA	P101.2 20 °C	STA
LP 12:0	0,47	0,07	0,43	0,19			0,52	0,00
LP 14:0	9,54	4,19	9,51	8,00			11,49	0,18
LP i14:0 ME			0,08	0,16				
LP 16:0 ME	19,40	3,27	9,32	10,33				
LP i16:0 MT			14,20	12,45	18,70	14,24	16,30	0,66
LP 16:1	2,81	0,43	3,99	6,57	13,85	9,80	6,53	6,53
LP 16:1w7c ME			3,11	0,49			1,95	0,02
LP 16:1w9c ME								
LP 18:0	3,03	0,25	1,80	1,48				
LP 18:1			4,55	1,96	8,75	1,41	1,32	0,08
LP 18:1w7c ME	13,01	5,40	7,60	7,83				
LP 18:1w9c ME			4,73	7,13	2,45	1,17	11,82	9,65
LP 18:2w3 ME			0,59	1,02			0,66	0,66
LP 18:2w6,9 ME	4,13	1,69	4,76	2,63	1,51	2,13	4,80	0,64
LP 18:3w6,9,12 ME			0,01	0,02			0,09	0,01
LP 18:4w3 ME	0,71	0,28	0,84	0,67			1,62	0,06
LP 20:0 ME	1,38	0,14	0,32	0,34			0,36	0,28
LP 20:1 ME	1,84	0,30	0,95	0,63			1,12	0,07
LP i20:0 ME								
LP 20:3w6,9,12 ME	2,99	0,49	2,51	1,78	3,06	0,66	0,24	0,24
LP 20:4w3,6,9,12 ME	1,25	0,22	0,86	0,61			0,35	0,00
LP 20:4w6,9,12,15 ME	3,48	0,86	1,03	0,93				
LP 20:5w3,6,9,12,15 ME			2,28	2,36			5,28	3,30
LP 22:0 ME	25,17	7,23	11,47	6,19	1,57	2,21	20,19	0,84
LP 22:4w3 ME	0,13	0,00	0,39	0,49	0,53	0,75	0,01	0,01
LP 22:4w6 ME	0,01	0,02	0,08	0,09			0,25	0,03
LP 22:5 ME					0,37	0,52		
LP 22:5w3 ME	0,35	0,07	0,41	0,21				
LP 22:5w6 ME	0,27	0,02	2,87	3,14	1,30	1,8354647		

Number of FAME profiles	<i>Pythium flavoense</i>		<i>Salisapilia tartarea</i>		<i>Salisapilia tartarea</i>		<i>Phytophthora lacustris</i>	
	3		6		3		7	
Fatty acids	V21.2 20 °C	STAB	LT7204 20 °C	STA	LT 7204 27°C	STA	P2Z.2 20°C	STA
LP 12:0	0,51	0,03						
LP 14:0	16,11	1,12	1,59	0,20	3,44	1,11	0,80	1,0803089
LP i14:0 ME			5,25	2,75				
LP 16:0 ME	13,99	1,16	0,00	0,01			6,28	10,869053
LP i16:0 MT	0,01	0,01	19,20	1,64	25,75	4,11	12,75	12,228776
LP 16:1	1,13	0,02					0,34	0,7679938
LP 16:1w7c ME			16,66	2,82	7,65	0,87	7,95	6,51
LP 16:1w9c ME								
LP 18:0	2,80	0,28						
LP 18:1			0,97	0,11	2,13	0,34	0,61	0,68
LP 18:1w7c ME	14,95	2,90					7,21	7,21
LP 18:1w9c ME			31,73	5,29	44,90	13,97	16,36	5,40
LP 18:2w3 ME							2,74	2,74
LP 18:2w6,9 ME	5,69	0,58	8,32	2,94	12,46	0,66	18,23	9,45
LP 18:3w6,9,12 ME			0,51	0,34			0,00	0,00
LP 18:4w3 ME	1,84	0,20	0,01	0,01				
LP 20:0 ME	0,09	0,13	0,10	0,02				
LP 20:1 ME	1,84	0,23	0,03	0,04				
LP i20:0 ME			0,34	0,03				
LP 20:3w6,9,12 ME	1,65	0,24						
LP 20:4w3,6,9,12 ME	2,93	0,34	3,03	0,36			2,0326963	1,7549787
LP 20:4w6,9,12,15 ME	0,86	0,05	1,93	0,24	1,68	1,47		
LP 20:5w3,6,9,12,15 ME								
LP 22:0 ME	20,66	4,33	2,43	0,47			9,2702376	9,6214758
LP 22:4w3 ME	0,23	0,02	6,06	0,64	0,29	0,50		
LP 22:4w6 ME	0,24	0,03	0,63	0,14	1,54	0,77	0,4458234	0,814973
LP 22:5 ME			0,07	0,01				
LP 22:5w3 ME	0,26	0,02						
LP 22:5w6 ME	0,21	0,03	0,14	0,02				

<i>Phytophthora lacustris</i>								
Number of FAME profiles	3		5		3		5	
Fatty acids	P2Z.5 27 °C STA		P100.18 20 °C STA		P100.18 27 °C STA		EMTS 1.2.1 20 °C STA	
LP 12:0			0,21	0,02			0,14	0,01
LP 14:0	1,54	1,18	1,75	2,15			4,61	1,39
LP i14:0 ME			2,93	1,93	1,32	0,69		
LP 16:0 ME	19,62	14,39	0,08	0,16			12,09	14,81
LP i16:0 MT	22,99	18,08	17,16	8,12	20,98	16,42	17,28	14,40
LP 16:1	2,96	4,19	22,58	23,95	38,63	19,19	0,76	1,52
LP 16:1w7c ME	4,85	3,54	3,98	1,19			4,19	2,47
LP 16:1w9c ME			1,12	0,87	0,49	0,69		
LP 18:0			3,36	1,65	2,72	1,72	0,59	0,83
LP 18:1	0,17	0,24	2,03	0,76	0,81	0,06	0,93	0,47
LP 18:1w7c ME								
LP 18:1w9c ME	9,79	1,64	4,14	2,68			10,60	5,38
LP 18:2w3 ME			2,64	2,58				
LP 18:2w6,9 ME	22,49	3,72	14,78	10,58	15,01	9,45	21,39	1,53
LP 18:3w6,9,12 ME			0,15	0,25	3,51	4,96	0,85	1,58
LP 18:4w3 ME			0,46	0,32			0,51	0,63
LP 20:0 ME			0,11	0,11			0,23	0,23
LP 20:1 ME			0,19	0,23			0,14	0,17
LP i20:0 ME			1,37	0,22	0,46	0,19		
LP 20:3w6,9,12 ME			0,17	0,15	0,12	0,09		
LP 20:4w3,6,9,12 ME	0,58	0,82	5,19	2,36	2,53	0,65	1,88	0,96
LP 20:4w6,9,12,15 ME	2,45	3,46						
LP 20:5w3,6,9,12,15 ME			0,94	1,88	3,12	4,26	4,01	0,17
LP 22:0 ME	5,93	4,49	6,63	8,03	3,90	2,83	11,26	0,24
LP 22:4w3 ME			0,52	0,23	0,55	0,28	0,10	0,13
LP 22:4w6 ME	4,19	3,02	0,26	0,23			1,09	1,17
LP 22:5 ME					0,10	0,14		
LP 22:5w3 ME								
LP 22:5w6 ME					0,69	0,51		

Number of FAME profiles	<i>Phytophthora lacustris</i>				<i>Phytophthora ramorum</i>			
	3		8		6		5	
	EMTS 1.2.1 27 °C		S7.1 20 °C		S7.1 27 °C		CBS 111 762 20 °C	
Fatty acids	STA	STA	STA	STA	STA	STA	STA	
LP 12:0			0,07	0,08			0,35	0,01
LP 14:0	0,62	0,88	2,18	2,11	2,48	1,54	13,48	3,81
LP i14:0 ME								
LP 16:0 ME			14,02	14,34	29,07	14,42	9,67	12,04
LP i16:0 MT	42,16	13,97	17,54	16,29	12,04	16,92	13,54	13,55
LP 16:1	0,99	1,40	0,82	1,64	1,21	1,71	5,86	7,29
LP 16:1w7c ME			3,94	3,49	1,55	3,47	4,44	0,48
LP 16:1w9c ME								
LP 18:0							2,06	2,08
LP 18:1	0,21	0,29	0,89	0,92	0,12	0,27	0,84	0,14
LP 18:1w7c ME			9,96	8,35	14,14	7,57	11,55	2,54
LP 18:1w9c ME	5,96	4,31	10,88	8,97	3,75	4,18	23,26	1,19
LP 18:2w3 ME								
LP 18:2w6,9 ME	17,38	12,46	18,84	2,17	21,82	9,55	6,81	5,64
LP 18:3w6,9,12 ME	12,85	18,18	0,04	0,08			0,02	0,02
LP 18:4w3 ME			0,37	0,45			2,33	0,38
LP 20:0 ME								
LP 20:1 ME			0,23	0,40			0,27	0,27
LP i20:0 ME								
LP 20:3w6,9,12 ME					0,15	0,32	2,56	2,56
LP 20:4w3,6,9,12 ME			2,20	0,79	1,96	1,72	2,57	0,90
LP 20:4w6,9,12,15 ME	2,70	3,82			2,24	3,16	0,72	1,42
LP 20:5w3,6,9,12,15 ME			0,85	1,69			1,35	0,27
LP 22:0 ME	3,91	5,52	11,42	1,83	10,28	5,79	11,43	3,22
LP 22:4w3 ME			0,24	0,41			0,19	0,19
LP 22:4w6 ME	3,54	5,01	0,65	1,09	3,68	6,66	1,14	1,55
LP 22:5 ME								
LP 22:5w3 ME							0,18	0,01
LP 22:5w6 ME							0,04	0,05

